
Masters Theses

Student Theses and Dissertations

1971

Feed drive design for numerically controlled machine tools

Subash Bhatia

Follow this and additional works at: https://scholarsmine.mst.edu/masters_theses



Part of the [Mechanical Engineering Commons](#)

Department:

Recommended Citation

Bhatia, Subash, "Feed drive design for numerically controlled machine tools" (1971). *Masters Theses*. 5110.

https://scholarsmine.mst.edu/masters_theses/5110

This thesis is brought to you by Scholars' Mine, a service of the Missouri S&T Library and Learning Resources. This work is protected by U. S. Copyright Law. Unauthorized use including reproduction for redistribution requires the permission of the copyright holder. For more information, please contact scholarsmine@mst.edu.

111

FEED DRIVE DESIGN FOR NUMERICALLY CONTROLLED
MACHINE TOOLS

BY

SUBASH BHATIA, 1944

A THESIS

Presented to the Faculty of the Graduate School of the

UNIVERSITY OF MISSOURI - ROLLA

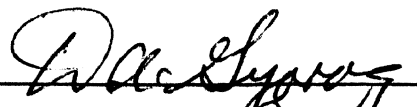
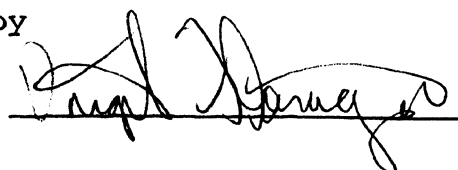
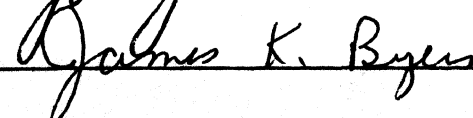
in Partial Fulfillment of the Requirements for the

Degree of

MASTER OF SCIENCE IN MECHANICAL ENGINEERING

1971

Approved by

 (Advisor) 


T2675
161 pages
c.1

202940

ABSTRACT

The various types of feed drive control systems used in numerical control of machine tools have been broadly classified. Further a step by step design has been presented for the feed drive of a numerical contouring control milling machine. The aim has been to develop a consistent strategy for tackling a variety of such problems. Consequently stress has been laid on principles and not on design figures.

ACKNOWLEDGEMENTS

The author wishes to extend his sincere thanks and appreciation to Dr. D.A. Gyorog for the guidance, encouragement and valuable suggestions throughout the course of this thesis.

The author is indebted to Mrs. Connie Hendrix for her cooperation in typing this manuscript.

TABLE OF CONTENTS

	Page
ABSTRACT	ii
ACKNOWLEDGEMENT	iii
LIST OF ILLUSTRATIONS	vi
LIST OF TABLES	ix
LIST OF SYMBOLS	x
I. INTRODUCTION	1
II. BASIC NUMERICAL CONTROL	5
III. SERVO SYSTEM ANALYSIS	30
A. Incremental Servos	30
B. Contactor Servos	35
C. Clutch Servomechanisms	39
D. Linear Electro-Hydraulic Servo	42
E. Electric Servos	45
F. Rotary Electro-Hydraulic Servo	51
IV. SERVO-SYSTEM SYNTHESIS AND DESIGN	54
A. Frequency Domain Specifications	57
B. Time Domain Specifications	58
C. Torque Motor Constants	65
D. Motor, Pump and Valve	65
E. Stabilization of Velocity Loop	71
F. Position Loop Compensation	85
G. Optimization of Transient Response	103
H. Operation of the Designed System	107

TABLE OF CONTENTS (continued)

	Page
V. THE MODERN DESIGN APPROACH	118
VI. CONCLUSIONS	123
BIBLIOGRAPHY	126
VITA	129
APPENDICES	130
A. Hydraulic Servo Analysis	130
A1. Linear Electro-Hydraulic Servo	130
A2. Valve-Controlled Motor	133
A3. Torque-Motor Analysis	138
B. Transfer Functions of Electric-Servo	145
C. Lag-Lead Compensator Characteristics	148

LIST OF ILLUSTRATIONS

Figure		Page
1a	'Point-to-Point' Operation	9
1b	'Continuous Path' Operation	9
2	Typical Cam Profile Machined on Contouring Control	12
3	'Bendix Dynapath System'	14
4	Block Diagram of a Contouring Control System .	15
5	Types of Non-Linear Controllers for 'Command Point Anticipation'	18
6	Digital-Analog Systems	22
7	Analog Systems	23
8a	Control Loop for 'Positioning Control' Employing Incremental Servos	31
8b	'Stepping Motor' (Electrical) Characteristics	31
9	Block Diagram of Electro-Hydraulic Pulse Motor	34
10	Contact Servomechanism Operation	36
11	Clutch Servomechanism	40
12	Linear Hydraulic Servo Motor	44
13	Electric Servo System	46
14	Ward-Leonard System	47
15	Thyratron Operation	49
16	Electro-Hydraulic Servo System with Rotary Motor	52
17	Digital-Analog Contouring Control System . . .	55
18	Equivalent Unity Feedback System	61

LIST OF ILLUSTRATIONS (continued)

Figure		Page
19	Typical Open-Loop Response for Torque Motors . . .	66
20	Basic System to be Checked for Response and Stability	69
21	Block Diagram with Velocity Loop Eliminated . . .	70
22	Series Compensation of Velocity Loop	72
23	Velocity Loop with Series Lag Compensator	74
24	Root Locus Plots for Lag Compensator	76
25	Series Lag-Lead Compensator	77
26	Locus Plots of Lag-Lead Compensator	79
27	Acceleration Feedback Compensation	80
28	Locus Plots for Acceleration Feedback	82
29	Compensation of Position Loop	84
30	Representation for Open Loop Frequency Response.	86
31	Open Loop Frequency Response	88
32	Open Loop Frequency Response for Compensated System	93
33	Block Diagram of Compensated System	94
34	Closed Loop Frequency Response	96
35	Response to Unit Step	101
36	Response to Unit Ramp	102
37	System to be Simulated on Analog Computer . . .	105
38	Study of System Operation	110
39	Sample - Data Representation of Feed Control System	120
40	Valve Controlled Cylinder and Piston	134

LIST OF ILLUSTRATIONS (continued)

Figure		Page
41	Valve Controlled Hydraulic Motor	136
42	Torque Motor	142
43	Electric Servo-System	147
44	Lag-Lead Compensator Characteristics	150

LIST OF TABLES

Table		Page
1	Root Locus Data for Series Lag Compensator	75
2	Root Locus Data for Lag-Lead Compensation	78
3	Root Locus Data for Acceleration Feedback	81
4	Open Loop Frequency Response Data	87
5	Open Loop Frequency Response Data for $G_c(s) = \frac{1+\tau_1 s}{1+\tau_2 s}$	91
6	Open Loop Frequency Response Data for $G_c(s) = \frac{(1+\tau_1 s)(1+\tau_2 s)}{\tau_1 \tau_2 s^2 + (\tau_1 + \tau_2 + \tau_{12})s + 1}$	92

LIST OF SYMBOLS

A_p	Area of piston	in^2
B_p	Viscous damping coefficient of piston and load	in-lb-sec
β_e	Bulk modulus of oil	p.s.i.
C_{ip}	Internal or crossport leakage coefficient of piston	$\text{in}^3/\text{sec/p.s.i.}$
C_{ep}	External leakage coefficient of piston	$\text{in}^3/\text{sec/p.s.i.}$
D	Operator d/dt	
D_m	Volumetric displacement of motor	in^3/rad
e_g	Error signal	volts
I_f	Field current in generator	amps
J_T	Load and motor inertia reflected to motor shaft	in-lb-sec^2
K_c	Flow pressure coefficient	$\text{in}^3/\text{sec/p.s.i.}$
K_e	Constant of back emf	
K_G	Gain constant for tachogenerator	volts/rad/sec
K_p	Gain constant for position error amplifier	
K_v	Gain constant for velocity error amplifier	
K_s	Gain of torque motor	ins/volt
L_{fg}	Inductance of field winding of generator	henrys
L_a	Inductance of motor armature winding	henrys
M_T	Mass of piston and load referred to piston	$\text{lbs-sec}^2/\text{in.}$

LIST OF SYMBOLS (continued)

Q_L	Flow rate	in^3/sec
R_a	Resistance of motor armature winding	ohms
R_{fg}	Resistance of field winding of generator	ohms
S	Laplace transform	
T_L	Arbitrary load torque	in-lb
T_M	Torque developed by motor	in-lb
τ_a	Motor armature time constant	
τ_{fg}	Time constant of field winding	
θ_o	Output shaft rotation	rads.
$\dot{\theta}_o$	Output shaft velocity	rads/sec
θ_i	Input shaft rotation	rads.
V_t	Total compressed volume of oil	in^3
ω_o	Natural frequency of torque motor armature and associated moving members	rads/sec.
$\omega_r = \frac{1}{\tau_v}$	Defines time constant for torque motor armature and associated moving members	rads/sec
X_i	Input signal	ins.
X_o	Output linear movement of load	ins.
X_v	Displacement of spool value from line-on-line position	ins.
ξ	Damping ratio	

I. INTRODUCTION

A major emphasis in control system analysis is to develop mathematical models for physical situations; models which satisfactorily describe the component dynamics. Obviously the model developed must describe the actual components and the physical problem in terms appropriate for analytical design, evaluation and testing. Unfortunately in most problems of any meaningful dimensions, the designer who attempts to develop the model, soon finds himself confronted with higher order transfer functions. Consequently even the simplest of physical problems lead to models of sufficient complexity to preclude the use of any conventional techniques for analysis of system stability, sensitivity and transient response. The only meaningful approach at this stage is to subdivide the problem into two major areas:

- a) For the initial design the system must be represented by a model which is simple enough to allow analysis to be carried out with the conventional techniques available to the system designer (with the possible aid of a digital computer to help with the mathematics).

- b) In the final analysis, using the preliminary design developed in the first step, the system dynamics are simulated with the analog or digital computer. At this stage the model may be made increasingly complex by adding branches to represent the various non-linearities which are invariably present. Based on this simulation the final dynamic and steady state characteristics for the system may be decided upon and the compensating element parameters fixed.

This in a broad sense is the procedure to be followed in designing any control system, and the same is true when designing feed drives for numerical control of machine tools. Almost all publications on this subject have tended to be descriptive, without attempting to present a unified approach to designing servo-systems suitable for numerical control both point-to-point and continuous path. A few papers^{8,9,10,15*} have suggested a similar approach for preliminary design. But though these would serve the purpose of initiating the potential designer on the right path, the problem has not been presented in sufficient detail nor any analysis presented, which could be used as a guideline by the aspiring designer.

*References listed in Bibliography

The purpose of this investigation is two fold. Firstly to synthesize the various types of feed drive control systems used in numerical control of machine tools. A broad classification has been attempted for the sole purpose of illustrating the applicability of the basic design method to these various types. Secondly to carry out the design of a feed drive servo system suitable for numerical contouring control.

The problem has been analyzed in sufficient depth as to offer a clear guideline for analysis of any number of similar problems. The aim has been to present a logical step by step analysis and consequently more stress has been laid on basic principles and not on the design figures themselves. The feed drive has been designed for a hypothetical machine tool. However, a sincere attempt has been made to assume basic data which is as close to real as possible. In brief, a feed drive has been designed for a numerical contouring control milling machine having the following performance requirements.

- a) Feed range from 0 to 40 inch/min.
- b) Excessively high table and load weight handling capability.
- c) Maximum velocity errors of .001" for normal contouring rates (maximum up to 5 inch/min) and .008" for skimming rates (maximum up to 40 inch/min).
- d) Overall loop sensitivity w.r.t. plant characteristics of 1/10 of 1%.

For sake of completeness certain brief comments on basic numerical control have been included. No attempt has been made to go into details as sufficient literature exists. Only areas having a direct bearing on the performance criteria of the feed drives have been commented on in detail.

II. BASIC NUMERICAL CONTROL

The topics included in this chapter can be divided into two parts. The first part deals with a brief description of numerical positioning and contouring control. Certain comments on programming have also been included in this section. The second part presents a brief synthesis of a typical control system used with contouring machine tools. Numerical control has been broadly classified on the basis of applications into two types viz. 'point-to-point' and 'continuous path'. In both types the major control function is the automatic motion of the workpiece, relative to the cutting tool, as commanded by the input data.

Numerical position control as applied to drilling boring and punching machines is characterized by intermittent cutting operations. The positioning cycle itself is free from disturbing factors such as cutting forces, etc. Furthermore the control itself is concerned with the position commanded by the input and the path traversed is of no consequence. Maximum feed rate is applied to approach the desired position with the final approach made at a 'crawling rate' to avoid overshoot due to inertia. When in position the table is clamped mechanically or by servo. Most position control machine tools require

positioning accuracies finer than .001 inch/ft. Recent extension of numerical control to jigboring machines (which offer maximum rewards by way of economic savings) calls for accuracies within .00005 inch/ft. This is where the ingenuity of the control system designer enters the control problem solution. The factors which have to be considered while designing servo-systems suitable for such control are:

1. Achieve a sufficiently high gain at the same time maintaining stability.
2. Match the servo design to machine tool characteristics taking into account such inherent nonlinearities of the controlled element such as backlash, coulomb friction, stickslip effects, machine resonances, etc.
3. Design a control loop insensitive enough to give uniform accuracy for a service period of a number of years.

This is no easy task. The problem is complicated by factors such as valve drift, changing characteristics of the plant with increasing usage e.g. friction of the machine slides, etc. Obviously the problem is not just of designing a servo with a sufficient enough gain. Radical changes have had to be incorporated in m/c tools*.

*Machine tool

Various different servo designs have been tried ranging from the completely open loop type servos with stepping actuators to other conventional closed loop type. The latter have generally been found to be more reliable.

Numerical contouring control refers to operations where the control has to be exercised simultaneous on more than one axis with full coordination between all the controlled axes. Most common applications are milling machines, grinding machines, lathes, drafting machines and to some extent flame cutters. Here not only are we interested in reaching the commanded position but also the path taken. As the name implies the path of the workpiece relative to the cutter center line has to be controlled during the continuous cutting operation. Thus the control problem is basically that of controlling the feed rate along the three axes in strict relation with each other. The requirements on the servo are even more stringent and in addition to the factors previously mentioned the design calls for:

- 1) A servo with the least possible velocity error.
- 2) No appreciable transients in feed rates due to external cutting forces (very often of an intermittent nature).
- 3) Minimum individual response shaping i.e. maximum interchangeability.

Designing a control system to meet such exacting demands is indeed a formidable task. It is clear that in the

final analysis the only hope for carrying out a successful preliminary design is with the help of computer simulations. With the computer simulations also it will not be possible to take into account all the nonlinearities of the various elements in the control loop. Certain amount of final shaping will have to be carried out after installation of the control system in order to ensure satisfactory transient behavior. However, as pointed above, the whole idea of performing a satisfactory design is to minimize reliance on this final shaping.

The two block diagrams shown in Fig. 1 show a general comparison between point-to-point and continuous path N.C. The following important difference between the two needs to be stressed. For point-to-point work most programming can be easily carried out with the help of trigonometric tables and a desk calculator. As an example consider a part which has to be programmed for drilling of some holes on a point-to-point machine. In such a case the programmer has to define the absolute coordinates of the holes from some chosen datum. He enters the information on a manuscript together with the necessary coded information for starting and stopping the machine spindle and for correct cutting speeds. The information is then punched on a paper tape.

On the other hand for parts such as airplane wing sections, dies, cams etc. machining has to be done on

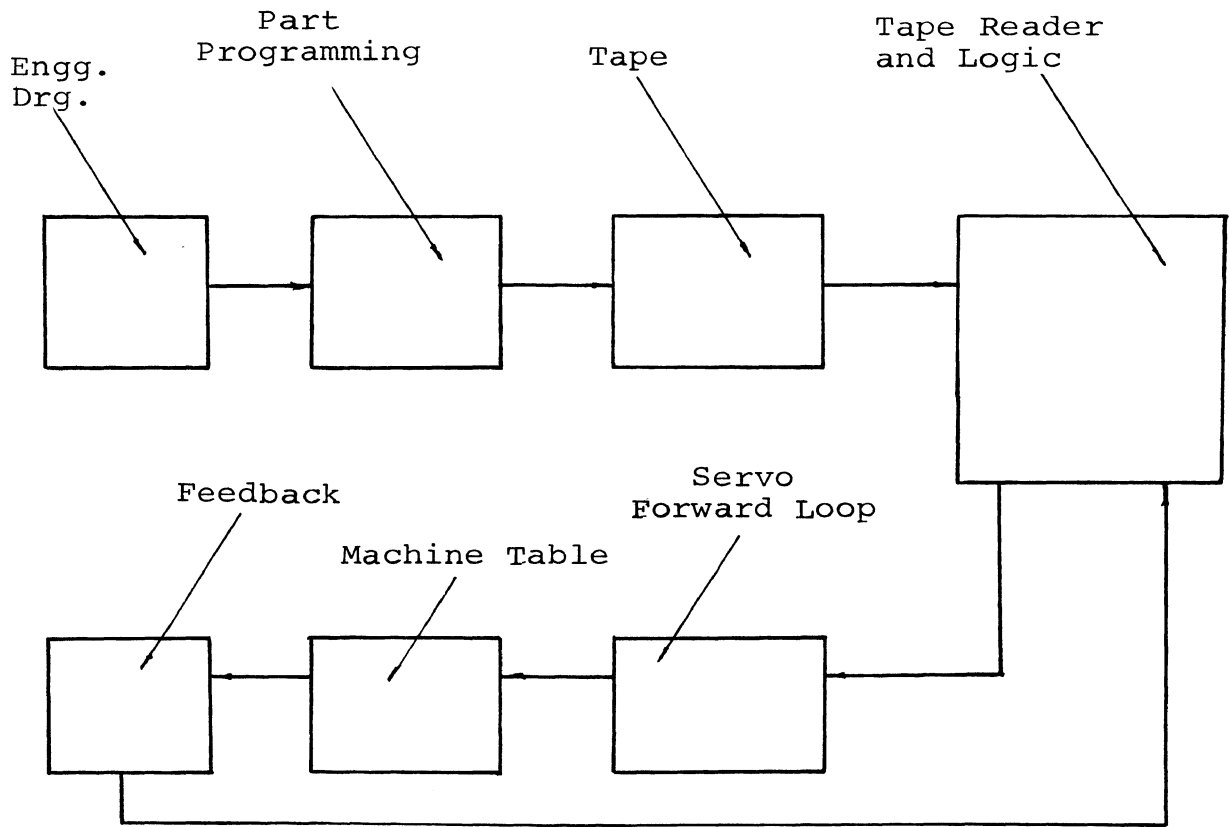


Fig. 1a. 'Point-to-Point' Operation

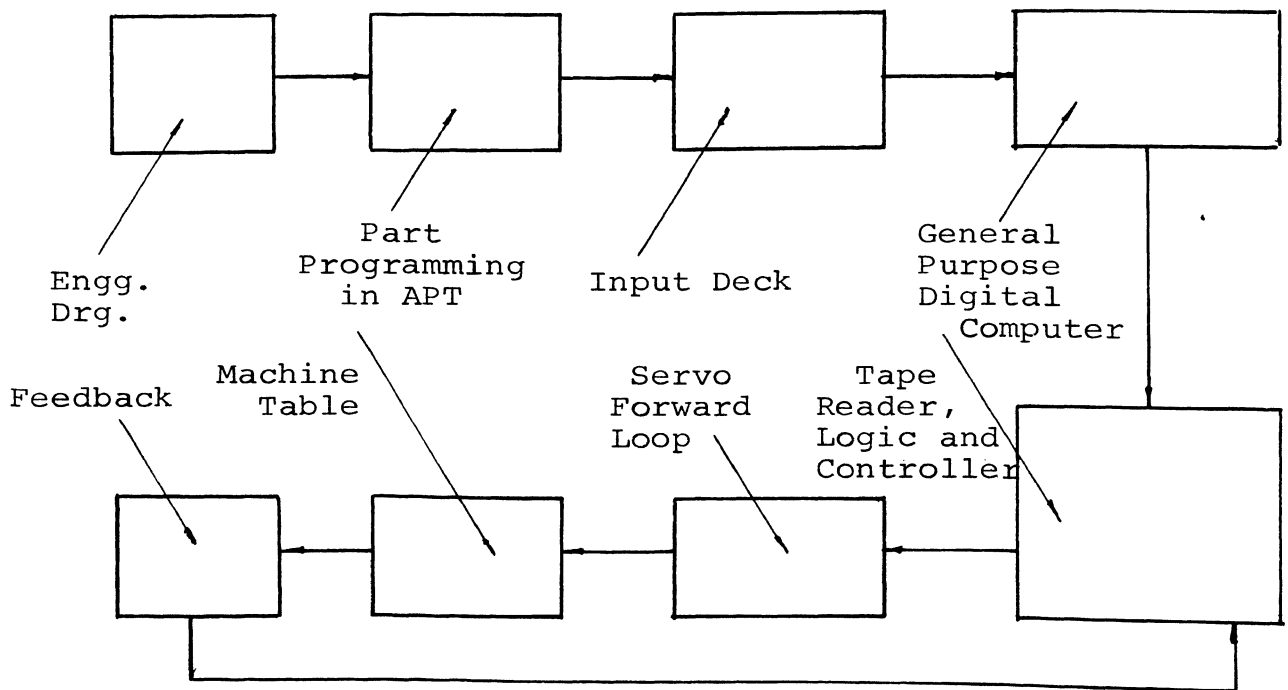


Fig. 1b. Continuous Path Operation

three, four or five axes contouring m/c tools. In such a case programming by hand is very nearly impossible excepting in the simplest cases. Coordinates of various end points of thousands of segments lying on the cutter center-path have to be defined. Here recourse is taken to the general purpose digital computer which, with the help of established computer routines, carries out the detailed computations and gives as its output the punched tape which forms the input to the machine control unit. A computer routine is usually written for a particular computer and will data process the input information to give a mathematical description of the cutter center path. This cutter center path information must be broken up into suitable spans and also into an acceptable form for a particular machine tool. This is achieved by a routine known as a 'post-processor'. For feeding basic part description to the computer special languages have been developed and of these the most comprehensive is 'Automatic Programming Tool' (APT). This is practically the only language which offers three axes coverage.

These in brief are the programming functions in a typical N.C. installation. The important factor is to carefully differentiate between those interpolation functions carried out by the general purpose computer and those carried out by the m/c tool control logic itself. Principle interpolation operations carried out by the

machine tool director are:

- a) linear interpolation,
- b) circular or parabolic interpolation.

Most contouring control m/c tools have linear and circular capabilities. In the case of 'Cincinnati Acramatic System' parabolic interpolation is also possible.

Obviously for reasons of economy, and the delay associated with increasingly higher order computation, higher order interpolation capabilities are never incorporated in the machine-tool logic. Thus all complex shapes have to be broken into segments definable by second order polynomials (parabola, circles depending upon m/c tool logic capabilities) and this is done externally with the help of digital computers. The tape input to the machine tool must carry the coordinate references for each segment in a separate block along with the feed rate number and other relevant information. Depending upon the part contour complexity and the desirable tolerance (manufacturing) the number of such segments might run into thousands and thus the need for the general purpose computer as a programming aid.

The part illustrated in Fig. 2 will have five programmed blocks shown:

- 1 and 4, linear blocks
- 2 , block containing commands for parabolic interpolation
- 3 and 5, blocks containing commands for circular interpolation

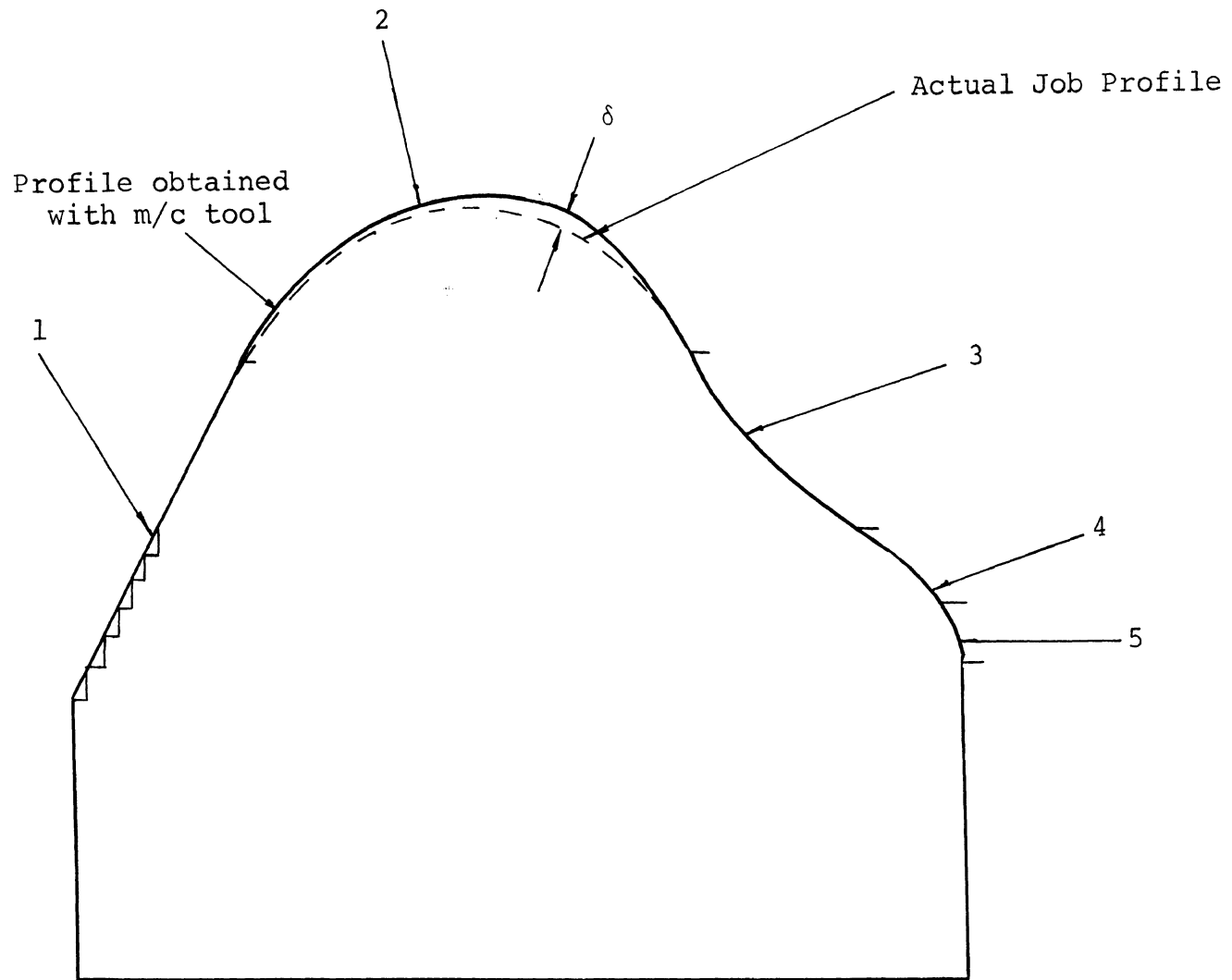


Fig. 2. Typical Cam Profile Machined on Contouring Control

δ is the maximum deviation of the interpolated profile from the actual profile as specified by part drawing where $\delta < \text{tolerance}$ (manufacturing) specified for the job.

This breakup of job contour into various segments, and expression of this data in a form acceptable to m/c tool director, is carried out externally with help of general purpose computer and special routines. It should be recognized here that because in most systems the m/c tool control unit can handle data and emit control signals only in the discrete sense the actual m/c tool travel is in the staircase fashion shown in Fig. 2.

Basic N.C. System - In this section a brief description of a typical n.c. unit is presented. The representation has been simplified in order to describe the major elements in the control system and their functions without having to go into the detailed circuitry of the logic unit. However, the references listed^{13,15,16} provide these details and the interested reader is referred to these references.

In line with the above thoughts attention is drawn to Fig. 3 which depicts a simplified version of the "Bendix Dynapath System" which has been successfully used with a number of contouring m/c tools and which in the present discussion can be assumed to be truly representative of this class of control systems in general. With some further simplifications the unit can be used for positioning controls also and therefore no separate figure has been

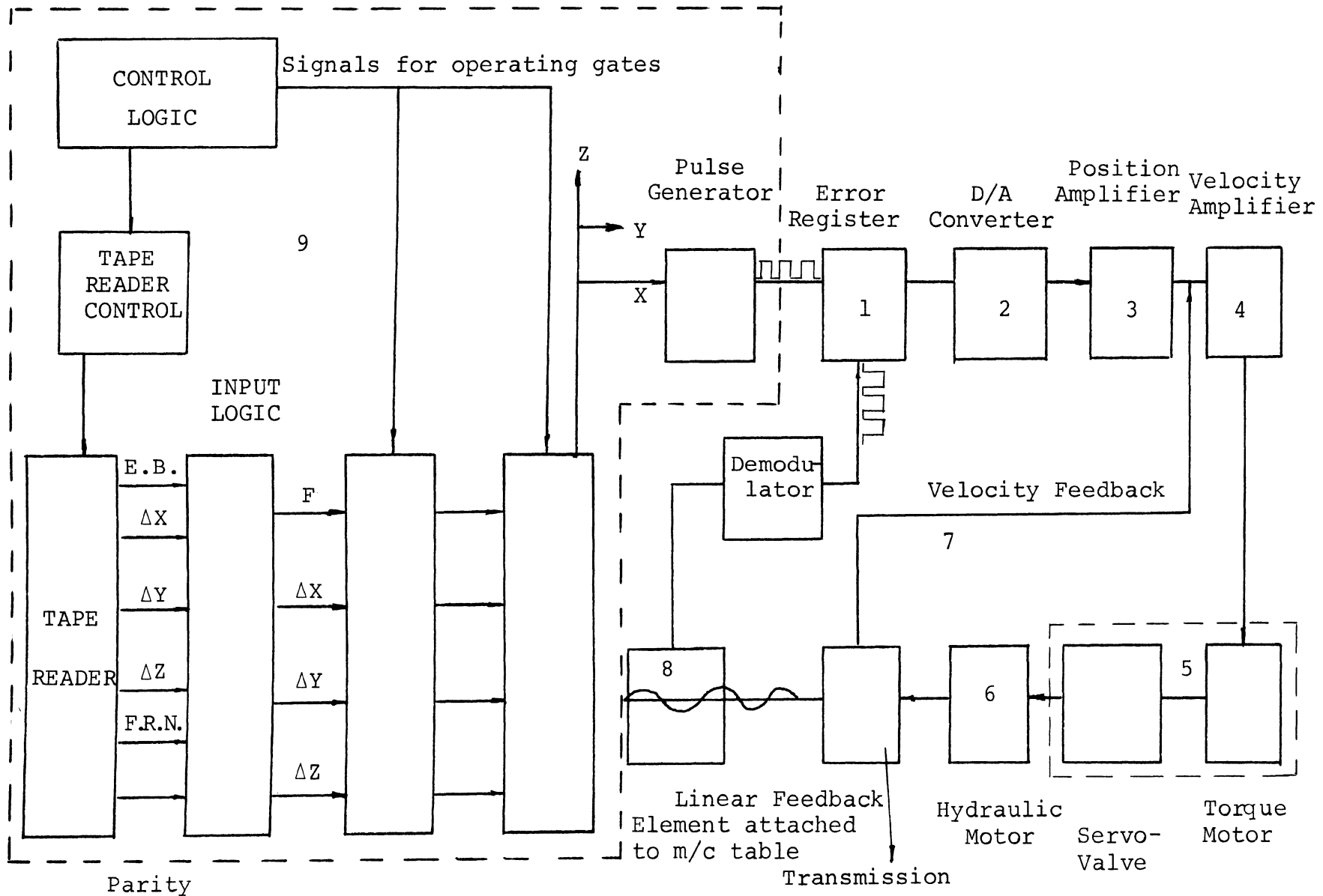


Fig. 3. 'Bendix Dynapath System'

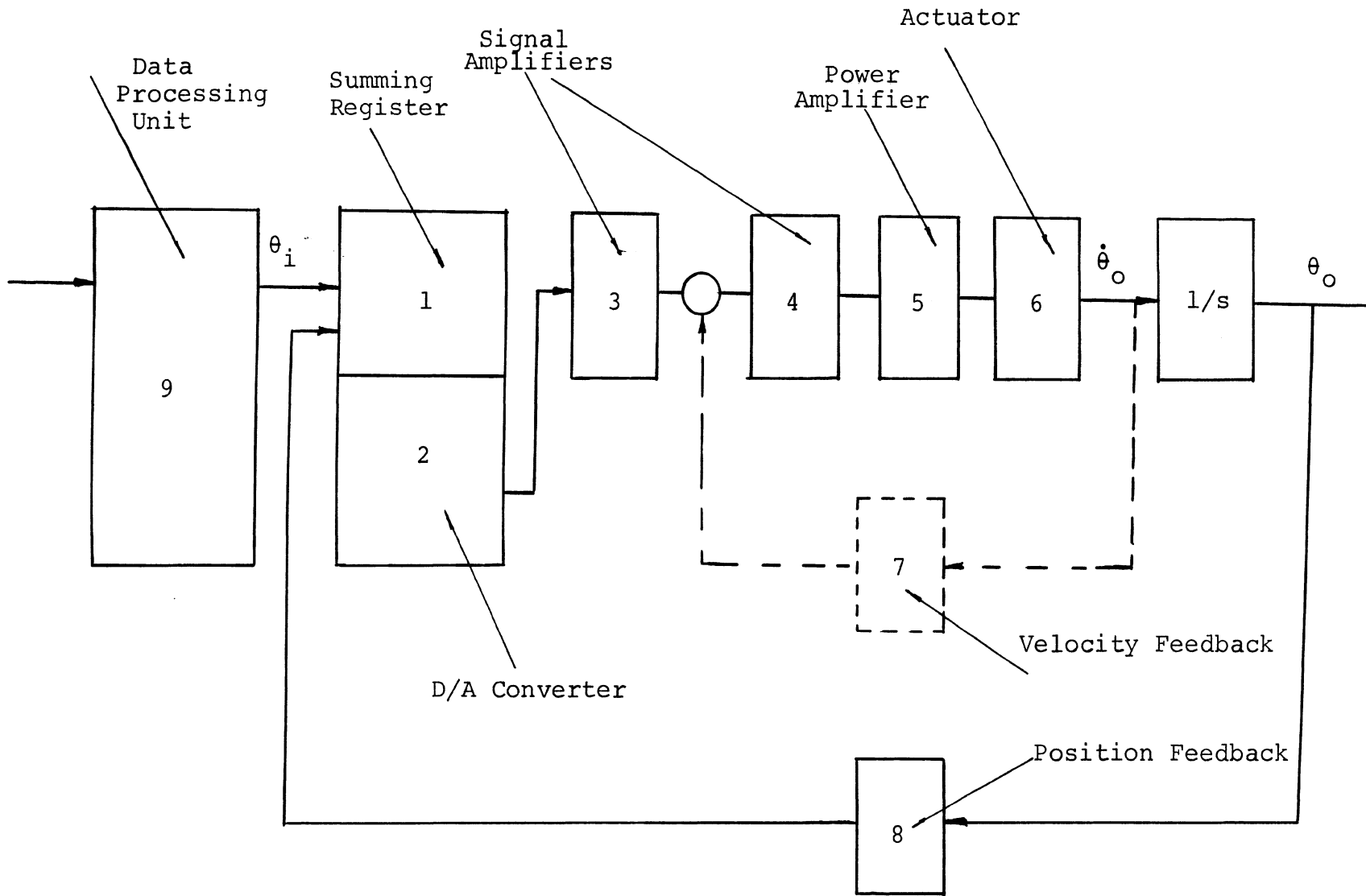


Fig. 4. Block Diagram of a 'Contouring Control System'

presented. Figure 4 shows the same system condensed into a block diagram form more suitable for purpose of analysis. The numbering of the blocks is such that the two figures can easily be correlated.

1. Summing or error register
2. Digital to analogue converter
3. Position error amplifier
4. Velocity error amplifier
5. Power amplifier (hydraulic or electrical)
6. Actuator
7. Velocity feedback
8. Position feedback
9. Director comprising of tape-reader, electronic data processing units and the control processing unit.

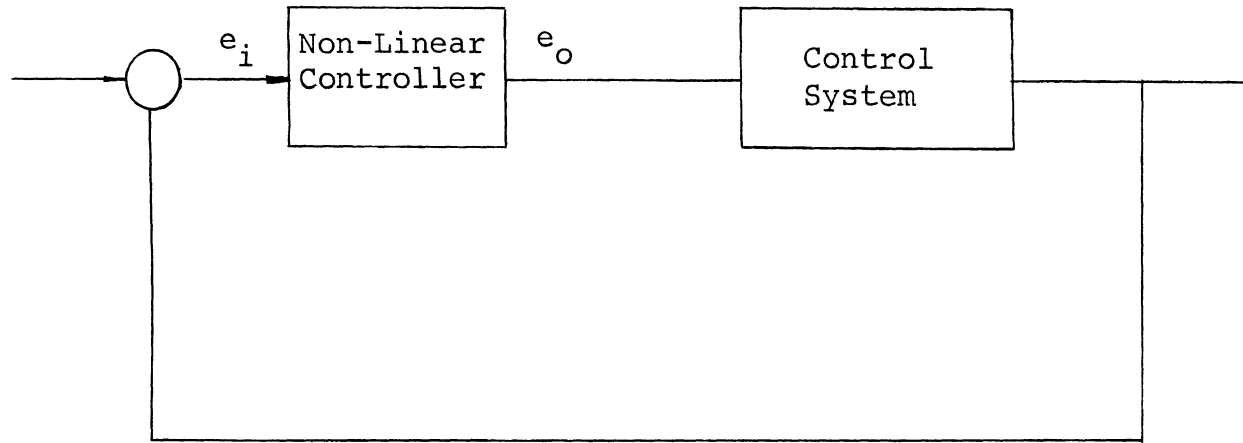
Elements 1 and 2 in combination serve as a digital controller. The input from the control processing unit to the digital controller is a string of pulses whose number and rate is proportional to the programmed incremental command and feed rate. The digital controller accepts command pulses and feedback pulses, each on either a plus or minus line, and develops a continuous voltage proportional to the integrated difference of the two.

Point-to-point systems are similar excepting that no velocity feedback loops are necessary as the cutting is intermittent and during cutting the machine table is always at rest.

The data processing and control functions performed by the m.c tool director (refer to Figs. 3 and 4) start by the photo-electric tape reader reading each programmed block and passing on the information to the temporary stores from where they have to be processed by the logic unit. For positioning systems a complete block of tape which has to be data processed will typically contain:

- a) incremental or absolute commands for the three axes.
- b) preparatory information specifying special stops, time delays, etc.
- c) commands for automatic tool selection from turret.
- d) miscellaneous functions such as speed selection, coolant on-off, spindle direction of rotation, automatic clamping of work piece, etc.

Normally this block of information may be assumed to contain 12 to 20 lines of information of which 8 to 12 lines may be decimal digits specifying the commands for the positioning of the machine table. This block would constitute a complete command and its execution would include the positioning and cutting cycle. The logic functions performed on this input are:



5a

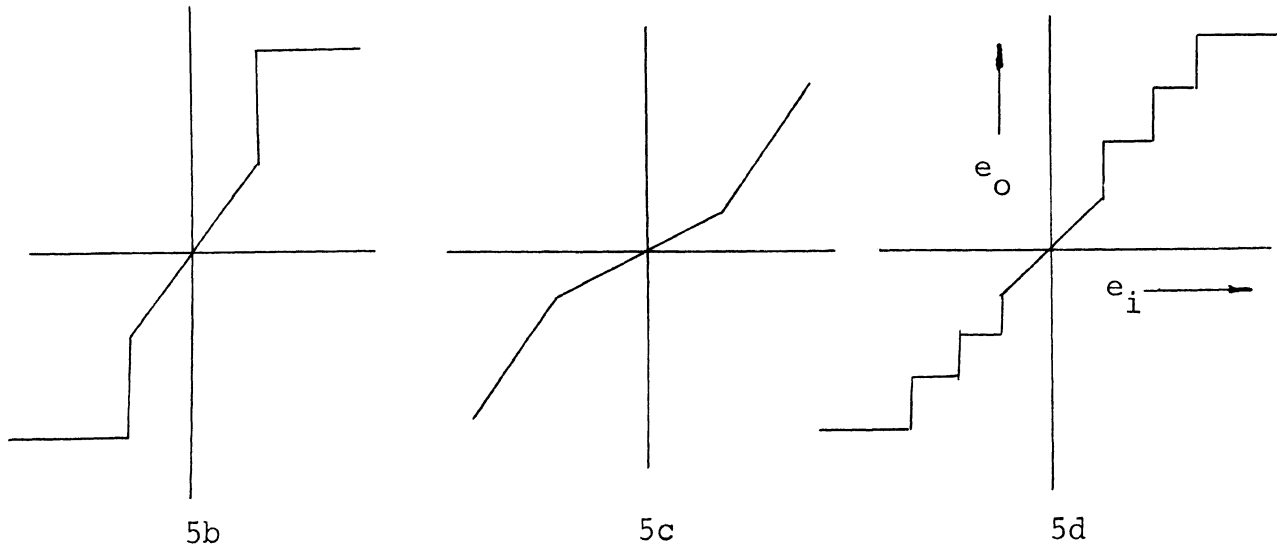


Fig. 5. Types of Non-Linear Controllers for 'Command Point Anticipation'

- a) Interpret various auxiliary commands and send out appropriate signals to m/c tool actuators.
- b) Generate the positioning commands (pulses or voltage) for the three axes.
- c) Automatic adjustments of traverse speeds during a non-cutting, point-to-point movement or commonly referred to as 'command point anticipation'.

For positioning systems this last is the most important logic function to be performed apart from the normal data processing functions. Figure 5 shows the various non-linear controllers which may be used to achieve 'command point anticipation' in positioning systems. For point-to-point systems since the inputs to the control system are always steps this controller is constantly acting on the error inputs to carry out suitable amplification. For obvious reasons controller 5d will probably give the best results. However, because of the number of steps involved the controller required will increase in complexity.

Other methods of achieving this end are discussed in later sections on 'Clutch', 'Contactor', and 'Stepping Type' servomechanisms. In the case of contouring control systems this digital controller is present in the control loop only when the inputs are step inputs which is the case for non-cutting rapid traverse positioning motions. For all cutting motions the inputs are generated ramp functions and at such times this non-linear controller does not form part of the control loop. Thus rapid traverse commands have to be programmed by special codes so as to enable the machine logic unit to distinguish these and channel the error signals through the non-linear controller. For ramp inputs there is a different form of accommodation required which has to be carried out external to the machine, i.e. while programming. This may be termed as introduction of 'acceleration' and 'deceleration' blocks and is discussed in detail in chapter 4.

Compared to point-to-point systems the programmed block for contouring control systems will contain certain additional information such as feed rates etc. Also since the information is for a continuous cutting cycle and the contours have to be represented by line segments or circular segments, each forming one block, the amount of input data will be very much more. In fact where a typical positioning control logic unit may have been handling 20 to 30 bits of information per second, the corresponding

contouring control unit (three to five axes typically) will have to handle up to 15000 bits/sec.

In addition to this tremendous difference in input data processing, the following additional arithmetic operations have to be performed by the logic unit.

- a) Simultaneous linear operation in three axes.
- b) Circular interpolation in one plane which can be changed over to any of the three main planes in accordance with the program.
- c) Cutter radius compensation (facility for automatic compensation of reduction in cutter diameter due to regrinding of worn cutters).
- d) Automatic retardation at corners programmable by special codes.

From the above it is obvious that the logic unit will be much more complex; a fact which is directly reflected in the cost difference between point-to-point and contouring control m/c tools. The latter carry a price tag of average \$65,000 as opposed to \$10,000 for the former.

Types of feed drives for N.C. - In this section brief comments are made on the principal types of feed control systems in use at the present. Although discussion primarily deals with continuous control systems, the concepts are equally applicable to positioning systems also. The most general classification of the different types of feed

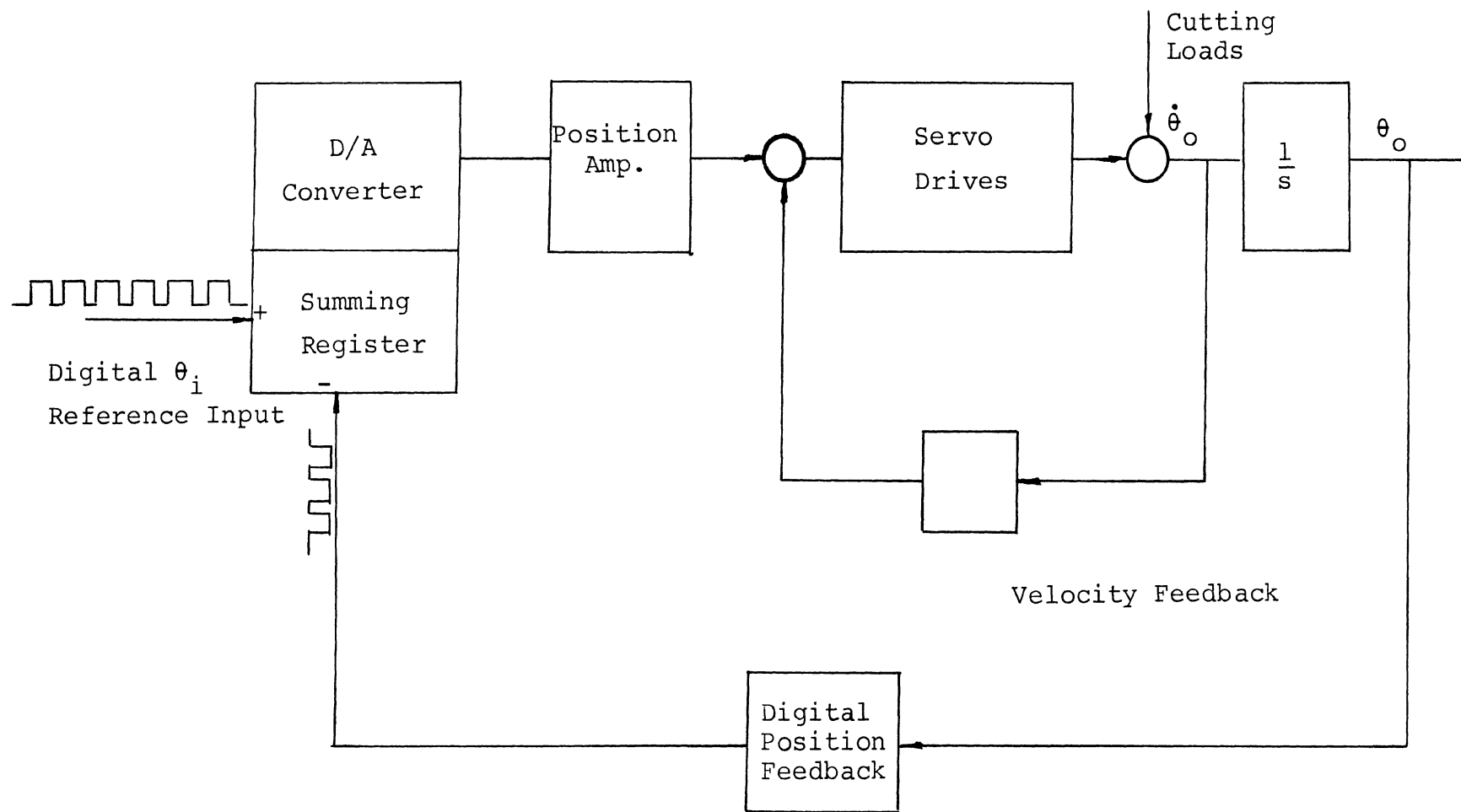


Fig. 6. 'Digital-Analog' System

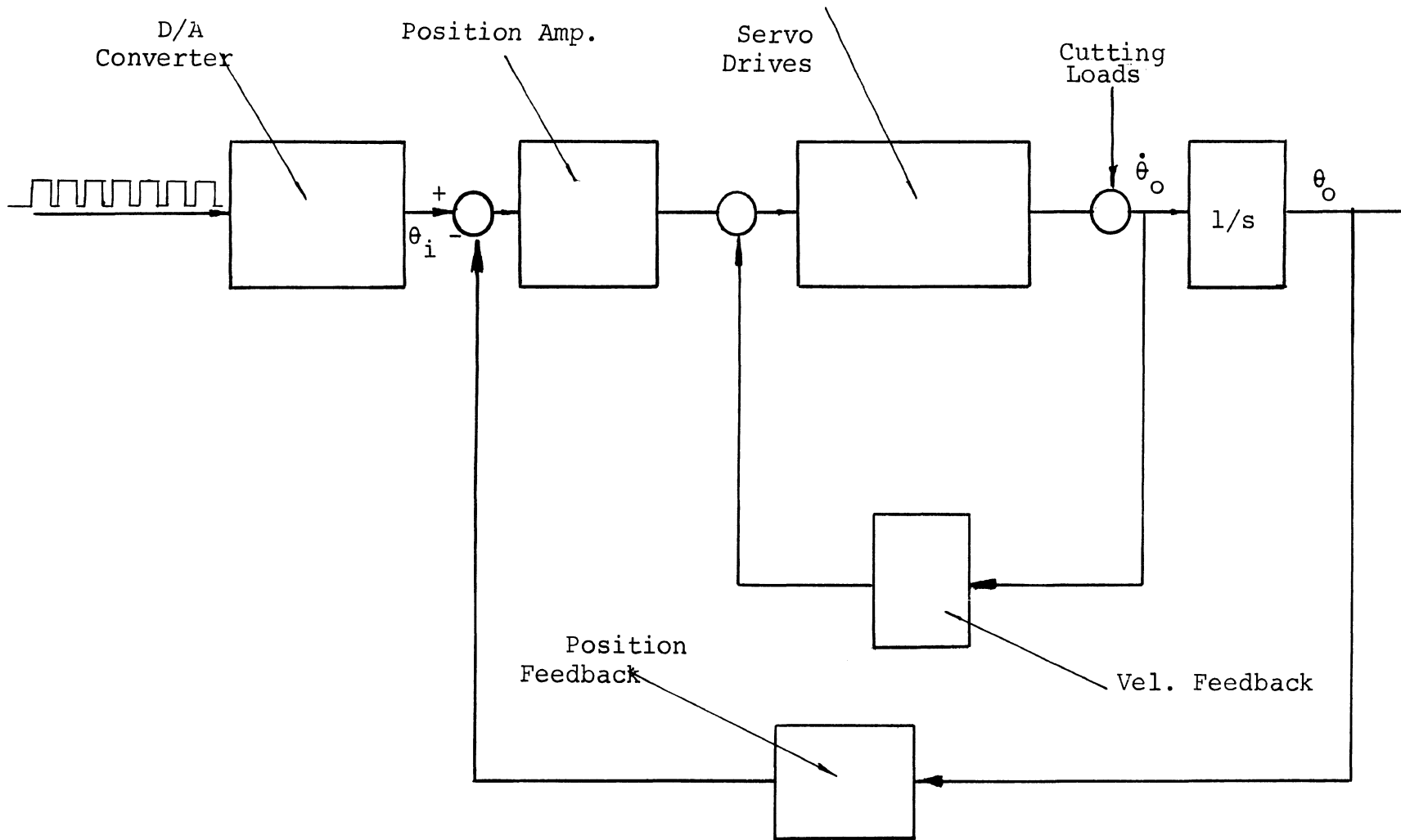


Fig. 7. Analog Systems

drives may be made on the basis of position feedback instrumentation.

Figure 6 gives a schematic diagram of a class of systems grouped under the title of 'Digital-Analog' systems. In these systems the position feedback pickup transmits one pulse for each basic increment of distance moved. Both the input and the feedback to the comparator (error registers) is digital and may be in an absolute or incremental basis. In the case of former the information will be coded thus involving parallel transmission along more than one line which has the advantage of reduced time delays.

By comparison the analog systems of Fig. 7 have the digital-to-analog conversion outside the control loop. Consequently the control loop itself is free of the sampling action of the digital to analog converter. The reference input to the control loop is a continuously varying voltage whose magnitude and rate of change depends on the desired position and feed rate. Interpolators generate continuously changing command information for linear or circular span segments whichever the case might be. The feedback pickups (transducers) consist of an array of rotary transformers and stepless switches analogous to the input interpolators. The difference between the input and feedback voltage levels forms the error signal to the control loop.

None of the above types holds any distinct advantage over the other and therefore it is not possible to credit or discredit either. However, certain appropriate comments can be made on the salient features of both. Theoretically it can be stated that the analog types of feedback being continuous in nature is capable of infinite resolution while the digital type of feedbacks are limited to the incremental distance assigned to each pulse (normally of the order of .0002"). However, in practice, it has been experienced that all the different types of analog pick ups used are subject to drift. Also signal contamination due to noise poses a serious problem. These two factors somewhat cancel any improved accuracy which would accrue from the infinite resolution capabilities. To reduce drift problems these transducers have to be highly precision engineered which results in very high manufacturing costs. The digital form of feedback suffers from the disadvantage of increased switching circuitry. Most manufacturers of N.C. systems tend to favor the digital form of feedback.

To give a better picture a brief description of the various different control systems in use has been included.

'Bendix Path Control System' works on an absolute digital coded feedback. The command pulse is assigned a weight of .0002". The feedback transducer employed is a rotary electromagnetic grating called a quantizer. The actuator is a hydraulic motor coupled to a servo-valve

which together with a constant pressure supply serves as the power amplifier. The error signal is applied to a solenoid which in turn actuates the servo-valve.

'North American Numill Control' is basically same as the Bendix system excepting that the transducer is not rotary but a linear optical grating which modulates the illumination to a semi-conductor photo-electric cell. The optical resolution of the grating coupled with some electrical multiplication gives a pulse weight of .0002" of slide displacement.

The 'Giddings and Lewis Numericord System' has the unique feature of having a logic unit which is completely diversified from the remaining m/c tool control. Thus one logic unit can be used to service a number of m/c tools. The logic unit is fed input on paper tape and it performs the various interpolations and other data processing functions giving as its output a magnetic tape which can be directly fed into the very much simplified m/c control unit. The resolution of this system is .0005". The input to the machine control loop comparator is a phase-modulated command signal. The other comparator input is produced by a feedback synchro rotated by a precision rack attached to the slide of the m/c tool. The comparator output is a D.C. voltage proportional to the sampled instantaneous displacement error between command and feedback. The power amplification is with an amplidyne which runs a d.c. motor,

the latter operating the machine slide drive.

The 'Cincinnati Acramatic System' is probably the only prominent one operating on an analog principle. The voltages correspond to absolute slide positions and both feed forward and feedback elements consist of rotary transformers, electronic scanners and stepless switching. The power amplifier and actuator are hydraulic.

We end this chapter with some brief remarks on the choice of actuators and associated drives for the machine slides. The two most common types of actuators are hydraulic motors, both rotary and linear, and electric motors. A third type which have found limited application are stepping motors.

Electric actuators are mostly variable speed armature controlled d.c. motors in which the amplified error signal is fed to the armature winding thus producing a proportional torque at the motor output. The amplification of the error signal is carried out in two stages. The error signal voltage is stepped up with some form of static amplifiers (push-pull transistor amplifiers etc.) while the major power amplification is by means of rotary amplifiers such as amplidynes, metadynes etc.

Common types of hydraulic actuators are cylinder piston combination (linear operation) and rotary motors. The power amplification is provided by a servo-valve and constant pressure supply fixed displacement pump combination.

Linear hydraulic actuators are restricted in use with m/c tools having short stroke requirements. This limitation is imposed because the mass of oil under compression behaves like a spring mass system and the greater the mass the lower the associated natural frequency. Also the greater the mass of oil to be handled the larger the pipes etc. The net effect is the response of low order resonant frequencies in the servo-control loop which lead to increased instability.

Comparing hydraulic actuators with electric ones the following distinguishing features should be noted.

- a) Hydraulic drives are characterized by their fast response and small time constants as compared to equivalent power electric drives.
- b) These are capable of transmitting power at low r.p.m. thus requiring fewer gear trains on the output side. This results in a substantial reduction in the possible backlash and compliance in the control loop thus giving a much better servo performance.
- c) Generally these have better torque to inertia ratios.

Some of the major disadvantages associated with these drives are higher cost, servo-valve drift and oil cooling and filtration problems. For most work of limited accuracy and for powering large m/c tools electric drives are adequate. Where high precision work is involved and where the additional cost can be justified hydraulic actuators are used.

On the question of type of drives for the machine slides it is adequate to mention that for most work the rotary motor with lead screw and nut combination are employed. For machine tools having long travel it is normal to use rack and pinion type drives as the use of former would-be coupled with problem of compliance of long lead screws.

III. SERVO SYSTEMS ANALYSIS

For contouring control applications by far the most commonly used drive mechanisms are electro-hydraulic servo-systems. Consequently the major part of analysis has been restricted to these. However, it needs to be pointed out that the design method followed can well be adapted for feed drives having electrical actuators or any other form of hydraulic actuators. Also, as mentioned earlier, positioning systems are simplifications of the contouring type hence the analysis technique can well be applied to these.

There are, however, three types of position control systems which cannot be covered by the method of analysis developed here. For the sake of completeness brief reference to these has been included. The drive systems for these can be broadly categorized as 'Incremental Servos', 'Clutch Servos' and 'Contactor Servos'. All these have found limited application in numerical positioning control.

A. Incremental Servos

These are characterized by the use of stepping motors as actuators and by the fact that these are essentially open loop systems. For each input pulse the output shaft of the stepping motor assumes a new increment of angular position. A one-to-one correspondence of output shaft position to input signals results from the use of

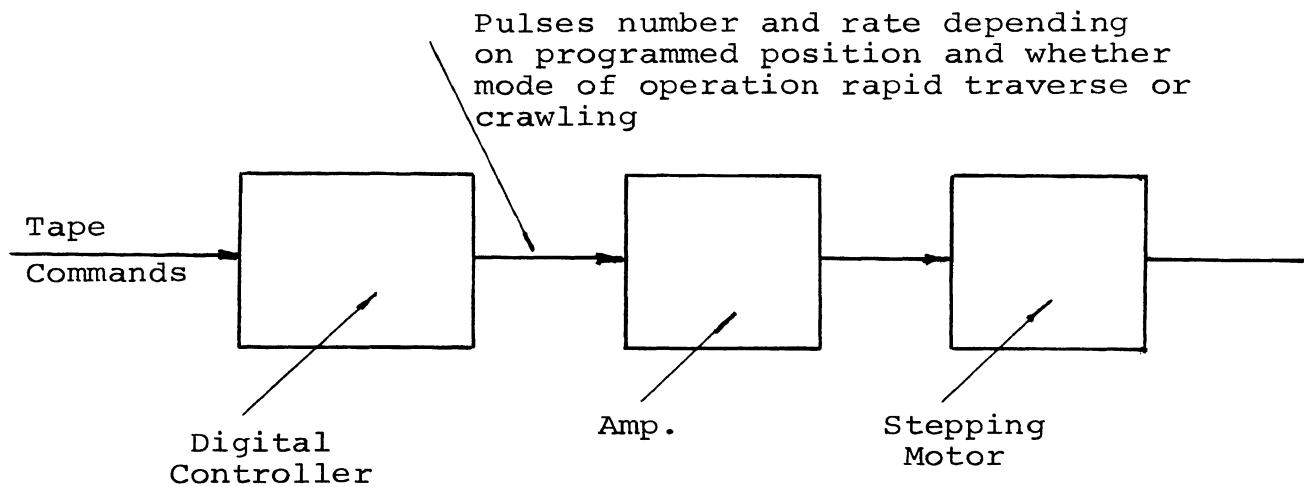


Fig. 8a. Control Loop for 'Positioning Control' Employing Incremental Servos

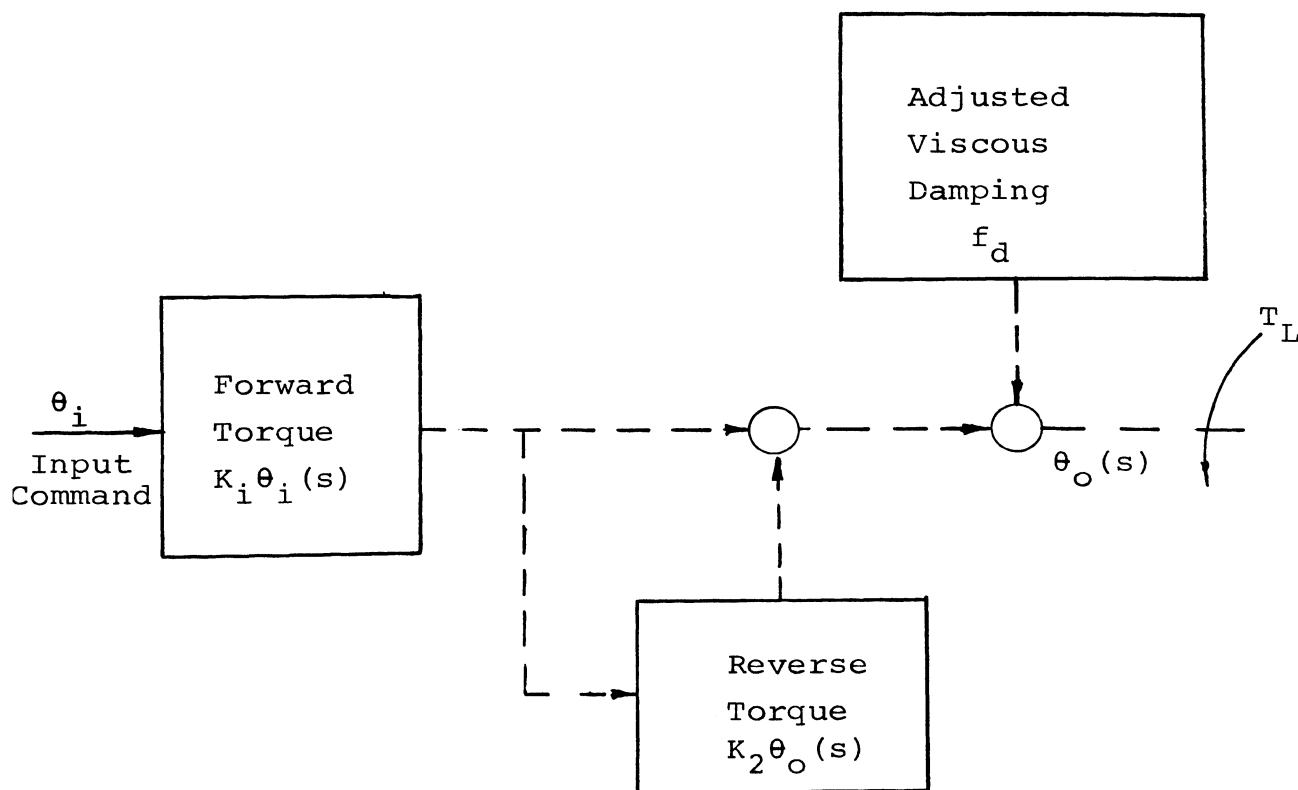


Fig. 8b. 'Stepping Motor' (Electrical) Characteristics

some kind of detenting (electrical or mechanical). The increment speed of the output shaft is directly proportional to the input pulse rate. The motor derives its linearity from a carefully designed mechanical or electrical detenting which results in an exact discrete shaft advancement for each input pulse. Linearity is maintained provided the input pulse rate stays within the performance capabilities determined by the fundamental time constant. Chief limiting factor is the frequency response as the stepping motor is capable of responding satisfactorily only up to a limited input pulse rate.

The block diagrams of Figs. 8a and 8b give the basic operation for this class of servos. As soon as a forward driving torque is applied (on receipt of a pulse) the motor begins to simultaneously generate a reverse stepping torque. When net torque on output member reaches zero, it gets damped to zero velocity. Motor dynamics can be expressed as

$$K_1 \theta_i(s) - K_2 \theta_0(s) = [J_t s^2 + (B_m + f_d) s] \theta_o(s)$$

or

$$\frac{\theta_o(s)}{\theta_i(s)} = \frac{K_1}{J_t s^2 + (B_m + f_d) s + K_2}$$

As can be seen the transfer function for response to a pulse input is analogous to the response of a continuous input servo. Obviously f_d and B_m must yield a damping

ratio which will cause the device to settle in a sufficiently quiescent state before the start of a new step cycle.

Another type of actuator in use with these control systems is the 'Electro-Hydraulic' pulse motor shown in Fig. 9. The electro-hydraulic pulse motor is distinguished from the conventional electro-hydraulic servo in several ways.

- 1) It accepts pulses instead of analog commands.
- 2) A stepper motor controls command signals instead of the usual solenoid or torque motor.
- 3) The rotary pilot valve closes an internal feedback loop and meters oil.
- 4) The motor is in the same housing as the valve providing good hydraulic stiffness.

For each command pulse received to the ring circuit it produces three output pulses which in turn are amplified and drive the stepping motor. The gear train output shaft turns through a fixed increment for each command pulse.

The advantage of this arrangement is the internal feedback achieved by mechanically coupling the hydraulic motor output shaft to the pilot valve sleeve. The difference between relative angular position of core and sleeve represents servo error. Thus steady state velocity errors will depend on amplitude of input velocity and the operation of the loop may be considered analogous to the conventional velocity servos working on continuous inputs. Within load and response limits this actuator performs well

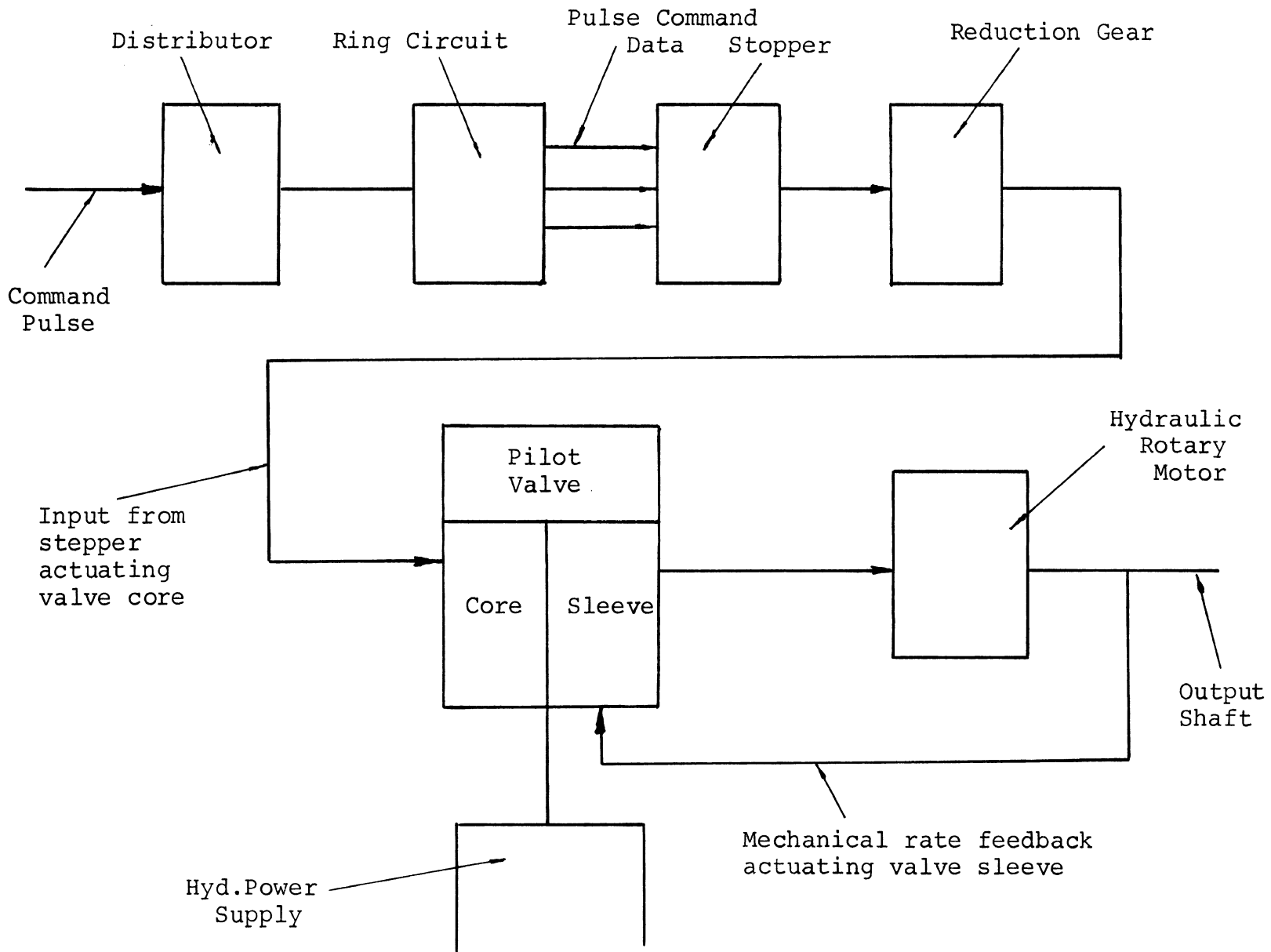


Fig. 9. Block Diagram of 'Electro-Hydraulic' Pulse Motors

and eliminates the need for both external digital-to-analog converters and feedback instrumentation.

B. Contactor Servos

In the present context these can be said to form the basis for a class of digital-to-analog type numerical controls. Theoretically these are important because of the applicability of an optimization criterion. Physically this type of servo system is characterized by a switching mechanism (controlled by the digital controller) which allows either maximum positive or maximum negative torque to be applied at its output as a discontinuous function of the system error. Figure 10a shows the block diagram representation of the principle elements. The actuator is a field controlled d.c. motor. The digital controller acts on the system error and switches the motor field current from a maximum value in one direction of flow to a maximum value in the opposite direction.

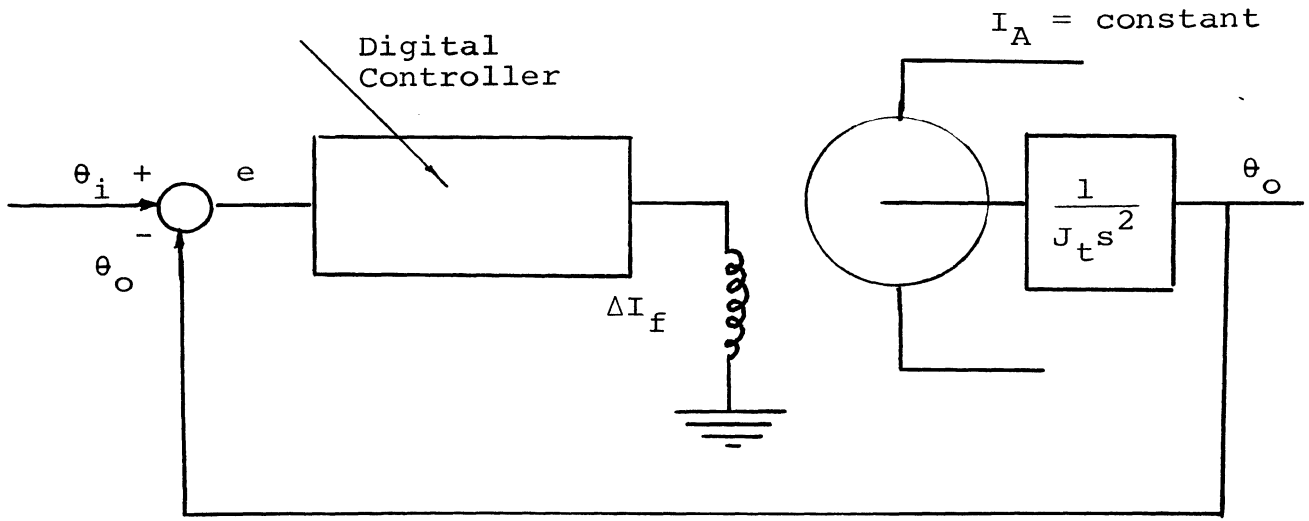
Neglecting the time constant of the motor field and output damping, the system equations are

$$\begin{aligned} e &= \theta_i - \theta_o \\ T_m &= J_t s^2 e \end{aligned}$$

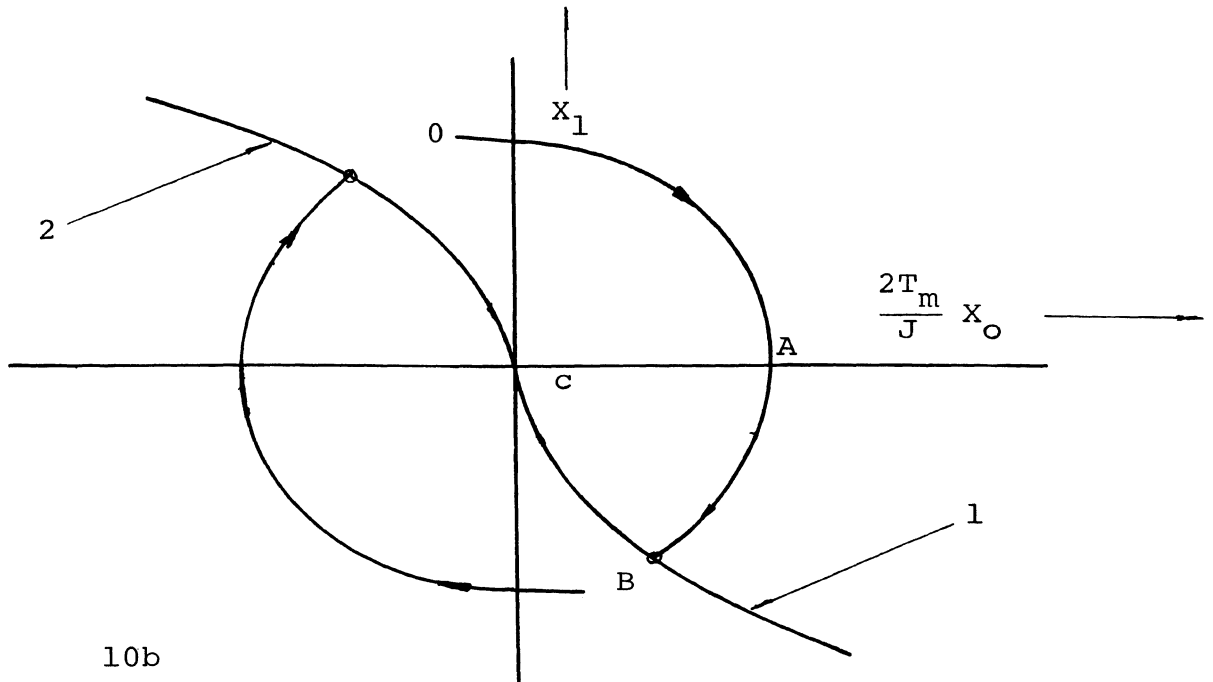
or for this ideal system the governing differential equation is

$$s^2 e = -\delta T_m / J_t$$

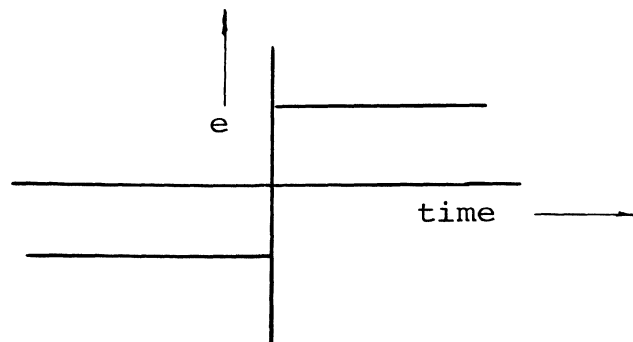
where $\delta = \pm 1$ and is termed the switching function.



10a



10b



10c

Fig. 10. Contactor Servomechanism Operation

Defining $x_0 = e$ and $x_1 = Dx_0 = De$ as the state variables the phase plane equations are

$$Dx_1 = -\delta T_m/J_t$$

$$Dx_0 = x_1$$

from which we can further write

$$x_1 dx_1 = -\delta \frac{T_m}{J_t} dx_0$$

and integrating we get

$$\frac{x_1^2}{2} = -\delta \frac{T_m}{J_t} x_0 + K$$

where K - constant of integration.

The phase portrait of this servo consists, therefore, of two families of parabolas (since $\delta = \pm 1$) all having vertices on the x_0 axis as shown in Fig. 10b. Hopkins* has demonstrated that the optimum switching criteria

$$\delta = +1 \text{ for } x_1 |x_1| + 2 \frac{T_m}{J_t} x_0 > 0$$

and

$$\delta = -1 \text{ for } x_1 |x_1| + 2 \frac{T_m}{J_t} x_0 < 0$$

will carry the representative point directly into the origin without any overshoot. Curves 1 and 2 on the phase portrait are the optimum switching curves. Path ABC represents the

*Hopkin, A.M, A Phase Plane Approach to the Compensation of Saturating Servomechanisms, Trans. AIEE, Vol. 70, Part I, pp 631-39, 1951.

the error, error-rate response of the system to a step input of position and path DABC gives the time history for a step input of velocity.

The point to be noted is that for such an ideal servo only one switching operation is necessary for the representative point to reach the origin regardless of its starting position. Also since the servo is operating at maximum acceleration or deceleration at all times, its response will be optimum for second order systems.

For practical systems to be operated on the above principles certain factors, which impose serious limitations on the ideal case, should be noted.

1. Since the final optimum switching phase trajectories for positive or negative output torque always pass through the origin of the phase-space, the system at equilibrium finds itself in an oscillatory state where its output torque is continually being switched back and forth from maximum positive to maximum negative values.
2. Where the plant transfer function is of a higher order the optimum switching criteria become increasingly complex. In general the n th order system requires ' $n-1$ ' switching criteria to reduce its error and the $n-1$ st derivatives

to zero simultaneously. Thus the controller required becomes increasingly complex for higher orders.

3. The switching criteria are functions of the system parameters; small changes in these parameters will introduce errors into the switching program which get magnified as the order of the system increases. Parameters which influence these changes are output friction, load inertia etc.

To circumvent the problem of steady state oscillations about the null point two different approaches have been tried. The first approach is to introduce a dead zone of operation near the region of zero error. Thus the controller output is of the form shown in Fig. 10c. The disadvantage is the increased position error which has to be accepted. Another method which has been found more satisfactory in practice is to switch the servo over to a linear mode of operation when in the vicinity of the origin of its phase space. Disadvantage is the increased complexity and cost of the control system.

C. Clutch Servomechanisms

These are mostly employed for position controls and their major advantage lies in the ease with which these can be arranged to provide speed control in discrete steps.

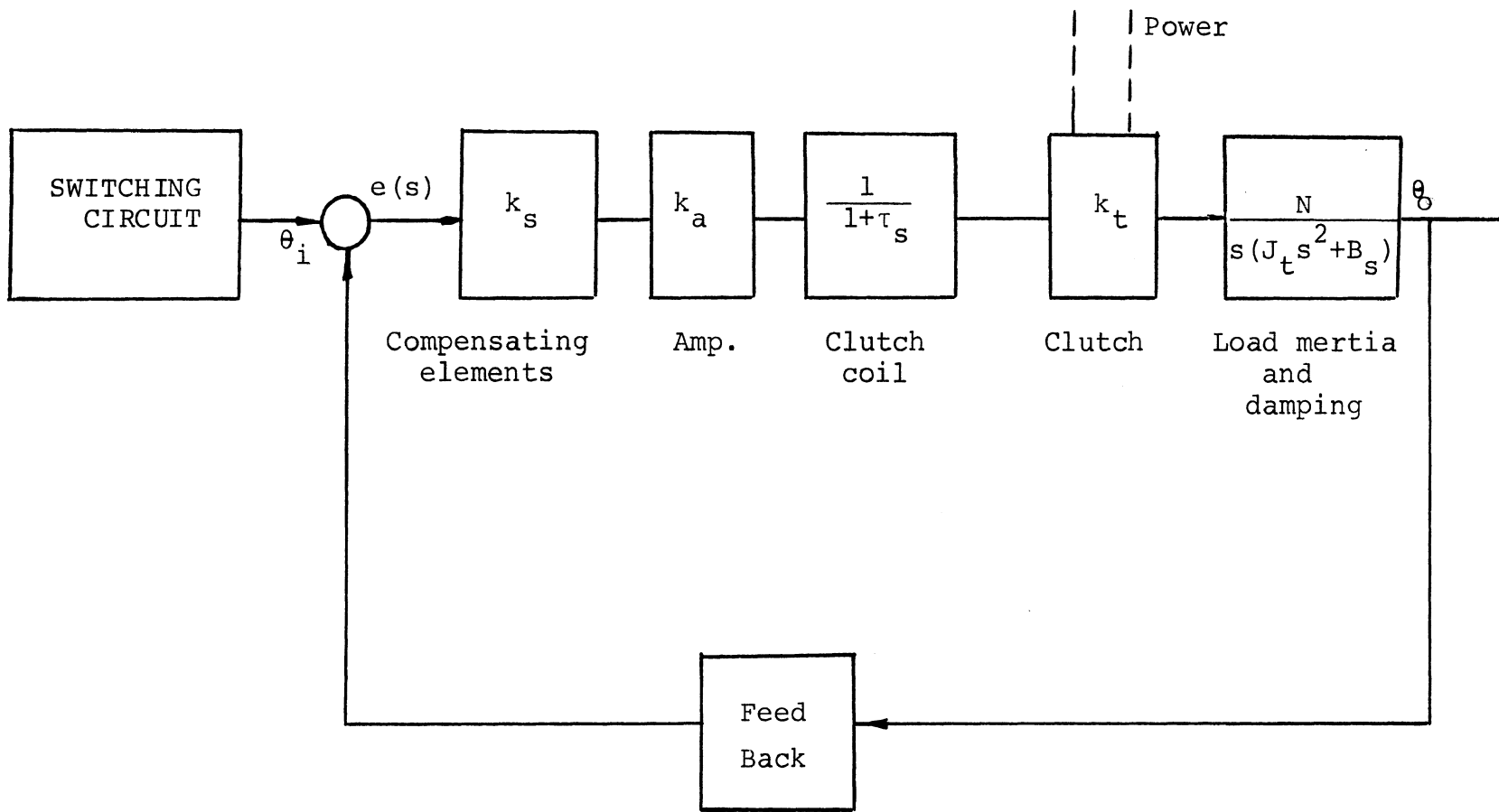


Fig. 11. Clutch Servomechanisms

Thus depending on the number of clutches employed the rapid traverse speed of positioning may be stepped down in a number of discrete steps to an ultimate 'crawling rate' as the targeted position is approached. This speed reduction is essential to avoid machine table overshoots which unnecessarily result in hunting of the servo about its null position.

In general this class of servo-mechanisms employ a clutch or clutch brake combination for the actuator. The power source for the system is a constant speed electric motor. The clutch acts as a torque transmitter and controls the coupling between the constant speed drive motor and the load. A servo-amplifier (electrical) controls the clutch, and the degree of coupling between the input and output shafts is proportional to the magnitude of the error signal. The clutches employed for m/c tool controls are categorized as non-linear because of the on-off nature of operation and the most commonly used ones are the friction disc variety.

A non-linear clutch servo has a relay type of operation. The clutch is operated either full off or full on. When the error signal is above the threshold magnitude, the clutch is fully engaged, and delivers full torque to the load. The performance of this type of system can be improved by employing a clutch brake combination. Figure 11 is the block diagram of a typical system.

The overall transfer function is

$$\frac{\theta_o(s)}{e(s)} = \frac{K_o N K_t}{s(1+\tau s)(J_t s^2 + Bs) + K_o N K_t}$$

where $K_o = K_a K_s$

N = gear transmission

K_t = represents the nonlinearity since the clutch is transmitting only when the signal is above a threshold value. This operation is similar to the one shown in Fig. 9c excepting that each clutch has a linear mode of operation.

We now come to the three major types of servo drives which are most commonly used in conjunction with precision m/c tools both positioning and contouring. The following sections contain the block diagram representation for these systems. The step by step derivations have been presented in the appendix.

D. Linear Electro-Hydraulic Servo

The major elements in the control loop are

1. Position error amplifier
2. Solenoid (torque motor)
3. Hydraulic power amplification consisting of servo valve supplied by constant delivery pump which maintains a constant pressure input to the valve.
4. Double ended piston-cylinder which is the actuator.

5. Position feedback transducer.

The typical transfer functions are represented in the block diagram of Fig. 12 and for derivation of the same the reader is referred to Appendix A sections 1 and 3. The following points of importance, in connection with the above representation, may be noted.

In writing expression for the load it has been assumed that force developed by servo is used for acceleration of the mass and in overcoming viscous friction loads. No spring type loads have been taken into account. Although these will normally be present in the form of compliance of the piston rod etc. these are of a negligible nature so that the mechanical members in the power transmission loop can be considered to be rigid bodies. However, in simulating the system on the computer, this term may also be included and the effects studied.

Servo-valve orifices have been assumed matched and symmetrical. In practice most will have a slight underlap. However, this assumption has no detrimental effect on the analysis, and the simplified transfer function represented above are the ones almost always used in practice for design purposes.

The expressions representing the servo-valve action are linearized ones as is the normal practice. The normal designed operating range is such that these linearized equations represent the action satisfactorily. However

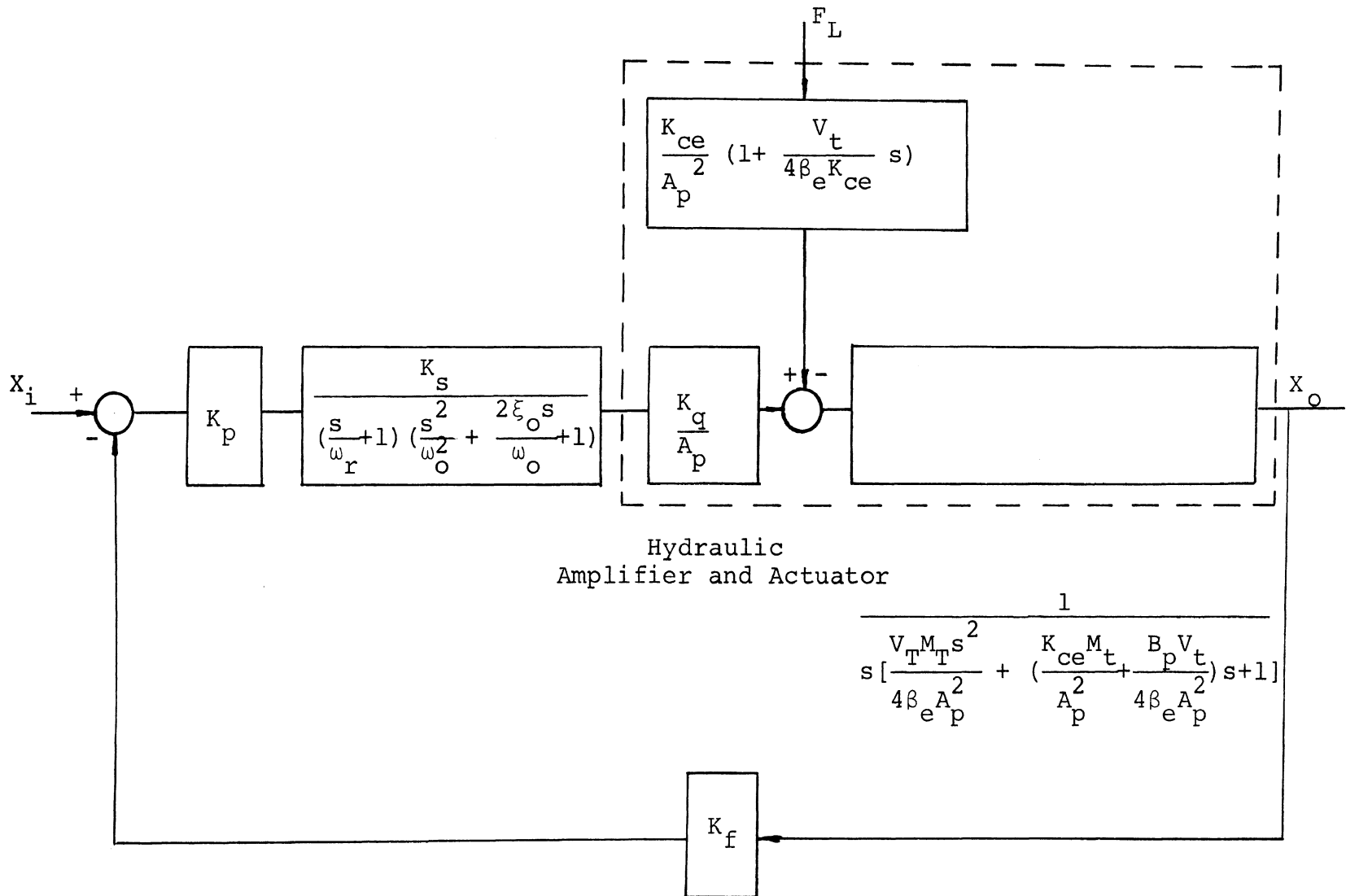


Fig. 12. Linear Hydraulic Servo Motor

it should be mentioned here that the actual flow equation may be simulated on the computer. For most m/c tool applications, the external loads which can cause changes in operating conditions are quite small as compared to the inertia of the table and therefore saturation conditions are very rarely encountered in practice.

The above comments are equally applicable to rotary hydraulic servos.

E. Electric Servos

The block diagram in Fig. 13 is for an armature controlled d.c. motor operated system. The power amplification is provided by a motor (constant speed) - generator set typically referred to as a Ward-Leonard drive. For development of transfer functions reader is referred to Appendix B. The following additional comments should be noted.

The Ward-Leonard is one of the many types of rotary amplification systems possible. The other commonly used forms are the 'amplidyne' and 'metadyne'.

Figure 14 shows the block diagram for a Ward-Leonard drive. As can be seen there is no closed loop dependence. Because of this two of the commonest problems are:

1. Changes in load torque result in changes in speed which are reflected all the way back to the a.c. motor.
2. Variations of the line voltage and frequency will cause variations in speed of the a.c. motor, and ultimately variations in load speed even when external torque is constant.

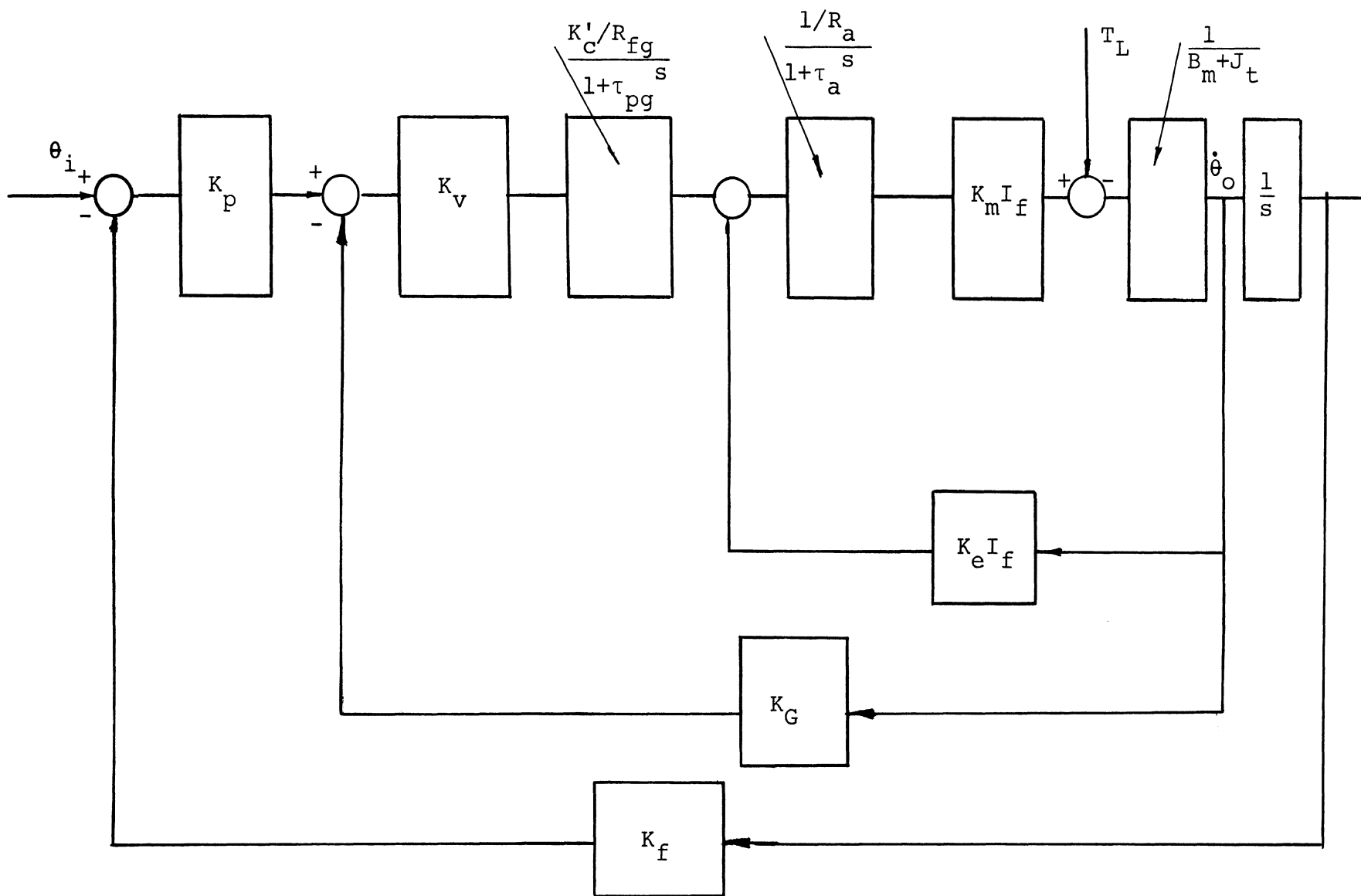


Fig. 13. Electric Servo System

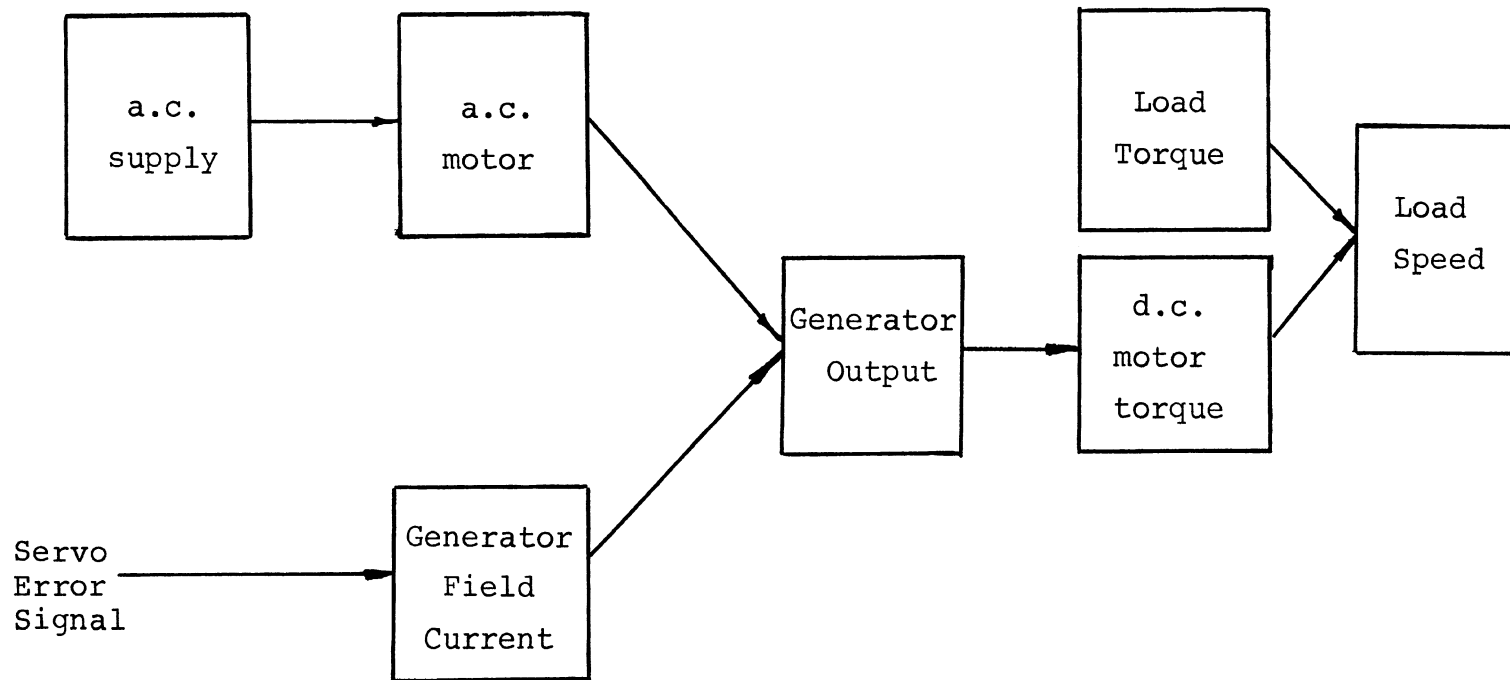


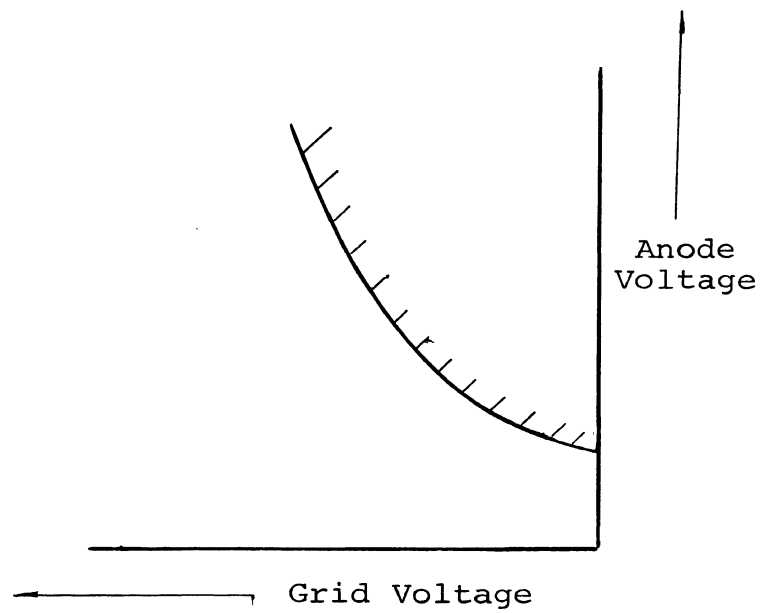
Fig. 14. Ward-Leonard System

Amplidyne is equivalent to two normal generators connected in cascade with the armature of the first feeding the field of the second. Transfer function can be expressed as

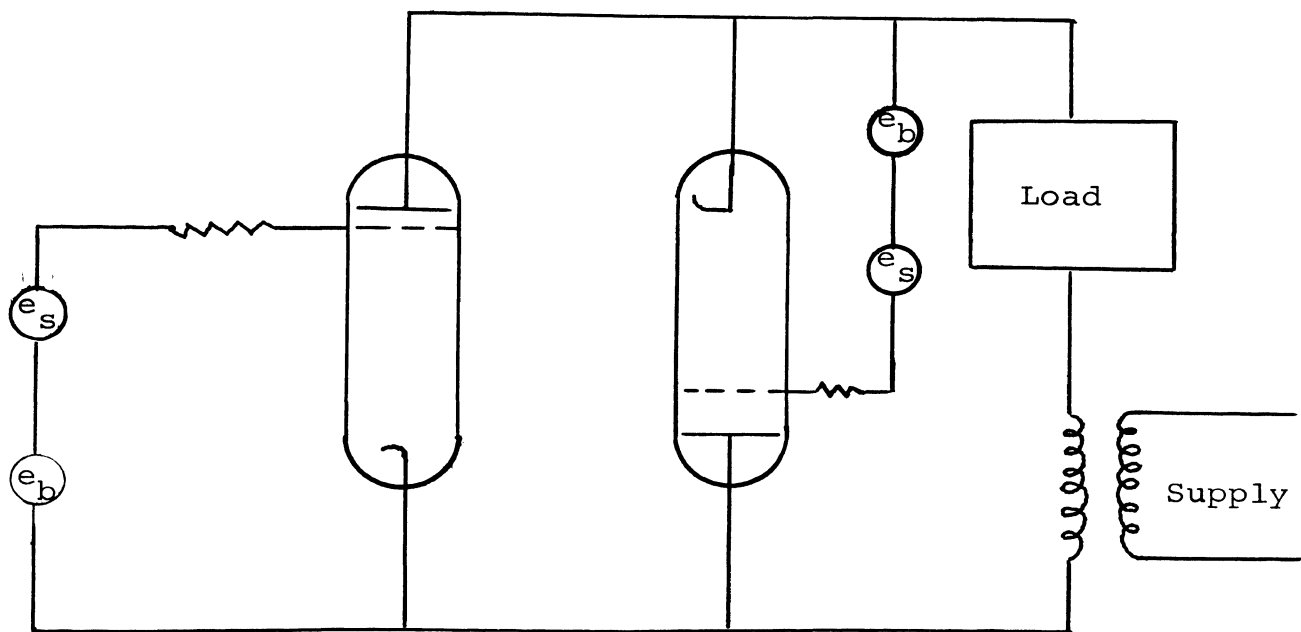
$$\frac{e_o}{e_i} = \frac{K}{(1 + \tau_1 s)(1 + \tau_2 s)}$$

For constant excitation it produces a constant voltage output. The transient performance is effectively that of two simple time lags in cascade. The time constants τ_1 and τ_2 may be quite large and for this reason it is normal in using an amplidyne to provide externally a minor feedback loop around the machine to increase the rapidity of its response. Metadyne is essentially the same as the amplidyne excepting that this has overall series negative feedback. For constant excitation it tends to produce a more or less constant output current. The effect of overall negative feedback is to improve response and to reduce overall gain.

In addition to the rotary forms of power amplification described above servo systems also employ static type of power amplifiers of which the most common is the 'thyatron'. These are simply gas filled tubes. Figure 15a shows the common control characteristics of a thyatron. If at any time the anode voltage, being +ve relative to cathode, and the grid voltage are such that the operating point crosses to the shaded side of the curve than the valve 'strikes' i.e.



15a



15b

Fig. 15. Thyatron Operation

starts to conduct. Once conduction has started the grid loses control and the only method of extinguishing the arc is to reduce the anode supply voltage below the burning voltage, and allow sufficient time for the gaseous ions to recombine before the anode potential is again allowed to become positive. Control of the thyatron is effected by any one of the following ways

1. d.c. control zero bias
2. d.c. control a.c. bias
3. a.c. control a.c. bias
4. phase shift control
5. pulse control.

For servo applications a circuit arrangement such as shown in Fig. 15b has to be used so that control of current can be effected in either direction. Considering the load to be a motor the circuit is so set that only one of the thyratrons is allowed to conduct and control the current, the other is permanently non-conducting until direction of motor is reversed.

Signal Amplifiers - In the present context these are the position error and velocity error amplifiers shown in the control loops. Commonly used type are the vacuum tube or transistor amplifiers. Since signal amplification of the order of several hundred is sometimes required a number of units have to be cascaded. Certain amount of

tube stabilization by internal feedback is also desirable. The common forms of tube arrangements used are listed below.

1. Cathode feedback
2. Cathode coupled amplifiers or the push-pull type

A common problem associated with these is the drift which is invariably present. The gain characteristics keep varying with use. Drift is mainly due to the changes in d.c. supply voltage, heater voltage and changing properties of the tubes with time and ambient temperatures. One way to circumvent this problem is to have a.c. coupled amplifiers so that inter tube couplings do not pass drift effects from one stage to another.

F. Rotary Electro-Hydraulic Servos

For most precision contouring control applications this is the form of drive most frequently employed and for that reason the detailed design carried out in this paper is for such a system. The basic control loop is similar to the one presented for linear hydraulic actuators with the exceptions that the receiving unit is now a rotary motor and an additional velocity feedback loop is added. The common type of rotary motors in use are the gear, valve and piston type. Of these the piston type has the lowest internal leakage and therefore is generally more acceptable.

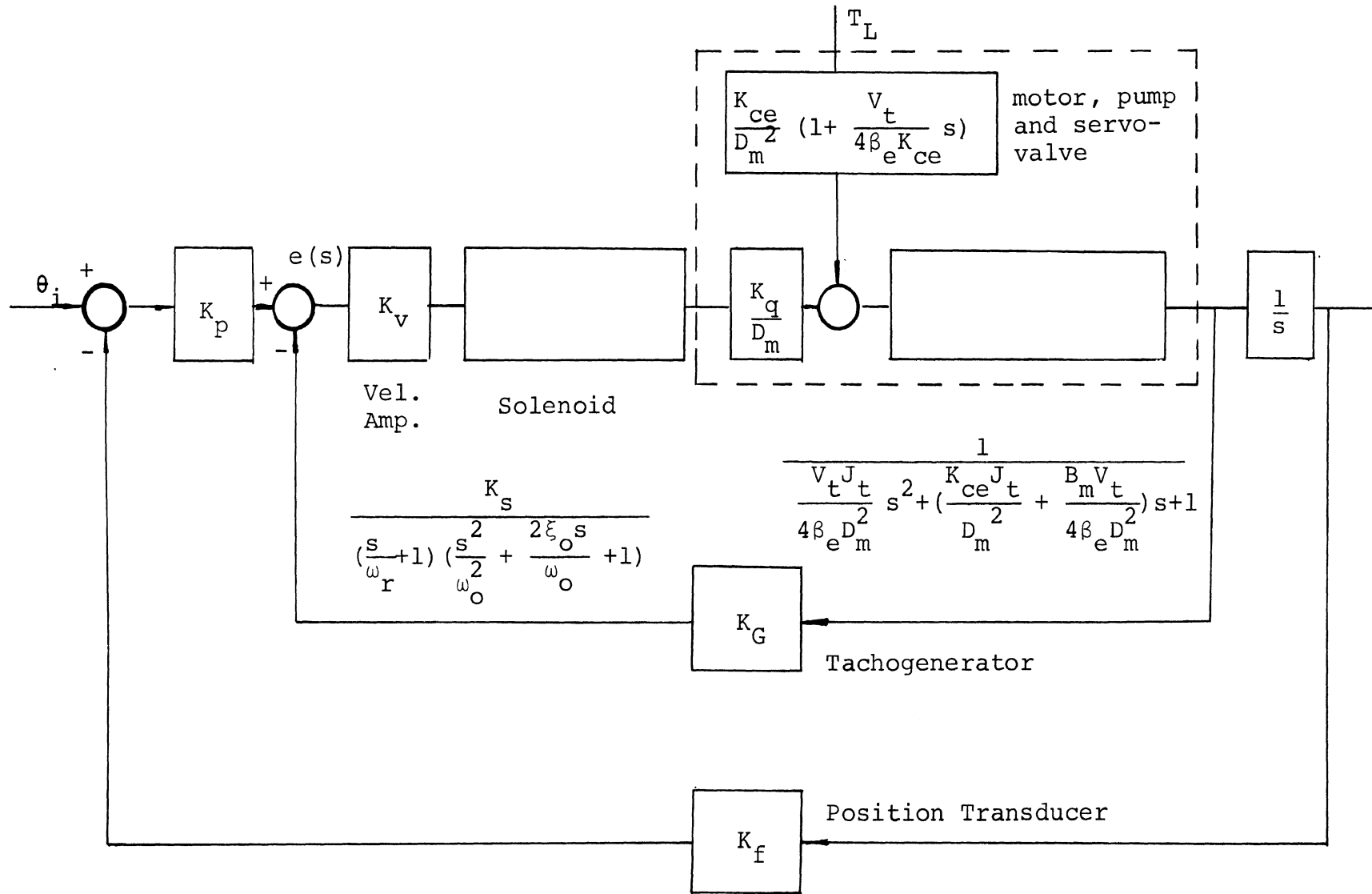


Fig. 16. Electro-Hydraulic Servo System with Rotary Motor

The basic block diagrams and transfer functions are shown in Fig. 16. For derivation of transfer functions refer to Appendix A, sections 2 and 3.

IV. SERVO-SYSTEM SYNTHESIS AND DESIGN

In the last section of Chapter III the three most common types of control systems have been discussed. It should be noted that for all the cases the representation has been for analog type systems. This might appear quite strange, especially in light of the remarks made earlier, that most systems tend to be the D/A type. This omission is of no consequence as the method of analysis does not differ. The D/A type systems will be characterized by a quantizing element in the feedback loop and a digital to analog converter in the feed forward part. Figure 17 shows the block diagram for a typical D/A contouring control loop. It can be seen that the basic amplification and actuation is exactly the same as for the system depicted in Fig. 16.

For the system shown the command pulse generator generates pulses for each axis of motion. The number of pulses generated for each axis is proportional to the distance the machine slide must move. The pulse rate is proportional to the slide speed. The accumulated difference between the command and feedback pulses is sampled periodically and converted into an analog error signal. In the steady state the analog signal will approach the velocity error between the command and feedback. Depending upon the velocity constant for the loop this may be as low

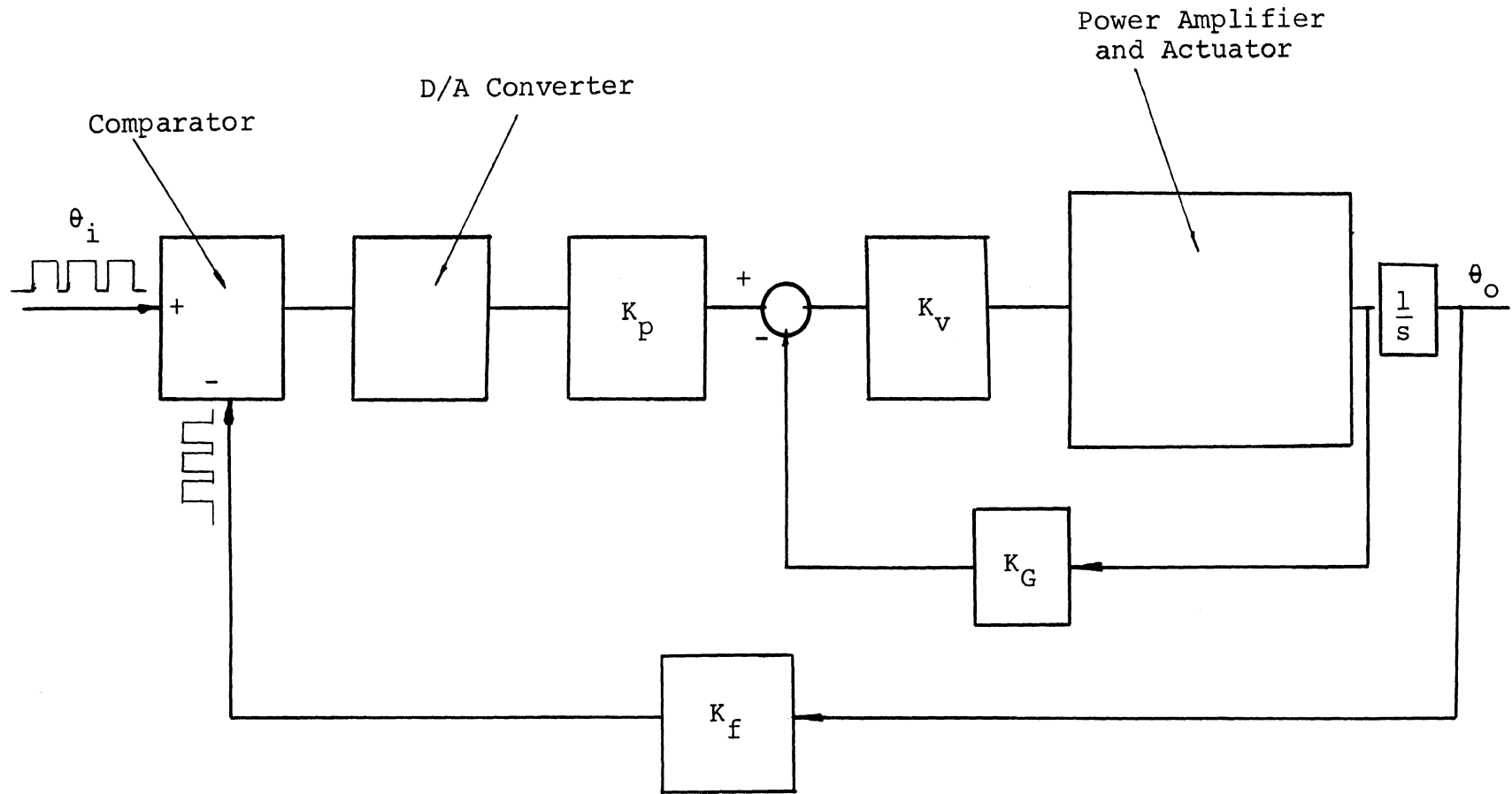


Fig. 17. Digital-Analog Contouring Control System

as corresponding to two or three pulses.

Many investigations carried out in the past seem to lead to the conclusion that the quantizing element in the feedback does not significantly effect the behavior of the closed loop. The quantizers may therefore be considered to behave linearly without introducing any lag in the system. Therefore the transfer function of the feedback element can be a simple constant. These points are amplified a bit further in a later section. With these brief comments we now proceed ahead with the design of a control servo having the configuration of Fig. 16.

Before embarking on the detailed design it is necessary to lay down the specifications which we expect our control system to meet. Broadly speaking the system must be stable and also must exhibit an optimum transient performance. In addition, it must successfully meet the accuracy requirements imposed by the inherent properties of the controlled process. For the system to be stable the functional relations between the coefficients defined by the Routh-Hurwitz criterion must hold. Also for our purpose it is preferable that both the entire system as well as the inner velocity loop be stable independently. In the present context the following specifications will be seen to cover the above requirements adequately.

A. Frequency Domain Specifications

- a) $M_{\text{peak}} = \left[\frac{C(j\omega)}{R(j\omega)} \right]_{\text{max}}$ - defined as the maximum value of the closed loop transfer function. This specification has the property of placing restrictions on the worst possible steady state response to periodic inputs. Also it can be related to the transient response of the system. A value of 1.3 has been empirically found to be acceptable for most applications and is retained for our purpose.
- b) Bandwidth - is defined as the range of frequencies between zero and the frequency corresponding to which the normalized closed loop transfer function has the magnitude .707. In deciding a suitable value two conflicting arguments have to be considered. For the system to exhibit a sufficient speed of response for ramp inputs the B.W. specification must cover the highest input ramp frequency that is likely to be encountered. On the other hand, if noise and secondary resonances are likely to be present, then the B.W. specification must be such as to guarantee a sharp cut off of all noise and structural resonances. Keeping in view the normal m/c tool characteristics a reasonable value of B.W. is 275 radians/sec (50 c.p.s.)

B. Time Domain Specifications

Commonly used parameters are delay time (T_D), rise time (T_R), settling time (T_S), percentage overshoot, damping characteristics, etc. Choice of specific design variables for optimization of transient response depends completely on the criteria which are applied in judging how well the output follows the input. A general form of measure of transient 'goodness' is the function

$$E = \int_0^{\infty} F[e(t), t] dt$$

where 'F' is some function of error $e(t)$ and time 't'.

Some of the well known special cases of the above are

$$E = \int_0^{\infty} e^2(t) dt$$

$$E = \int_0^{\infty} e(t) dt$$

$$E = \int_0^{\infty} |e(t)| dt$$

$$E = \int_0^{\infty} t |e(t)| dt .$$

None of these has universal applicability and the choice is dictated by the type of response which is termed optimum by the designer. A common approach is to carry out the optimization of a number of such indices and then select one which gives the best transient for the specific 'case in hand'. This selection can easily be accomplished with the help of an analog computer.

Lastly, to meet the accuracy and sensitivity requirements it is necessary to specify the appropriate error constants. For the type 1 system in question it is necessary to indicate the 'velocity constant' which will determine how closely a ramp input is followed by the system.

The following basic assumptions have been made in laying out the design procedure which follows.

1. Load is rigidly connected to motor shaft
2. Amplifier and transducer dynamics are negligible in comparison to load dynamics
3. Supply pressure to valve is constant
4. No losses in pipes etc. outside those taken into account in developing the transfer functions.
5. In an actual control loop the feedback signals are taken from the machine slides. This results in the inclusion of a number of mechanical elements in the control loop. In all typical set ups the mechanical design of the various machine members is such that their natural frequencies of vibrations are well above the crossover frequency of the open loop response, which in turn effectively limits the bandwidth of the servo. Thus for the dynamic analysis all these elements can be effectively ignored.

6. For the sake of simplicity the gear transmission ratio has been taken as unity. This in no way effects the dynamic analysis carried out. It should be noted, however, that in arriving at the value of J_t the reflected inertia of the load has to be included and therefore, to this extent, the transmission ratio does feature in the representation in the figure on page 52.

By appropriate choice of units the block diagram of Fig. 16 can be easily reduced to the form shown in Fig. 18. In carrying out this simplification the effect of T_L has been neglected. For preliminary design work this is a perfectly valid assumption. The magnitude of T_L under normal operating conditions will not exceed 10% of the torque developed by the motor.¹ The idea therefore is to develop the design without considering T_L . After the design has been completed the effects due to T_L may be studied during the simulation stage. The simplification of the block diagram to an equivalent unity feedback system enables us to consider the position and velocity loops separately. The units for various parameters of Fig. 18 will be as shown

$$K_p' = K_p/K_g \times K_f \quad \frac{\text{rad/sec}}{\text{volts}} \times \frac{\text{volts}}{\text{rad}} = 1/\text{sec}$$

where K_p is a constant.

$$K_v' = K_v K_g \quad \text{volts/rad/sec.}$$

Since gearing ratio is assumed unity K_f may be considered as unity. Thus the scaling of the input reference signal

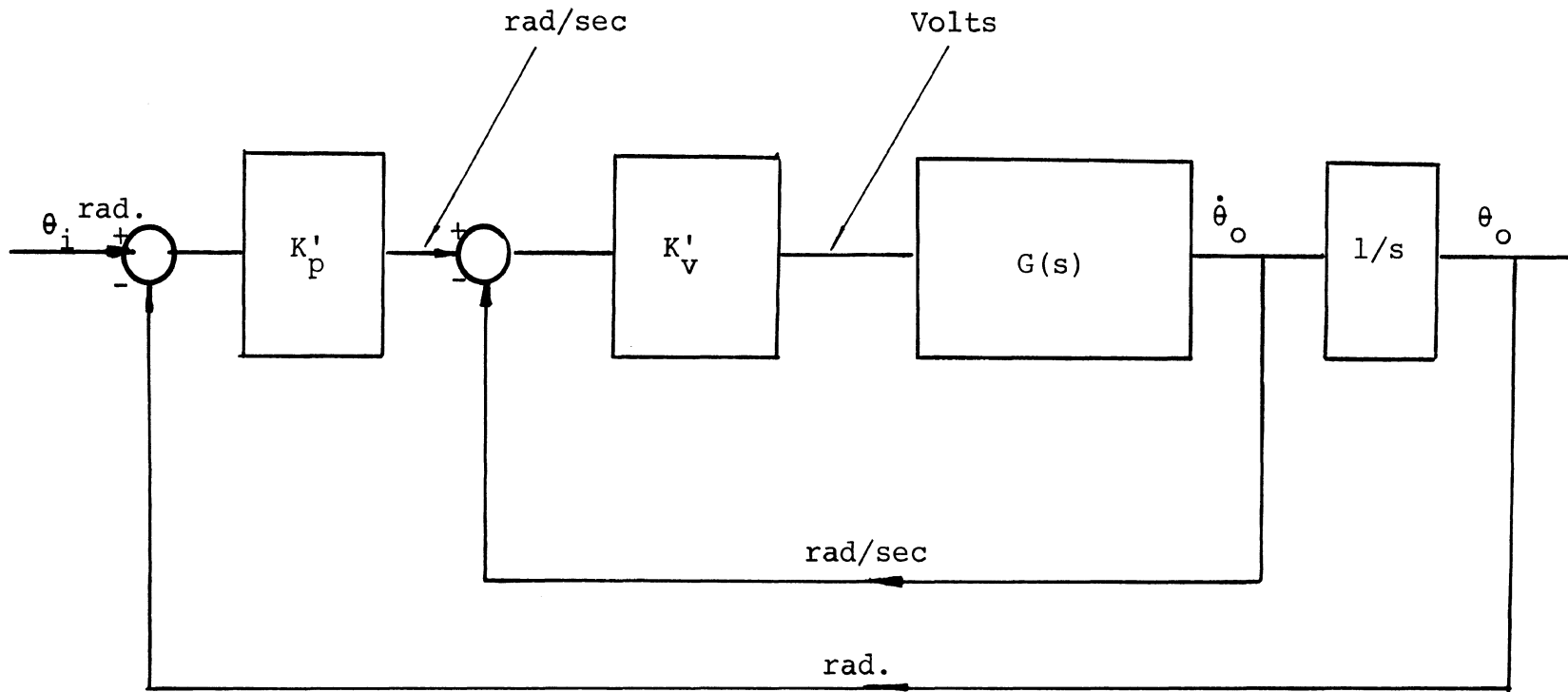


Fig. 18. Equivalent Unity Feedback System

is assumed such that 1 volt represents 1 rad. of angular movement of lead screw.

$G(s)$ is lumped transfer function for torque motor and actuator.

The overall transfer function for the block diagram can be expressed as

$$\begin{aligned} \frac{\theta_o}{\theta_i} = T(s) &= \frac{K_p' K_v' G(s)/s}{1 + K_v' G(s) + K_p' K_v' G(s)/s} \\ &= \frac{K_p' K_v' G(s)/s}{1 + G(s) K_v' (1 + K_p'/s)} \end{aligned}$$

Defining sensitivity w.r.t. plant characteristics as S_G we have

$$S_G = \frac{1}{1 + G(s) K_v' (1 + K_p'/s)}$$

Now $G(s) K_v' (1 + K_p'/s) \gg 1$ (true for all feedbacks), therefore

$$|G(s) K_v' (1 + K_p'/s)| = 1/S_G$$

or

$$|G(s) K_v' + G(s) K_v' K_p' s| = 1/S_G \quad (1)$$

To satisfy the general performance requirements laid down earlier, i.e. the velocity error should be less than .001" for input commands up to 5 inch/min (normal feedrates for contouring) the velocity constant C_v for the loop should be

$$\frac{5}{C_v \times 60} = .001$$

or

$$C_v = \frac{5}{.001 \times 60} \approx 80 \text{ for preliminary design.}$$

Since by definition velocity error coefficient for this system is

$$C_v = \lim_{s \rightarrow 0} s [k'_p \frac{K'_v G(s)}{1 + K'_v G(s)}] 1/s$$

therefore

$$\lim_{s \rightarrow 0} \left\{ \frac{K'_p K'_v G(s)}{1 + K'_v G(s)} \right\} \approx 80 \quad (2)$$

Thus equations (1) and (2) define the criteria for sensitivity and steady state accuracy of the control system and these can be used to make a preliminary estimate of system gains.

On the basis of sensitivity criterion we can state that a desirable sensitivity value of .1 of 1 percent²¹ would minimize the effect on the overall transmittance of variations in plant characteristics. Thus from Equ. (1)

$$\left| G(s)K'_v + \frac{G(s)}{s} K'_v K'_p \right| = \frac{100}{.1} = 1000$$

or

$$\left| G(s)K'_v (1 + K'_p s) \right| = 1000$$

$$\left| G(s)K'_v K'_p \right| = 1000 \quad \text{since } K'_p \gg 1$$

It is desirable that the velocity loop have a fast response so that any feed rate variations caused by cutter loads are quickly compensated. Also the major drift characteristics are normally in the velocity loop thus necessitating a high gain.

Based on these criterion a preliminary choice of $|G(s)K'_v| = 300$ is made which gives $K'_p \approx 3.33$. Thus it can be stated that the sensitivity requirements will be adequately met if $K'_p > 3.33$. Now equation (2) defines the gains on the basis of the need for a high velocity constant. Since $K'_v G(s) = 300$ and 1 in the denominator can effectively be neglected which gives us

$$K'_p = 80 > 3.33$$

These, therefore, are the magnitude of gains desirable to meet the two basic requirements imposed on the system. Our next job therefore is to consider the stability criterion for the system i.e. the tendency of the system to come to rest after termination of the input signal. Before it is possible to carry out any stability analysis, it is necessary to substitute actual values for various time constants and natural frequencies in the control loop. Since this paper is primarily concerned with establishing design procedures it is sufficient for our purpose to assume typical values for these parameters. A number of different sources in literature were used to obtain these typical values.

C. Torque Motor Constants

Transfer function for this element derived in Appendix A is

$$K = \frac{K_s e_g}{(s/\omega_r + 1) \left(\frac{s^2}{\omega_o^2} + \frac{2\xi_o}{\omega_o} s + 1 \right)}$$

The frequency response characteristics for typical torque motors are as shown in Fig. 18 and it can be seen that

ω_r - for typical elements is 15 c.p.s. or 95 rads/sec

ω_o - natural frequency of moving members is of the order of 125 c.p.s. or 775 rads/sec.

K_s - gain is typically of the order of 10

Thus for our design purposes, choosing these values and noting that the 2nd order term has effectively a very high crossover frequency well beyond the expected bandwidth of the servo, we can safely reduce the transfer function of the solenoid to

$$K = \frac{10 e_g}{(1 + 1/95 s)} = \frac{10 e_g}{(1 + .0105s)}$$

D. Motor, Pump and Valve

Appendix A section 2 gives the transfer function for these elements as

$$\theta_o = \frac{(K_g - D_m) x_v}{s \left(\frac{s^2}{\omega_n^2} + \frac{2\xi_1}{\omega_n} s + 1 \right)}$$

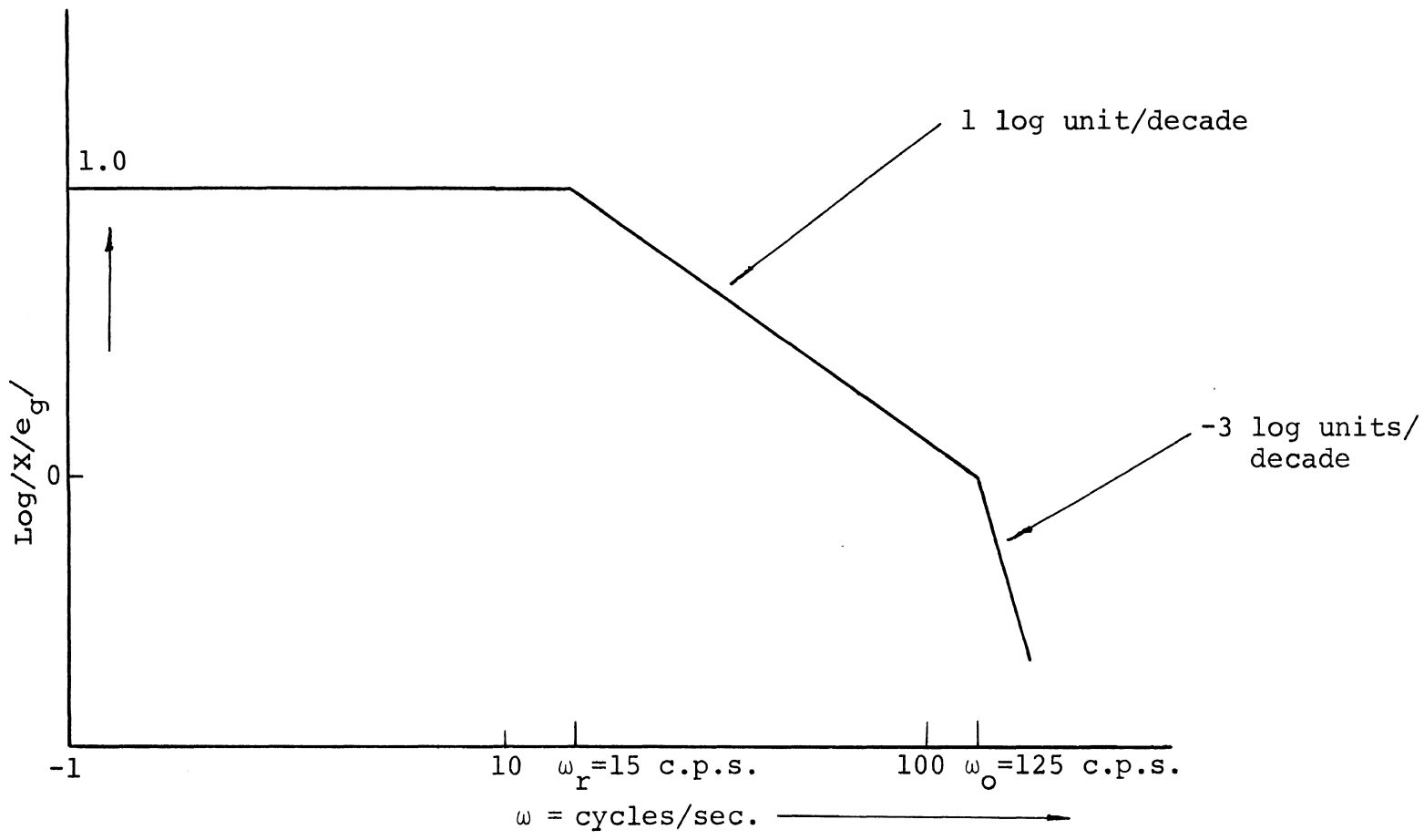


Fig. 19. Typical Open Loop Response for Torque Motors¹⁸

where

$$\omega_n = \left(\frac{4\beta_e D_m^2}{V_t J_t} \right)^{1/2}$$

is the undamped natural frequency typically referred to as the "hydraulic natural frequency" and is due to the interaction of the inertia with the trapped oil springs and this establishes the overall response of the valve motor combination. Typical values for a 1/2 h.p. unit, sufficient for feed drive of one axis, will be

$$\beta_e^{18} = 100,000 \text{ p.s.i.}$$

$$J_t^1 = \text{inertia of motor and gearing and reflected inertia of machine table weight, designed job weight and lead screw inertia is } .120 \text{ in-lbs-sec}^2$$

$$D_m^6 = .053 \text{ in}^3/\text{rev for motor operating at } 1000 \text{ r.p.m.}$$

$$V_t^6 = .30 \text{ in}^3$$

Substituting these values we get

$$\omega_n = \sqrt{\frac{4 \times 100,000 \times (.053)^2}{.3 \times .120}} = 125 \text{ rads/sec.}$$

Also typically the computed values of ω_n are some 40% or so higher than measured values.¹⁸ Therefore for design purposes the value of ω_n may be taken to be ≈ 75.0 rads/sec which is roughly 12 cycles/sec. ' ξ_1 ' is defined as the hydraulic damping ratio and is

$$= \frac{K_{ce}}{D_m} \left(\frac{\beta_e J_t}{v_t} \right)^{1/2} + \frac{B_m}{4D_m} \left(\frac{v_t}{\beta_e J_t} \right)^{1/2}$$

A typical value of $\xi_1 = 0.5$ may be assumed initially.

K_q - valve flow gain and is defined for a fixed pressure drop across the orifice, normally 1000 p.s.i., as flow rate p.u. axial movement of spool. This constant can be obtained from the operating curves of the valve. For our purpose it is adequate to assume that $K_q/D_m = 1$.

Thus substituting the values for these various constants we get the block diagram of Fig. 20. This is the control loop which has to be subjected to a stability analysis. Figure 21 shows the block diagram obtained by eliminating the inner velocity loop. From this figure

$$\frac{\theta_o}{\theta_i} = \frac{10K'_v K'_p}{s[(1+.0105s) \left(\frac{s^2}{75^2} + \frac{1.0s}{75} + 1 \right) + 10K'_v] + 10K'_v K'_p}$$

The characteristic equation for this transfer function is

$$s[(1+.0105s) \left(\frac{s^2}{75^2} + \frac{s}{75} + 1 \right) + 10K'_v] + 10K'_v K'_p = 0$$

Substituting $K'_p = 80$ and $K'_v = 30$ in this expression and simplifying we get

$$s^4 + 178.75s^3 + 13406s^2 + 1693.125 \times 10^5 s + 1354.5 \times 10^7 = 0$$

A preliminary investigation of this characteristic equation using Routh-Hurwitz criterion indicates that there are

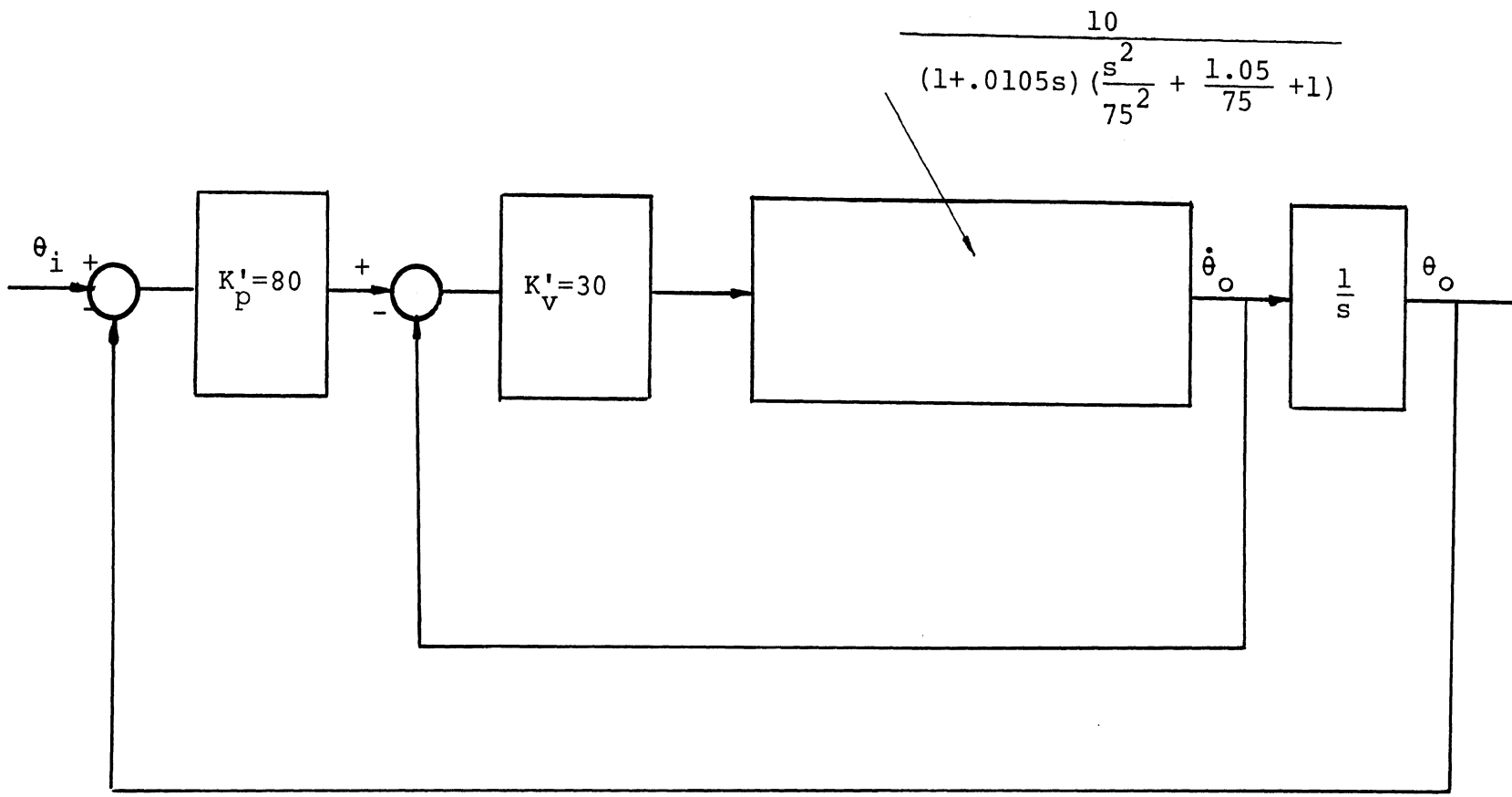


Fig. 20. Basic System to be Checked for Response and Stability

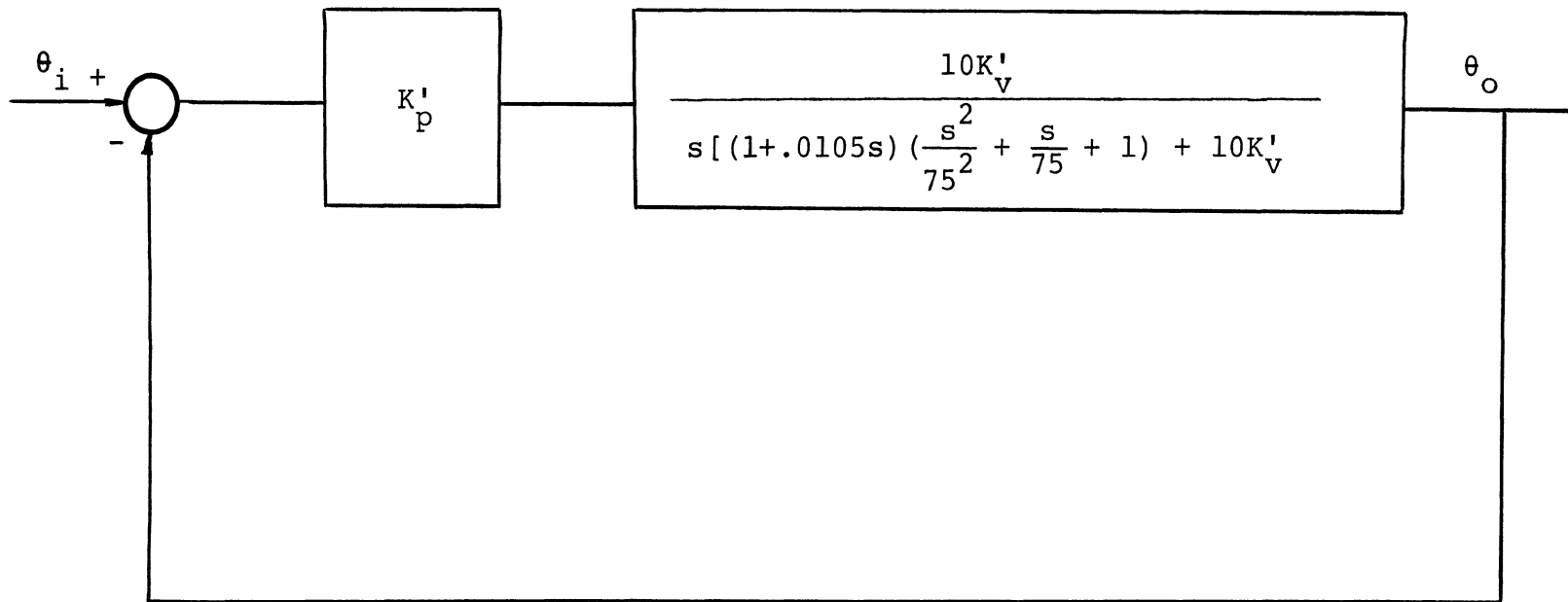


Fig. 21. Block Diagram with Velocity Loop Eliminated

two zeroes located to the right of the imaginary axis. Thus the system is basically unstable. To insure stable operation of the system it is necessary that both the velocity loop as well as the position loop be stable. The need for this becomes apparent in the sections that follow.

E. Stabilization of Velocity Loop

It has been pointed out earlier that a high gain in this loop is necessary in order to obviate the damaging effects of drift in valve and amplifier characteristics, and also the plant. Furthermore it is also desirable that this control loop be stable although this stability is not critical to the operation of the system. In addition to filling the need mentioned above this part of control system also helps in rapidly damping out any velocity transients set up by changing loads. As compared to the outer loop this part has a faster response. Thus corrective action in case of transients gets initiated in this minor loop and is subsequently taken over by the outer loop. This collective action is one of the reasons on the basis of which we have made the statement that stability of this is not critical.

A casual examination of the transfer functions and the gains involved in Fig. 22 clearly indicates that any stability which can be achieved has to be at the cost of reduced gain. However, since a high gain is more critical a proper balance has to be achieved. Three different

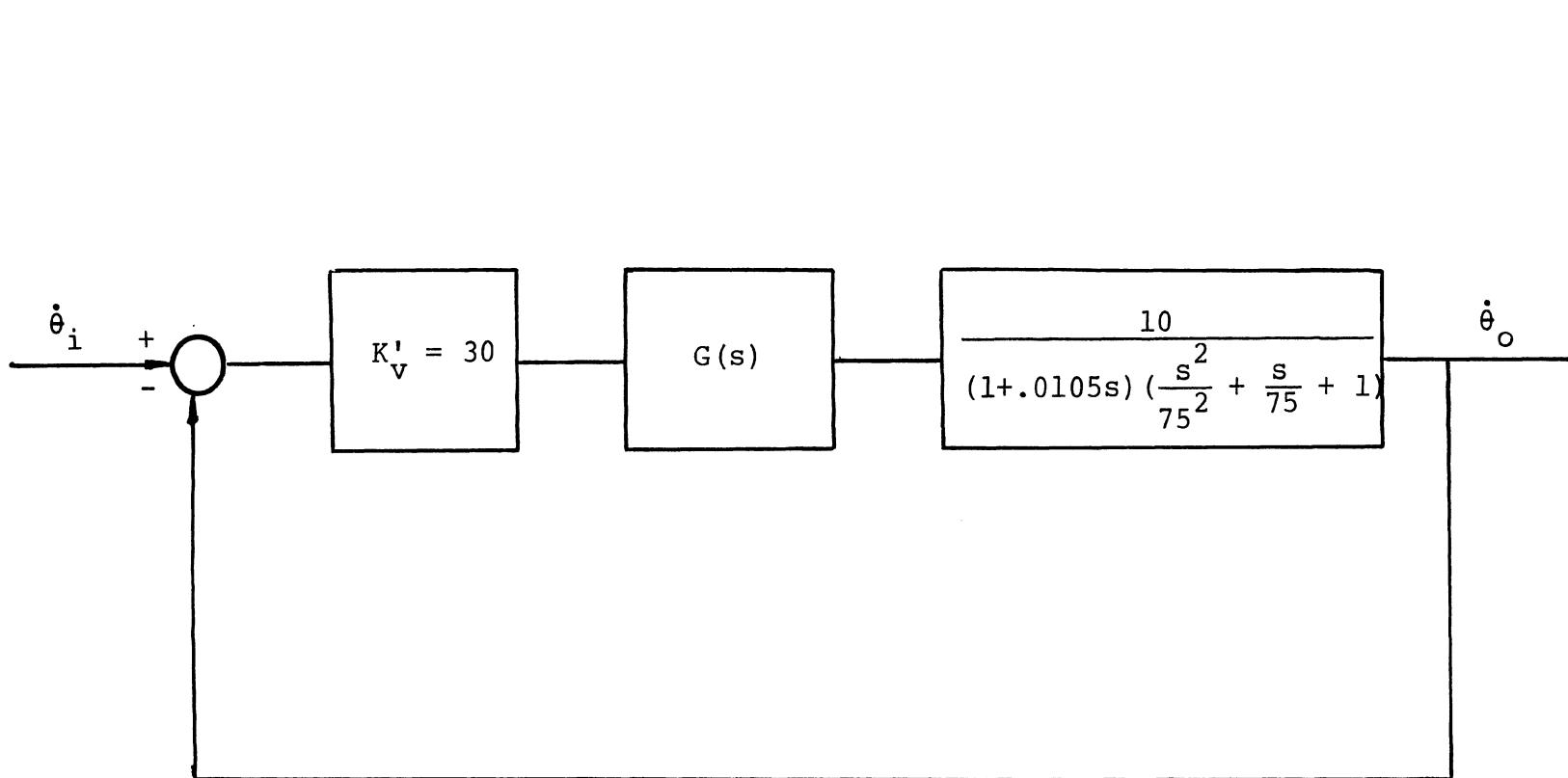


Fig. 22. Series Compensation of Velocity Loop

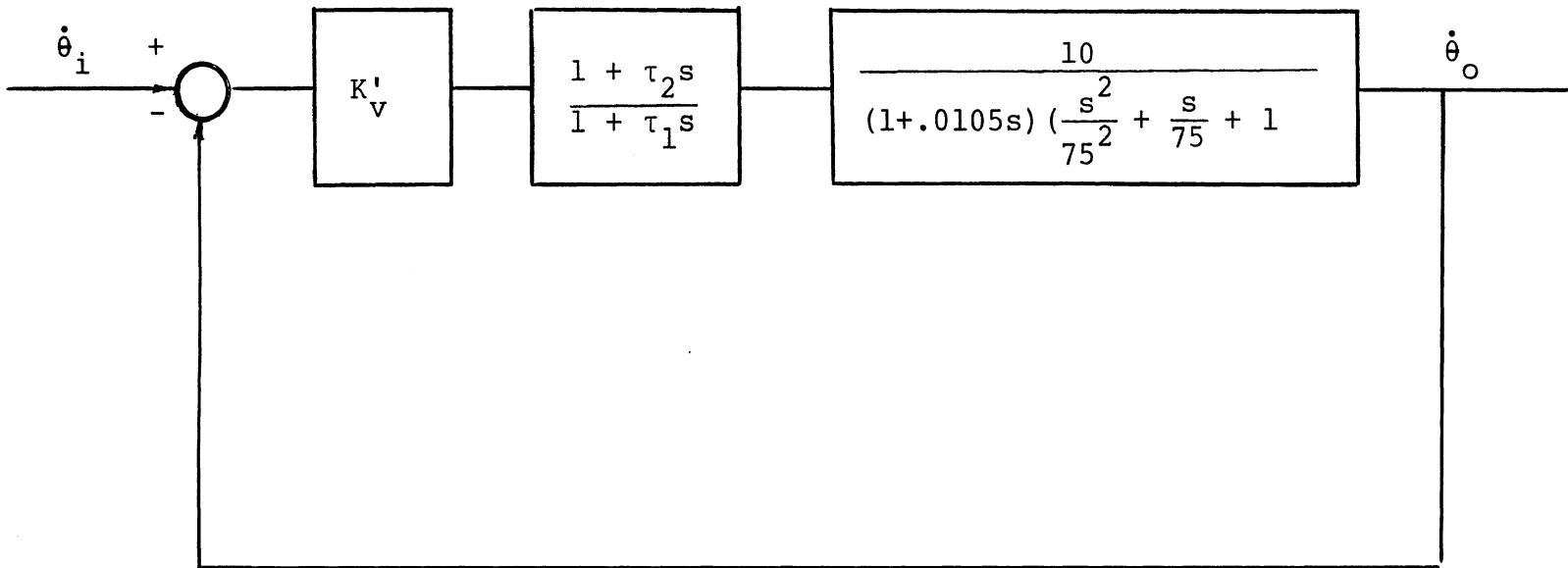
forms of compensation were tried.

- a) Series lag network - Figs. 23,24 and Table 1
- b) Series lag-lead network - Figs. 25, 26 and Table 2
- c) Acceleration feedback - Figs. 27, 28 and Table 3

The root locii plots shown were plotted with the help of a digital computer. The following general comments about the performance of the compensators are in order.

The series-lag network is capable of stabilizing the circuit only at the cost of a considerable reduction in gain over a wide frequency range. Thus utilization of this compensator will lead to inefficient performance of the control system when m/c tool encounters high frequency load transients. As opposed to this the series lag-lead compensator offers a greater range of frequencies over which a high gain can be maintained and therefore the operation of the control loop is more efficient. The acceleration feedback gives stable operation for only higher values of K_a . However, as the value of K_a is increased the damping of the dominant poles decreases. Also an important observation is that the undamped natural frequency associated with this pair is very high and this does ensure a very low rise time i.e. the circuit operation will be very fast.

Another approach which seems feasible is to use a combination of acceleration feedback and series lag-lead compensation so as to make use of advantages of both. This



Characteristic equation is

$$[.0105s^3 + 1.75s^2 + 131.25s + 5625](1 + \tau_1 s) + 750K'_V s + 56250K'_V = 0$$

Fig. 23. Velocity Loop With Series Lag Compensator

$\tau_1 =$	$\tau_2 =$	K'_V	Roots of Equation			
			Root I	Root II	Root III	Root IV
1	1/75	5	-112.8	-46.98	-8.0+J73.11	-8.0-J73.11
		10	-125.43	-60.12	4.7+J86.6	4.7-J86.6
		20	-145.9	-67.6	18.7+J105.3	18.7-J105.3
		30	-161.76	-70.15	27.9+J118.9	27.9-J118.9
2	1/75	5	-106.19	-28.8	-20.2+J65.3	-20.2-J65.3
		10	-112.7	-46.7	-8.0+J72.9	-8.0-J72.9
		20	-125.3	-60.0	4.92+J86.5	4.92-J86.5
		30	-136.3	-65.0	12.9+J96.8	12.9-J96.8
4	1/75	5	-103.0	-14.2	-29.0+J63.7	-29.0-J63.7
		10	-106.1	-28.6	-20.2+J65.3	-20.2-J65.3
		20	-112.7	-46.6	-7.95+J72.9	-7.95-J72.9
		30	-119.18	-55.16	-.44 +J80.2	-.44 -J80.2

Table 1. Root Locus Data for Series Lag Compensation

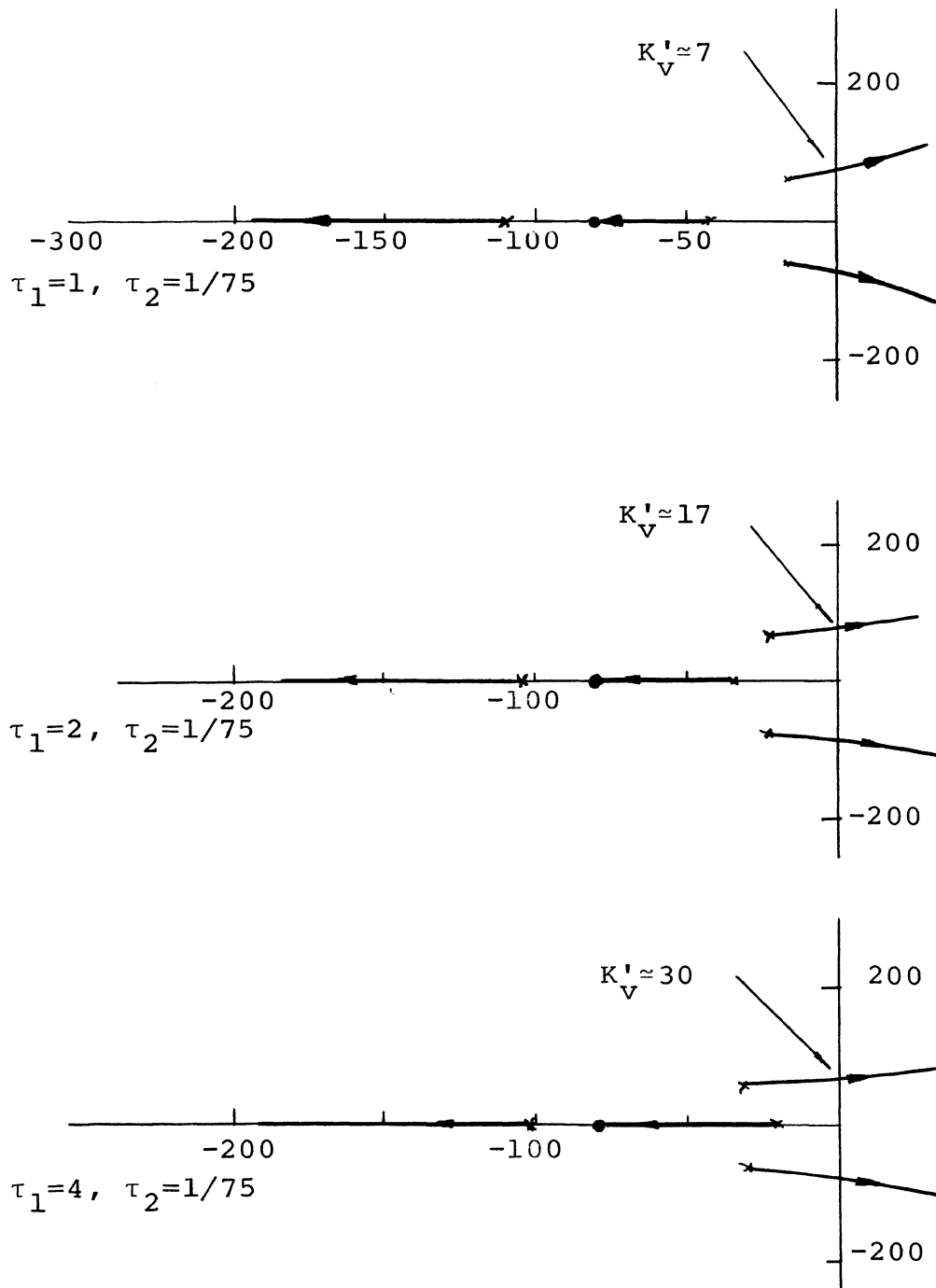
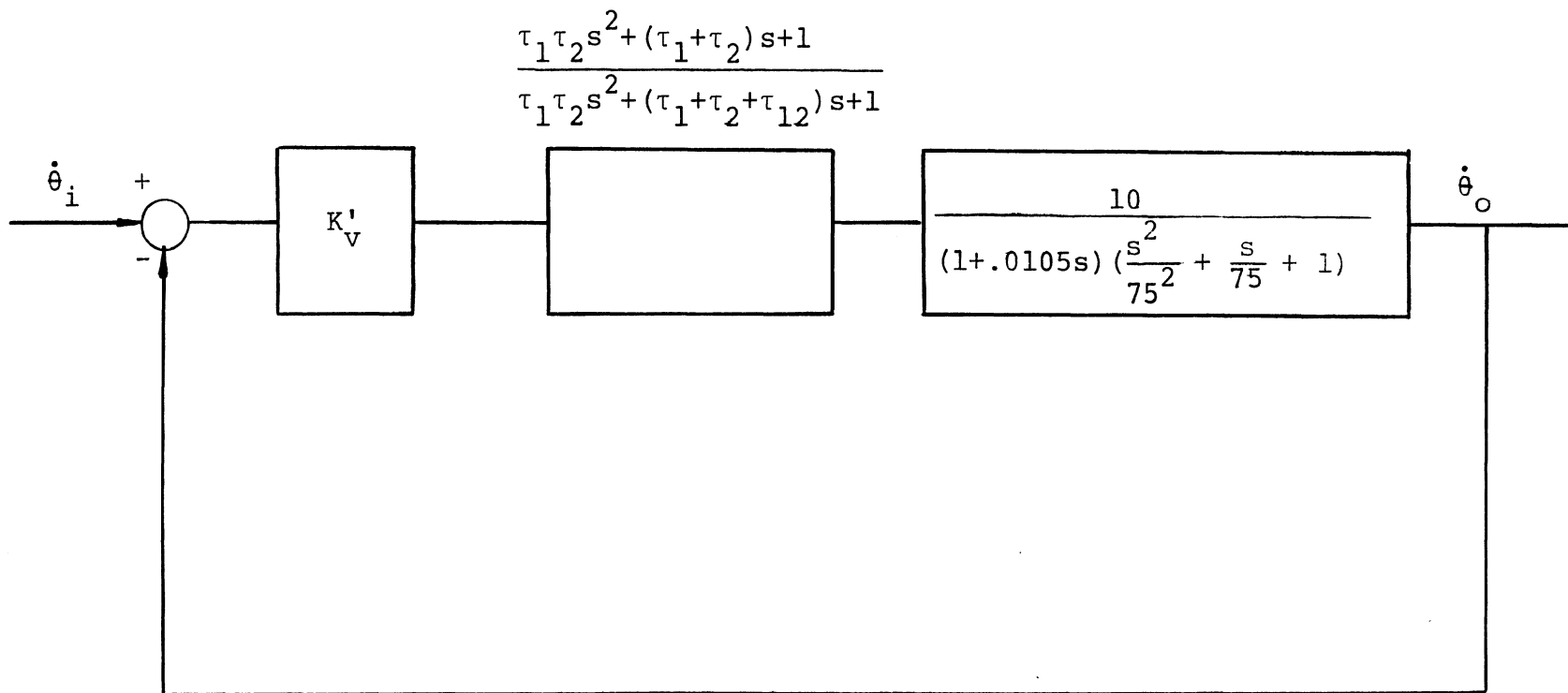


Fig. 24. Root Locus Plots for Lag Compensator



Characteristic equation is

$$1 + 10K'_V \left[\frac{\tau_1\tau_2s^2 + (\tau_1 + \tau_2)s + 1}{\tau_1\tau_2s^2 + (\tau_1 + \tau_2 + \tau_{12})s + 1} \right] \left[\frac{1}{(1+.0105s) \left(\frac{s^2}{75^2} + \frac{s}{75} + 1 \right)} \right] = 0$$

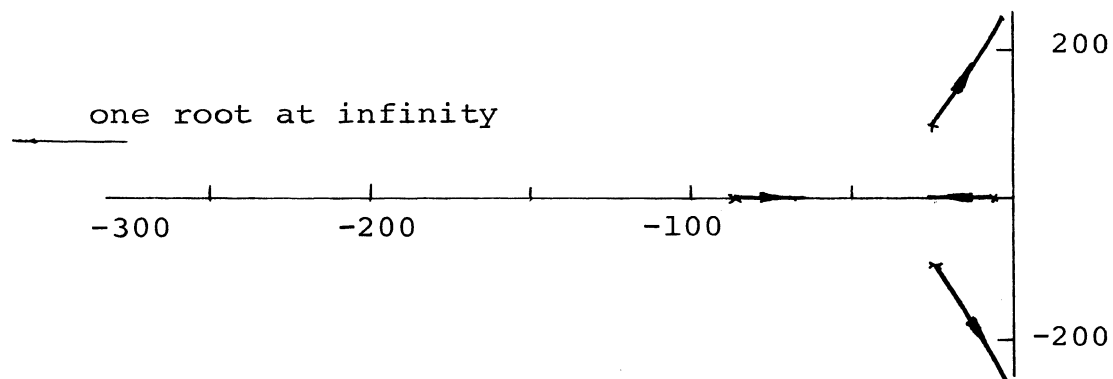
Fig. 25. Series Lag-Lead Compensator

τ_1	τ_{12}	K'_V	Roots				
			1	2	3	4	5
20/75	10	5	-1.94	-163.0	-2890.2	- 5.4+J93.6	-5.4-J93.6
		10	-2.54	-138.7	-2893.7	-15.5+J124	-15.5-J124.0
		20	-3.0	-109.9	-2900.0	-26.2+J179.5	-26.2-J179.5
		30	-3.2	-97.8	-2907.6	-28.8+J225.7	-28.8-J225.7
20/75	5	5	-2.44	-91.6	-1498.0	-33.9+J151.3	-33.9-J151.3
		10	-2.95	-84.4	-1510.9	-30.8+J203.6	-30.8-J203.6
		20	-3.30	-79.9	-1535.4	-20.6+J279.2	-20.6-J279.2
		30	-3.4	-78.3	-1558.5	-9.7+J336.5	-9.7-J336.5
15/75	10	30	-4.31	-78.05	-3841.6	-40.5+J217.8	-40.5-J217.8
10/75	10	30	-6.23	-58.53	-5714.5	-51.5+J207.4	-51.5-J207.4

$$\tau_2 = 1/75$$

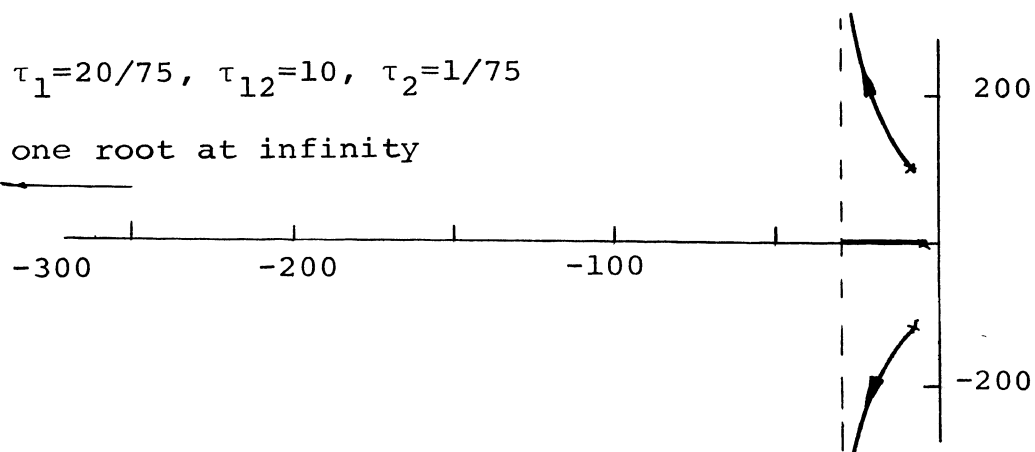
Table 2. Root Locus Data for Lag-Lead Compensator

$$\tau_1=20/75, \tau_{12}=5, \tau_2=1/75$$



$$\tau_1=20/75, \tau_{12}=10, \tau_2=1/75$$

one root at infinity



$$\tau_{12}=10, \tau_1=10/75, \tau_2=1/75$$

one root at infinity

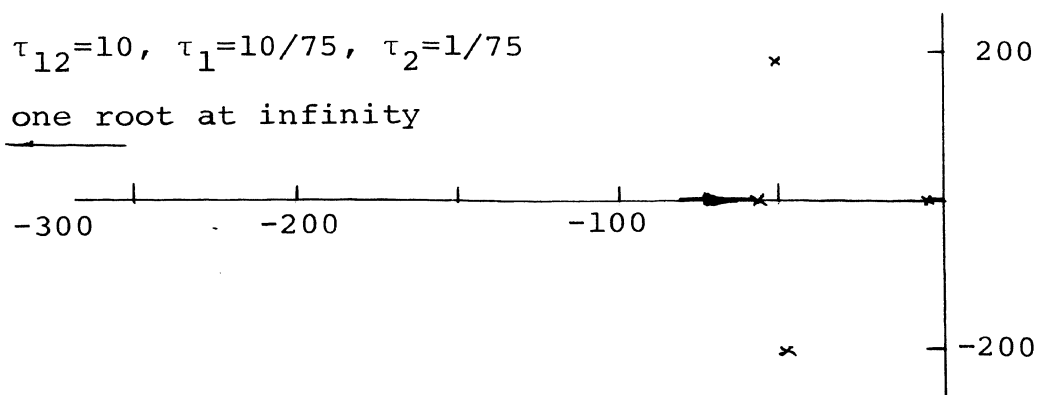
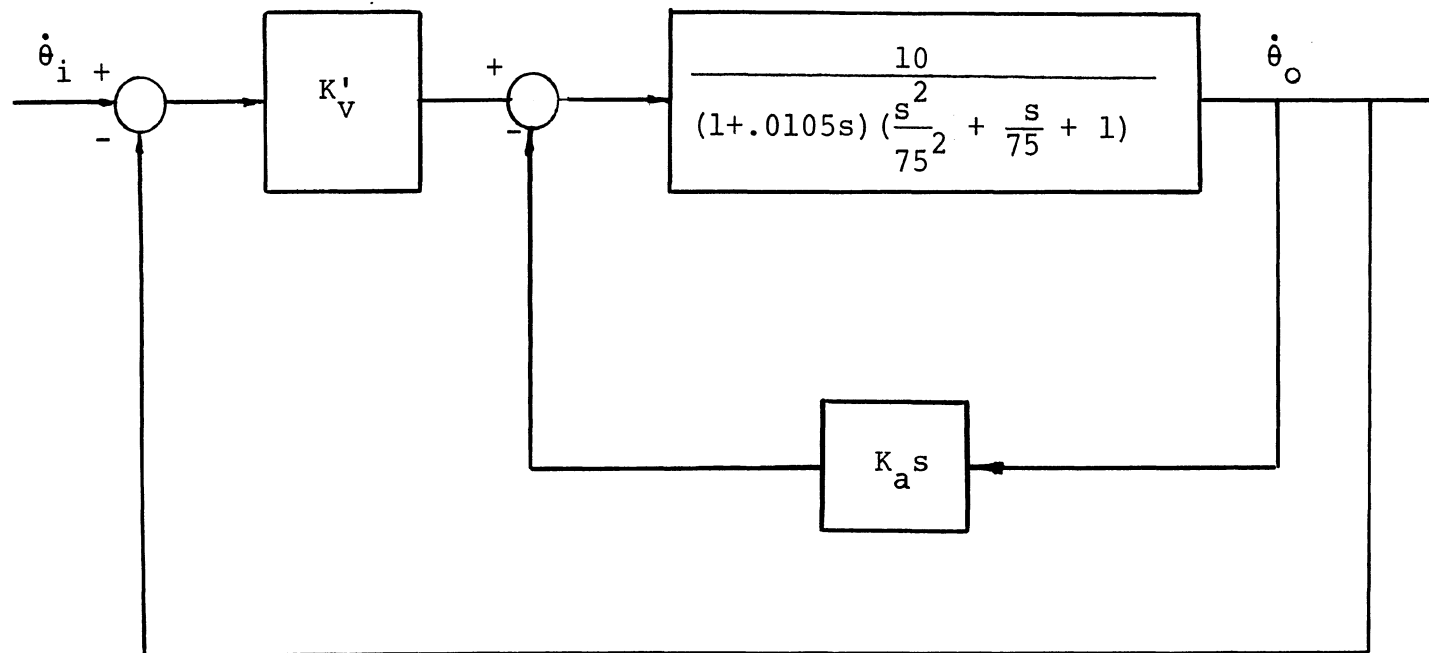


Fig. 26. Locus Plots of Lag-Lead Compensator



Characteristic equation is

$$.0105s^3 + 1.75s^2 + [131.25 + 56250K_a]s + 5625[1 + 10K'_V] = 0$$

Fig. 27. Acceleration Feedback Compensation

K_a	K'_v	ROOTS		
		1	2	3
1/4	10	- 80.1	-47.4+J840.4	-47.4-J840.4
	20	-158.4	- 8.2+J844.7	- 8.2-J844.7
	30	-232.0	28.5+J853.6	28.5-J853.6
	40	-299.3	62.1+J865.8	62.1-J865.8
1/2	10	- 40.1	-67.4+J1187.1	-67.4-J1187.1
	20	- 80.0	-47.4+J1187.2	-47.4-J1187.2
	30	-119.8	-27.5+J1188.2	-27.5-J1188.2
	40	-159.1	- 7.9+J1190.2	- 7.9-J1190.2
1	10	- 20.12	-77.4+J1678.2	-77.4-J1678.2
	20	- 40.0	-67.4+J1677.9	-67.4-J1677.9
	30	- 60.06	-57.4+J1677.9	-57.4-J1677.9
	40	- 80.06	-47.4+J1678.0	-47.4-J1678.0

Table 3. Root Locus Data for Acceleration Feedback

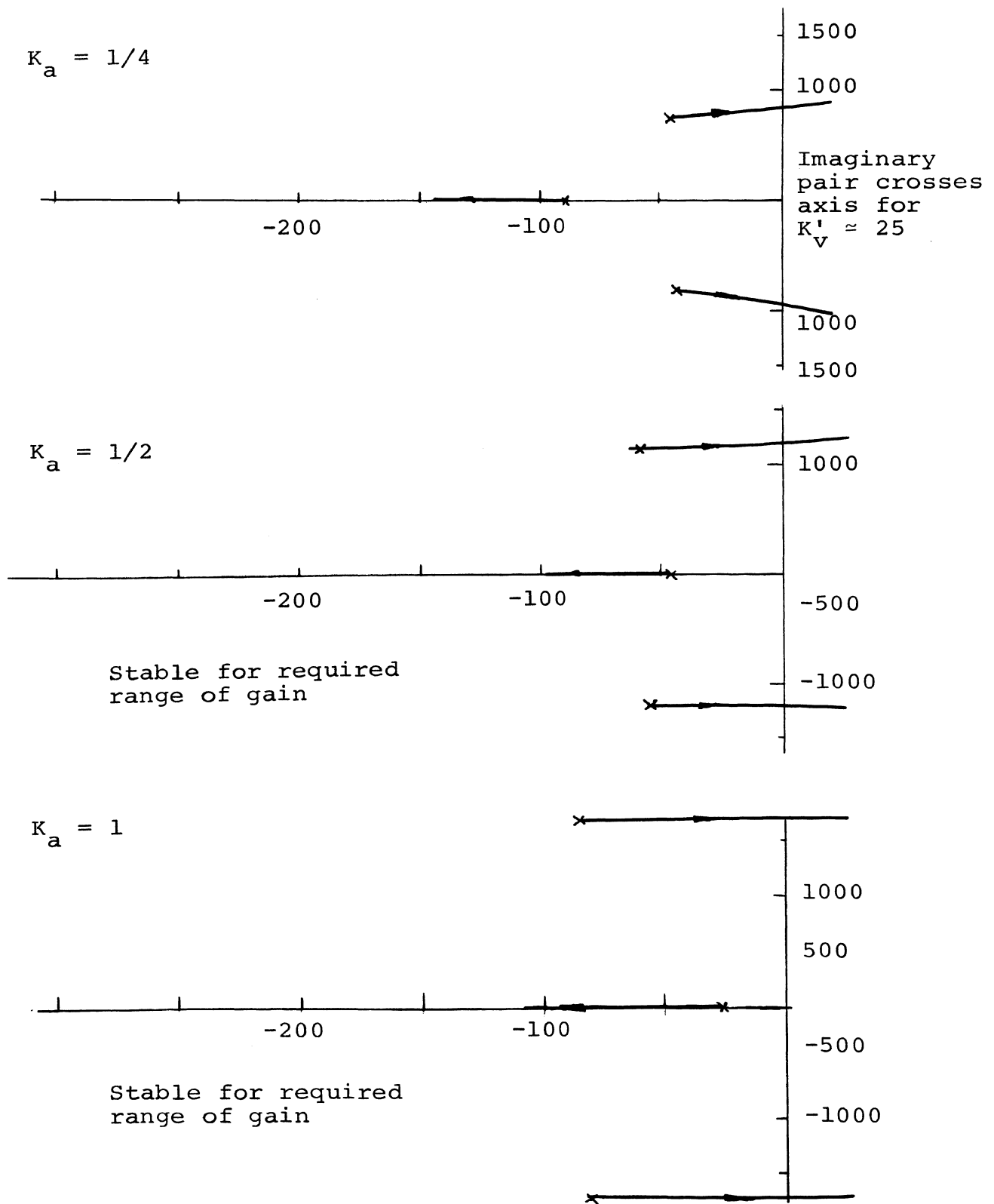
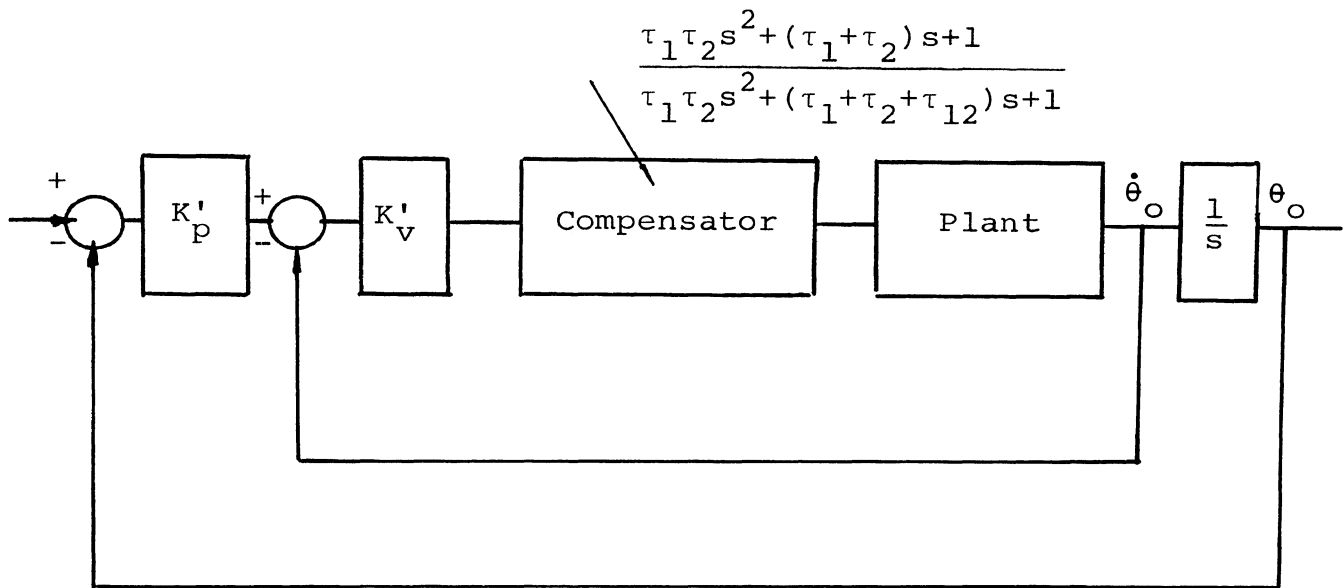


Fig. 28. Locus Plots for Acceleration Feedback

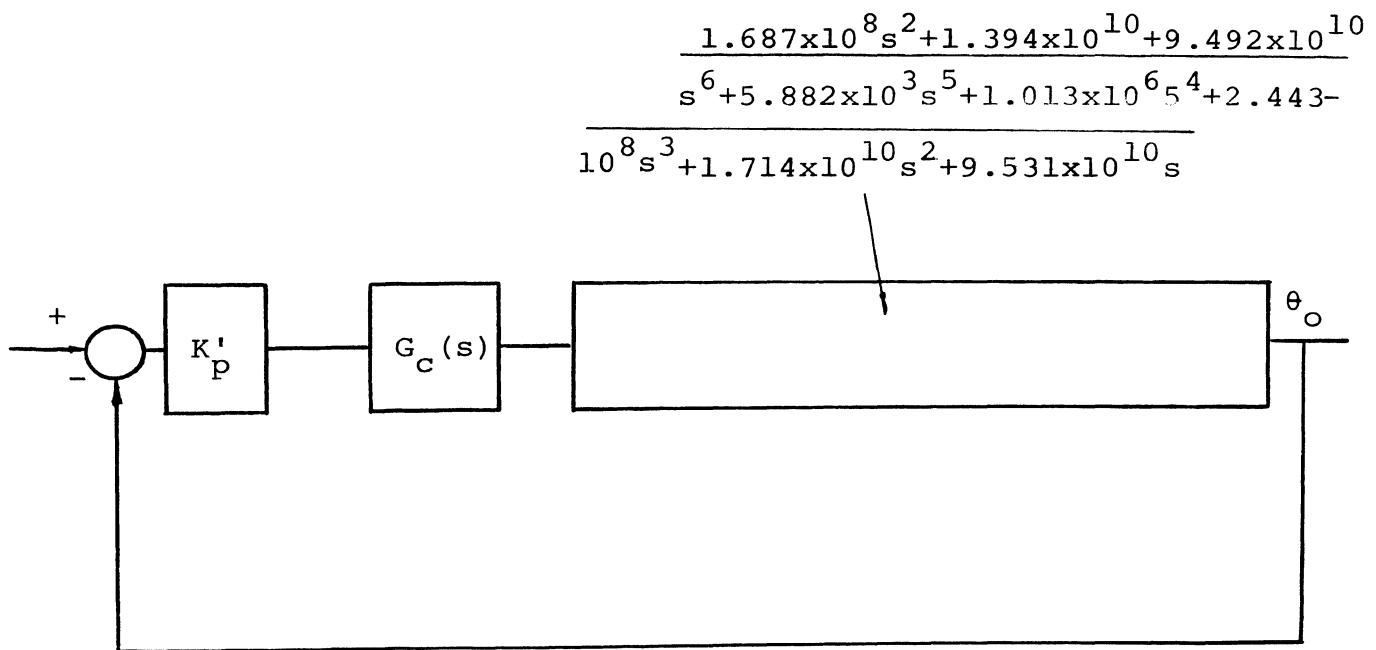
method could not be tried because of time limitations.

In deciding on the most feasible method of compensation factors such as physical implementation, cost etc. have to be borne in mind. Further a major consideration is the fact that for all control systems any drift in the feedback elements will directly be reflected in the system transmittance i.e. sensitivity with respect to change in feedback parameters is practically one. Since acceleration feedback will have to be through some physical sensors, which, unless made very accurately, (in which case cost will be high) are liable to drift, it is advisable in most instances to stay with series network type of compensation. These have the added advantage of being most economical and also offer ease in manipulation of parameters, a quality which comes in extremely handy while simulating for optimum transient response.

In line with the above discussion the choice of compensator naturally falls on a lag-lead type and this is shown in Fig. 29a. The choice of parameters was made after trying over a wide range of values. It should be pointed out that this choice may not be the optimum. However, in view of the fact that in the final simulation of the complete system the parameters of this compensator may also be subject to change to get the optimum transient response, it is recommended that not too much time be expended on optimizing the velocity loop compensator.



29a. $\tau_1 = 10/75, \tau_2 = 1/75, \tau_{12} = 10$



29b.

Characteristic equation is

$$s^6 + 5.882 \times 10^3 s^5 + 1.013 \times 10^6 s^4 + 2.443 \times 10^8 s^3 + 1.714 \times 10^{10} s^2 + 9.531 \times 10^{10} s + K'_p G_c(s) (1.687 \times 10^8 s^2 + 1.394 \times 10^{10} s + 9.492 \times 10^{10}) = 0$$

Fig. 29. Compensation of Position Loop

F. Position Loop Compensation

Figure 29a shows the control loop to be subjected to a stability analysis. We are now not only concerned with just getting all the roots of the characteristic equation in the left half plane but also with the degree of stability (i.e. gain and phase margins), bandwidth and all the other goodness factors mentioned earlier. The characteristic equation of Fig. 29b with $G_c(s) = 1$ is first subjected to a Routh-Harwitz test. The result indicates that for the required gain of $K'_p = 80$ all the roots are in the left half plane and the system is stable. To have some idea of the nature of response to be expected an open loop frequency response was plotted for the uncompensated system with $K'_p = 80$. Figure 30 shows the control system represented in a form more amenable for carrying out amplitude and phase calculations with help of digital computer. Table 4 gives the set of values obtained thus and Fig. 31 shows the log magnitude and phase versus frequency curves for the uncompensated system. Interpolation between the two curves shows that the uncompensated system will operate with a phase margin of 73° and a gain margin of 1.2. This large phase margin and small gain margin are evidently not conducive to efficient system performance. There is scope for shaping of this open loop plot to obtain better performance.

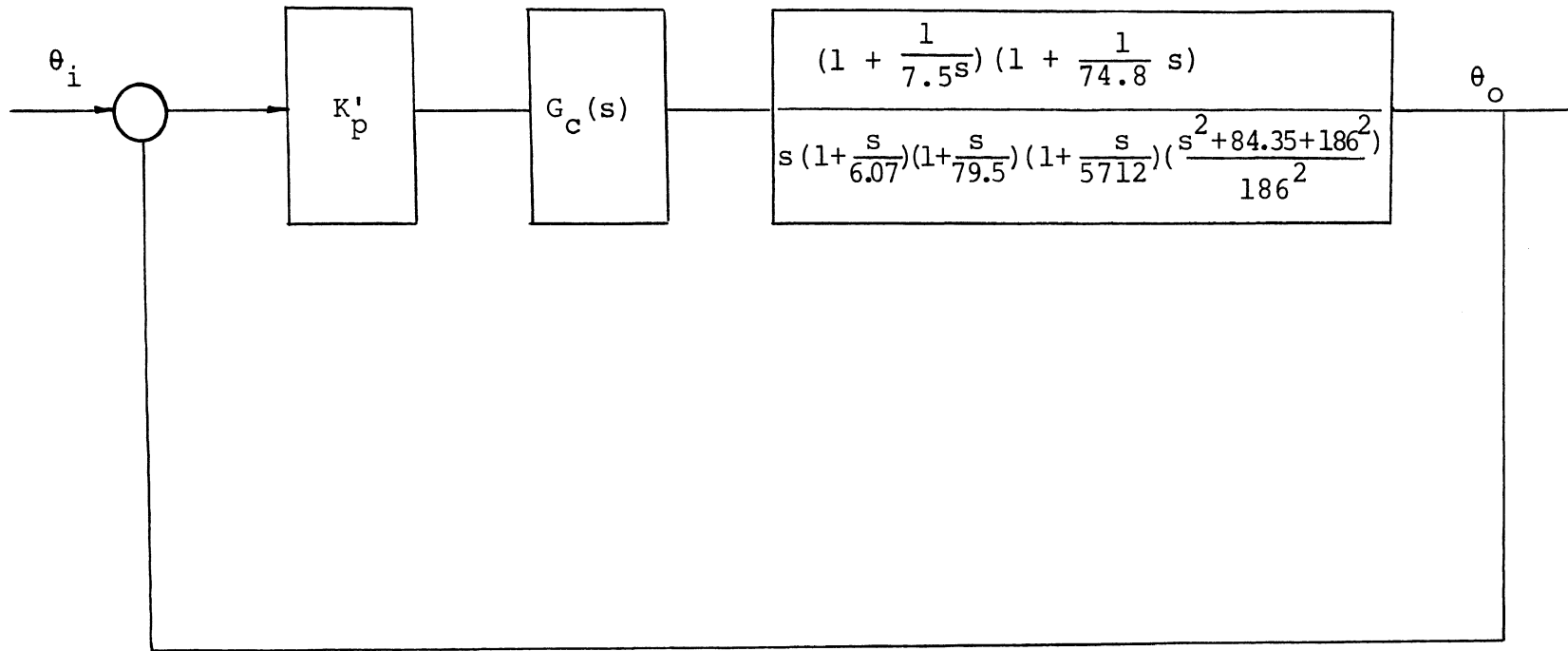


Fig. 30. Representation for Open Loop Frequency Response

Freq. ω rads/sec	Magn. $/\theta_o/\theta_2/$	Log magn. Log $\theta_o/\theta_i/$	Phase ϕ
1	79.637	1.901	-92°
5	14.856	1.192	-96.5°
10	6.944	.842	-97°
30	2.25	.352	-96°
50	1.414	.151	-98°
70	1.088	.037	-102°
100	.896	- .048	-109°
150	.896	- .048	-137°
200	.667	- .176	-200°
250	.281	- .568	-235°
300	.130	- .887	-248°
350	.073	-1.137	-254°
400	.046	-1.341	-258°
450	.031	-1.514	-261°
500	.022	-1.666	-264°

Table 4. Open Loop Frequency Response Data

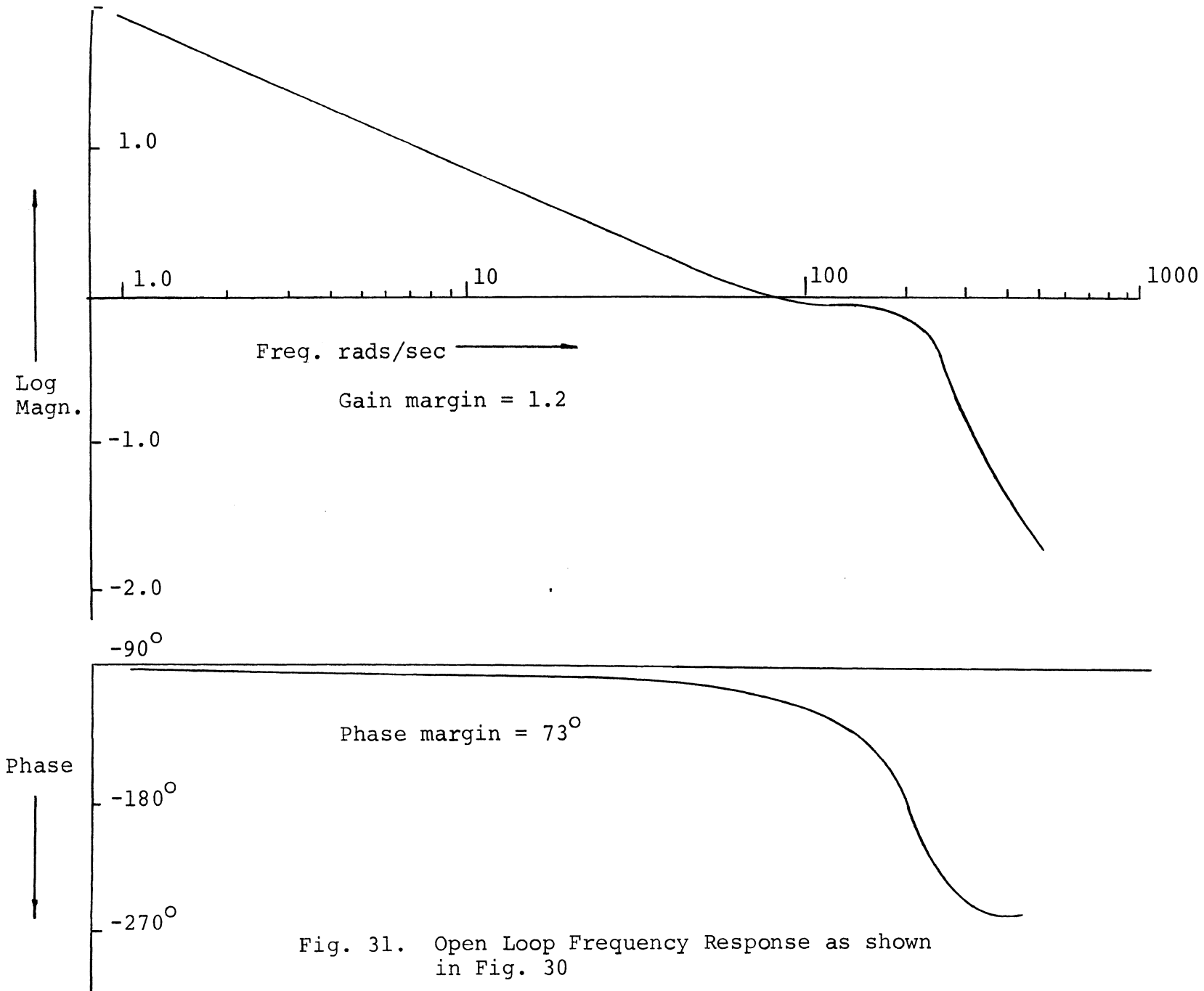


Fig. 31. Open Loop Frequency Response as shown in Fig. 30

Before deciding on the exact form of compensation there are two important points which merit our attention. Both these factors have major relevance to the fact that the control system being designed is for a numerical contouring control m/c tool. For reasons of accuracy it is desirable that:

- a) the control system have as high a velocity constant as possible,
- b) the gains for all the three axes must be the same and preferably the open loop steady state response curves be as similar as possible.

If only condition 'b' is fulfilled, the control system will reproduce programmed contours accurately, even in the absence of a high velocity constant. Need for stability places limitations on the maximum gains permissible for high order servos. Thus, while deciding forms of compensation and final gains for the position loop, it is desirable to satisfy both the above requirements as far as possible.

Two types of compensation were tried:

- 1) Series lag network with

$$G_c(s) = \frac{1 + \tau_1 s}{1 + \tau_2 s}$$

$$\tau_1 = 1/240$$

$$\tau_2 = 1/80$$

and

2) Series lag-lead network with

$$G_c(s) = \frac{(1+\tau_1 s)(1+\tau_2 s)}{\tau_1 \tau_2 s^2 + (\tau_1 + \tau_2 + \tau_{12})s + 1}$$

$$\tau_1 = 1/200$$

$$\tau_2 = 1/800$$

$$\tau_{12} = 1.35/200$$

Tables 5 and 6 give the frequency response data for the control system when cascaded in series with the above compensators and static gain $K'_p = 80.0$. Figure 32 shows the log amplitude and phase plots for the compensated system. Curves 1a and 1b in this figure are for compensator type 1 while 2a and 2b are for type 2. A simple analysis reveals that the type 2 compensator offers a better combination of phase and gain margins and thus forms the natural choice for this application.

Figure 33 shows the compensated system for which a closed loop frequency response analysis has been made in order to establish values for M peak and band width. Figure 34 shows the frequency response plots (closed loop) for the system with static gain K'_p equal to 80.0 and 120.0 respectively. In order to obtain the above data the following steps had to be carried out.

Freq. ω rads/sec	Magn. $ \theta_o / \theta_i $	Logmagn $\text{Log} \theta_o / \theta_i $	Phase ϕ
1	79.631	1.901	-92.5°
5	14.827	1.171	-98.5°
10	6.890	.838	-101°
30	2.107	.324	-109°
50	1.199	.079	-118°
70	.819	- .087	-126°
100	.560	- .252	137.5°
150	.421	- .375	-167°
200	.248	- .606	-227.5°
250	.117	- .933	-261°
300	.047	-1.326	-272°
350	.023	-1.638	-275°
400	.013	-1.898	-278°
450	.008	-2.121	-279.5°
500	.008	-2.118	-280°

Table 5. Open Loop Frequency Response Data for

$$G_c(s) = \frac{1+\tau_1 s}{1+\tau_2 s}$$

Freq. ω rads/sec	Magn $ \theta_o / \theta_i $	Log magn. Log $ \theta_o / \theta_i $	Phase ϕ
1	79.63	1.90	-92°
5	14.832	1.171	-98°
10	6.899	.839	-10°
30	2.132	.329	-106.5°
50	1.238	.093	-113°
70	.871	- .060	-120°
100	.630	- .201	-129.5°
150	.535	- .272	-155°
200	.359	- .445	-214°
250	.137	- .862	-246°
300	.064	-1.197	-255°
350	.035	-1.453	-257°
400	.022	-1.659	-258.5°
450	.015	-1.831	-258.5°
500	.011	-1.979	-258°

Table 6. Open Loop Frequency Response for

$$G_C(s) = \frac{(1+\tau_1s)(1+\tau_2s)}{\tau_1\tau_2s^2 + (\tau_1+\tau_2+\tau_{12})s+1}$$

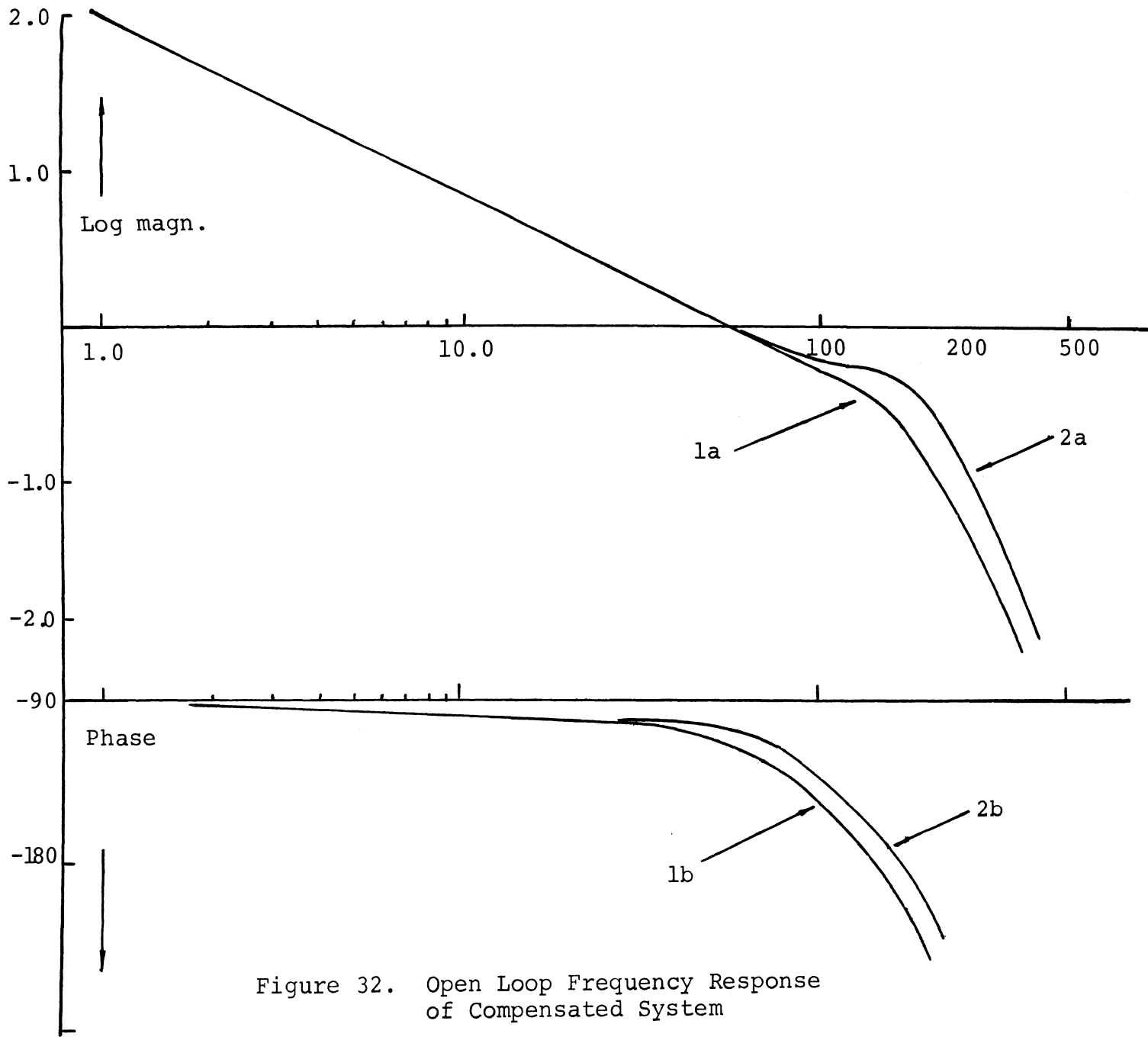


Figure 32. Open Loop Frequency Response of Compensated System

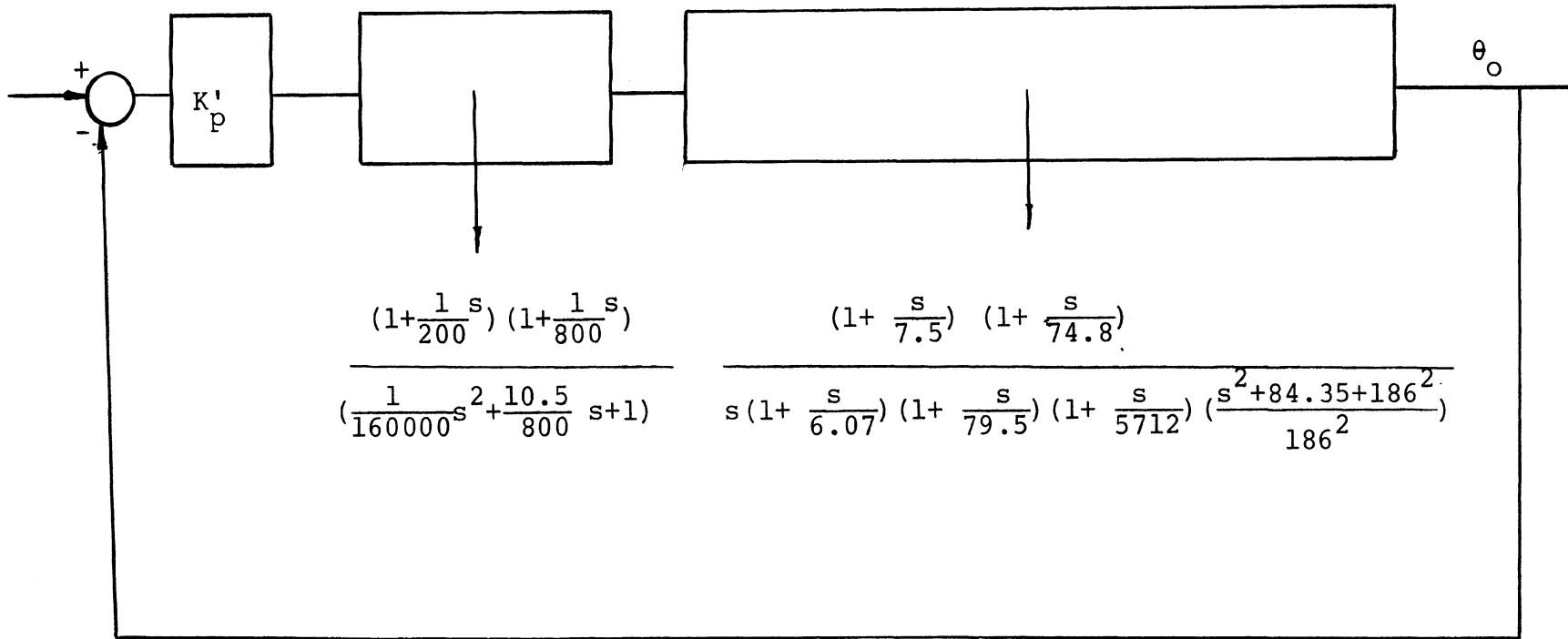


Fig. 33 Block Diagram of Compensated System

1) From Fig. 29 the system transfer function is

$$\frac{C(s)}{R(s)} = \frac{K'_p (s^2 + 1000s + 160,000) (1.687 \times 10^8 s^2 + 1.394 \times 10^{10} s + 9.492 \times 10^{10})}{(s^2 + 2080s + 160,000) (s^6 + 5.882 \times 10^3 s^5 + 1.013 \times 10^6 s^4 + 2.493 \times 10^8 s^3 + 1.714 \times 10^{10} s^2 + 9.531 \times 10^{10} s) + K'_p (s^2 + 1000s + 160,000) (1.687 \times 10^8 s^2 + 1.394 \times 10^{10} s + 9.492 \times 10^{10})}$$

- 2) The roots of the characteristic equation were then solved for with $K'_p = 80$ and 120 .
- 3) Finally the system transfer functions were expressed in the form shown and programmed on the digital computer to obtain magnitude and phase for the desired frequency range.

Static gain $K'_p = 80.0$

$$\frac{C}{R}(j\omega) = \frac{(1 + j \frac{\omega}{200}) (1 + j \frac{\omega}{800}) (1 + j \frac{\omega}{7.5}) (1 + j \frac{\omega}{74.8})}{(1 + j \frac{\omega}{7.1715}) (1 + j \frac{\omega}{75.4385}) (1 + j \frac{\omega}{5707.68}) (1 + j \frac{\omega}{2004.315})} \cdot \frac{1}{(1 - \frac{\omega^2}{6020} + j \frac{116.4\omega}{6020}) (1 - \frac{\omega^2}{30945.9} + j \frac{50.68\omega}{30945.9})}$$

Static gain $K'_p = 120.0$

$$\frac{C}{R}(j\omega) = \frac{(1 + j\omega/200) (1 + j\omega/800) (1 + j\omega/7.5) (1 + j\omega/74.8)}{(1 + j \frac{\omega}{75.409}) (1 + j \frac{\omega}{7.13}) (1 + j \frac{\omega}{5709.22}) (1 + j \frac{\omega}{2003.77})} \cdot \frac{1}{(1 - \frac{\omega^2}{9396} + j \frac{139.8\omega}{9396}) (1 - \frac{\omega^2}{29,900} + j \frac{27.13\omega}{29900})}$$

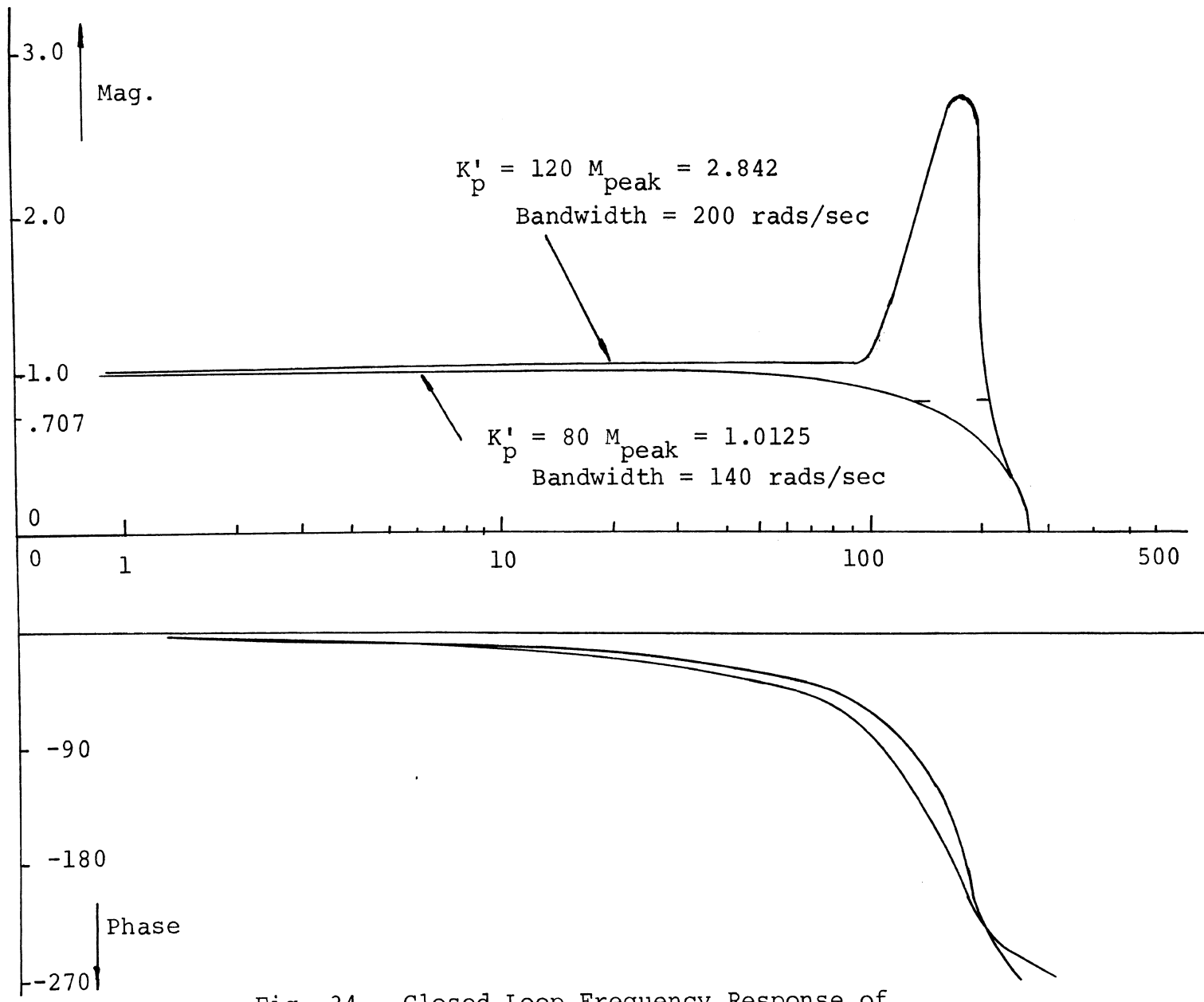


Fig. 34. Closed Loop Frequency Response of Compensated System

From the plots we get

$$K'_p = 80 \quad M_{\text{peak}} = 1.0125 \quad \text{bandwidth} = 140 \text{ rads/sec}$$

$$K'_p = 120 \quad M_{\text{peak}} = 2.84 \quad \text{bandwidth} = 200 \text{ rads/sec}$$

The last step of our preliminary design analysis is to check our system response in the time domain. To obtain the expression for the output as a function of time it is only necessary to express the system transfer functions $C/R(s)$ as partial fractions and then take the inverse Laplace transforms. The break up into partial fractions was accomplished with the help of a digital computer and the resulting time domain expressions are given below.

For our purposes it is sufficient to establish the time responses to a unit step and a unit ramp input. The following response expressions were obtained, as before, by breaking into partial fractions and taking the inverse transforms.

Gain $K'_p = 80.0$, $r(t) = 1.0$, $R(s) = 1/s$

$$c(t) = 1.0 + \frac{.1224e^{-7.1715t}}{7.1715} - \frac{.238e^{-75.4385t}}{75.4385} + \frac{4841.1e^{-51.3t}}{(51.3)(77.58)} \\ e^{-58.2t} \sin(51.31t-1.92) + \frac{8091.2}{(174.09)(175.9)} e^{-25.34t} \\ \sin(174.09t+2.7)$$

$$K'_p = 80.0 \quad r(t) = t, \quad R(s) = 1/s^2$$

$$C(t) = t - .01328 - \left(\frac{.1224}{7.1715^2}\right) e^{-7.1715t} + \left(\frac{.238}{75.4385^2}\right) e^{-75.4385t} \\ + \frac{4841.1}{(51.31)(77.58^2)} e^{-58.2t} \sin(51.31t + 1.94) + \\ \frac{8091.2}{(174.09)(175.9^2)} e^{-25.34t} \sin(174.09t + 4.32)$$

$$K'_p = 120.0, \quad r(t) = 1.0, \quad R(s) = 1/s$$

$$C(t) = 1.0 + \frac{.0748}{7.13} e^{-7.13t} - \frac{.1588}{75.409} e^{-75.409t} + \\ \frac{6352.1}{(67.15)(96.93)} e^{-69.9t} \sin(67.15t - 1.59) + \\ \frac{12384.6}{(172.38)(172.91)} e^{-13.565t} \sin(172.38t + 3.13)$$

$$K'_p = 120.0, \quad r(t) = t, \quad R(s) = 1/s^2$$

$$C(t) = t - .008857 - \left(\frac{.0748}{7.13^2}\right) e^{-7.13t} + \left(\frac{.1588}{75.409^2}\right) e^{-75.409t} \\ + \frac{6352.1}{(67.15)(96.3^2)} e^{-69.9t} \sin(67.15t - 3.96) + \\ \frac{12384.6}{172.38(172.91)^2} \sin(172.38t + 1.55)$$

It should be noted that the above expressions do not include the responses due to the two extreme outlying poles. These can effectively be ignored as they die out very fast and contribution to the response is negligible. Further it is

not possible to handle these on the computer. These expressions were then programmed and the responses plotted using a 'Calcomp' offline plotting system driven by IBM-360 Model 50. These plots are shown in Figs. 35 and 36. The following conclusion can be drawn from looking at nature of these plots. The transients due to step inputs take .35 seconds to die out in one case and approximately .5 seconds for system with higher gain. On the other hand the response to ramp inputs reaches its steady state value in less than .3 seconds for both the systems.

For the purpose of studying the transient behavior of higher order systems a very useful technique is to correlate system behavior to lower order systems. For details of the following correlation technique used the reader is referred to reference 20, pages 282 to 289. The relations for establishing correlations have been developed for type 1 and type 0 systems. These relations are repeated here.

<u>System Type</u>	<u>Condition On</u>	<u>Correlated</u>	<u>Relations Giving Parameters</u>
1) Type 1	$M_m > 1$	$\frac{C}{R} = \frac{to}{\omega_n} \frac{2}{s^2 + 2\xi\omega_n s + \omega_n^2}$	$M_m = \frac{1}{2\xi\sqrt{1-\xi^2}}$ $\frac{\omega_m}{\omega_n} = \sqrt{1-2\xi^2}$
2) Type 1	$M_m < 1$	$\frac{C}{R} = \frac{1}{1+\tau_c s}$	$\tau_c = 1/\omega_c$

<u>System Type</u>	<u>Condition On</u>	<u>Correlated</u>	<u>Relations</u> <u>Giving Parameters</u>
3) Type 0	$\frac{M_m}{K_o/(1+K_o)} \geq 1$	$\frac{C}{R} = \frac{[K_o/(1+K_o)]\omega_n^2}{s^2 + 2\xi\omega_n s + \omega_n^2}$	$M_m = \frac{K_o/(1+K_o)}{2\xi\sqrt{1-\xi^2}}$ $\frac{\omega_m}{\omega_n} = \sqrt{1-2\xi^2}$
4) Type 0	$\frac{M_m}{K_o/(1+K_o)} < 1$	$\frac{C}{R} = \frac{K_o/(1+K_o)}{1+\tau_c s}$	$\tau_c = 1/\omega_r$ $r = \frac{K_o}{\sqrt{1+(1+K_o)^2}}$

where the following parameters of the given high order system are defined as follows:

$\underline{M_m}$ - is the maximum value of closed loop frequency response.

$\underline{\omega_m}$ - frequency at which the closed loop frequency response is maximum.

$\underline{\omega_c}$ - is the frequency at which the open loop frequency response has a magnitude of unity.

$\underline{K_o}$ - is the gain of the type 0 system

$\underline{\omega_r}$ - is the frequency at which the open loop response has a magnitude equal to 'r'. For large values of K_o 'r' approaches unity.

Here onwards discussion is restricted to our system with gain = 80.0. This system has the following characteristics:

$$\begin{aligned} M_m &= 1.0125 \\ \omega_m &= 30 \text{ rads/sec} \end{aligned}$$

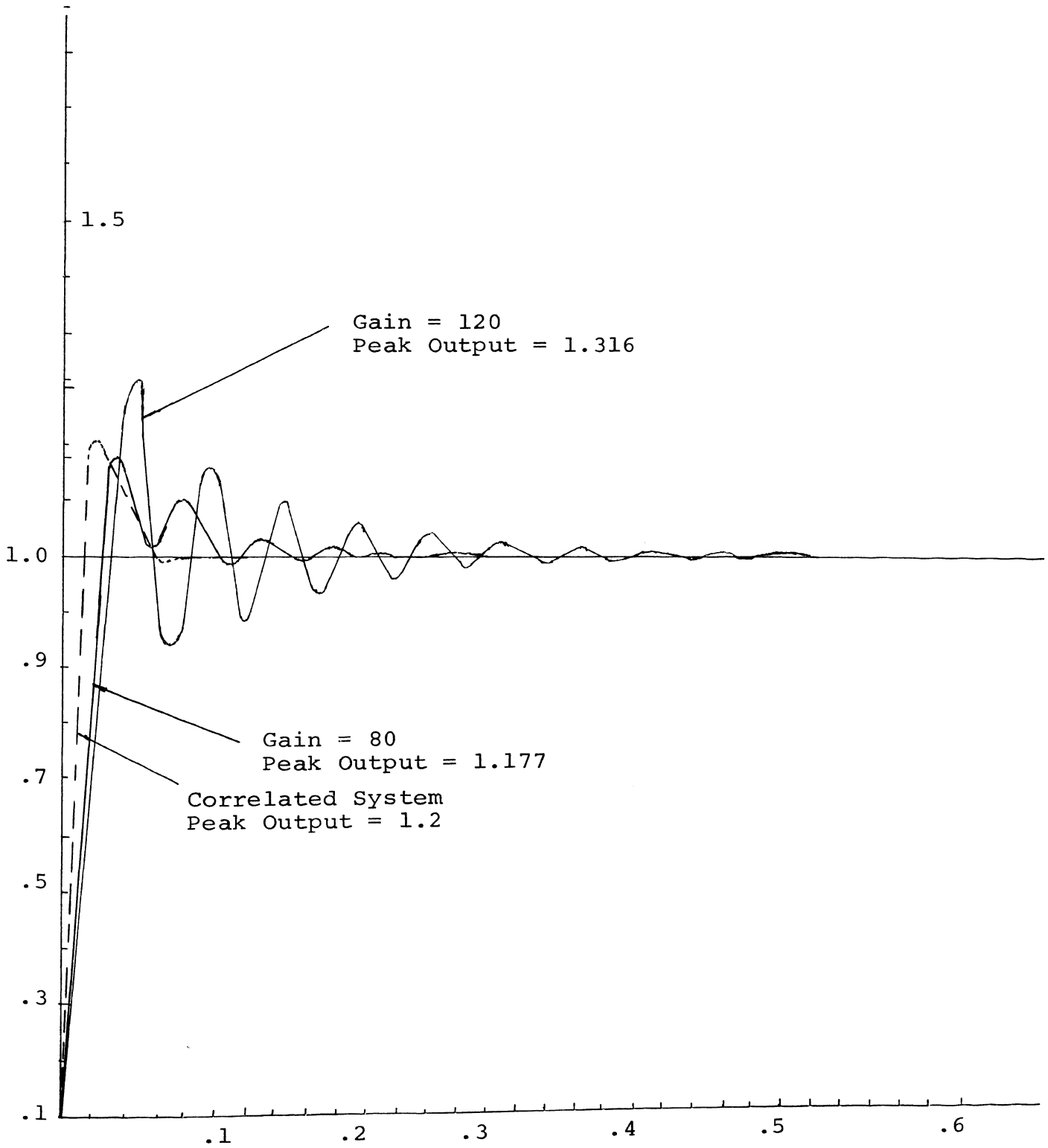


Fig. 35 Response to Unit Step

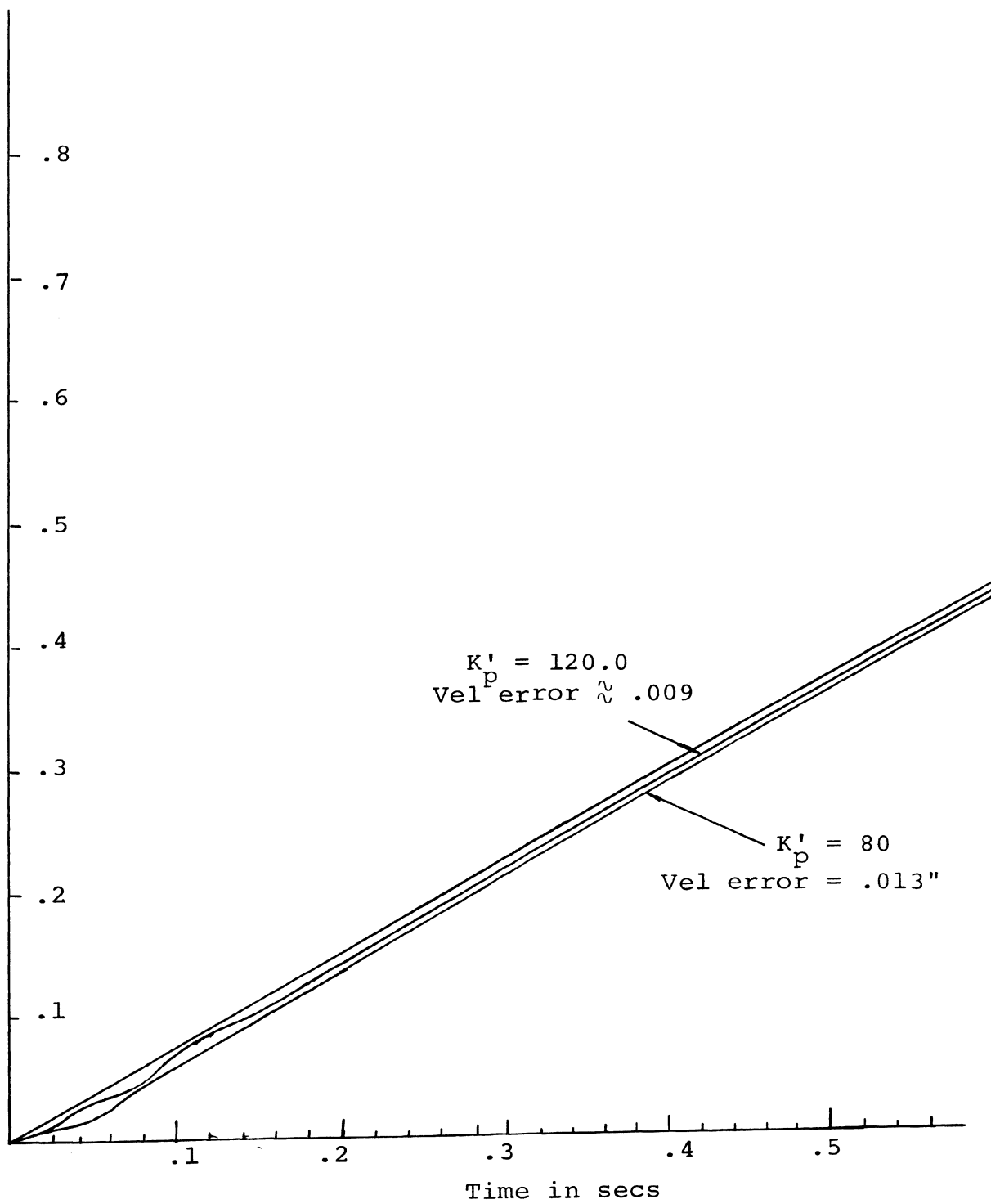


Fig. 36. Response to Unit Ramp

Using the relations

$$M_m = \frac{1}{2\xi\sqrt{1-\xi^2}}$$

we get $\xi = .69$ and

$$\frac{\omega_m}{\omega_n} = \sqrt{1-2\xi^2}$$

we get $\omega_n = 137.6$ rads/sec.

Therefore our system transient response can be approximated by the system having the following closed loop transfer function:

$$\frac{C}{R} = \frac{(137.6)^2}{s^2 + 2(.69)(137.6)s + (137.6)^2}$$

Response of this system to a unit step input is shown in Fig. 35. As can be seen the correlated system does not give a good approximation. This is chiefly because the higher order system does not exhibit any symmetrical under-shoots which is the case for any second order system. A similar correlation, if tried for the system with gain = 120, would probably give better results.

G. Optimization of Transient Response

The design technique followed in this chapter results in a control system which essentially has the desired steady state characteristics, but for which, there is no guarantee that the transient response will be equally good. Simultaneous optimization of both steady state and

transient characteristics is not possible. Transient properties have to be optimized by actual simulation of the final system using a digital or analog computer. Figure 37 shows the final system which has to be simulated by adjusting the parameters which have been shown as variables. The steady state design values are also shown in the figure. Before proceeding on to the actual optimization it is essential that one be fully conversant with the nature of dependence of the system response on the values of these parameters. Further it is also necessary to specify the range of values that have to be incorporated while physically implementing these controllers. Both of these ends can be achieved by being well conversant with the compensator characteristics. In our system we have only one type of compensator and its properties are briefly discussed in Appendix C.

Reverting to Fig. 37 the following general comments can be made regarding the simulation. Variation of parameters of the compensator in the velocity loop will not have any marked effect on the nature of system response to step or ramp inputs. However, these parameters do influence the response to velocity transients set up by changing T_L . The overall system response to position and velocity commands is greatly influenced by variation in parameters of the position loop compensator and also the signal amplification K'_p . A better understanding of the

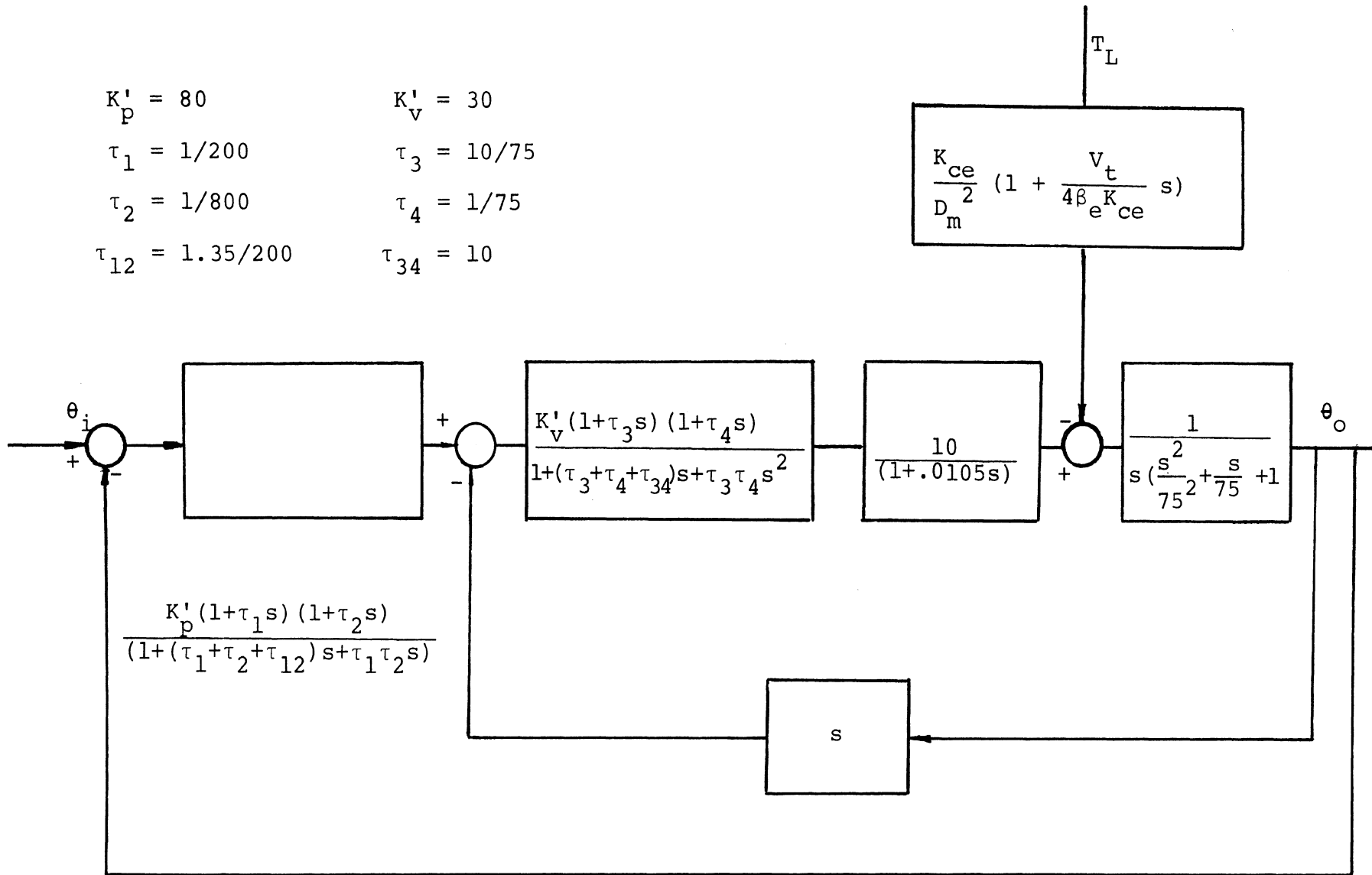


Fig. 37. System to be Simulated on Analog Computer

changes in system response can be made by noting the effect of changing parameters on the open loop frequency response of Fig. 31. In general it may be noted that any changes which lead to increase in the crossover frequency will result in a faster system response. Referring back to Fig. 44 it may be noted that increasing τ_{12} and keeping τ_1 and τ_2 same will result in a decrease in crossover frequency. Similarly we can deduce the following:

- a) moving breakpoint '1' (Fig. 44) to the right without changing τ_2 and τ_{12} will also decrease ω_c (crossover frequency).
- b) again merely changing τ_2 without changing τ_1 or τ_{12} will not have any substantial effect on system response.
- c) changes in K'_p will lead to proportional increases or decreases respectively in ω_c which in turn will proportionately effect the system transients.

It should, however, be noted that the best response will be obtained when an optimum combination of crossover frequency and phase margin is achieved. This is exactly what we hope to achieve through simulation.

H. Operation of the Designed System

It is always desirable that any preliminary design of a system be subjected to a simulation so as to insure compliance of all criteria which are essential for successful operation. In the particular case of a m/c tool contouring servomechanism a proof of successful design would be to simulate the actual machining of a profile, such as the one shown in Fig. 38. The desired feed rates and the number of blocks to be programmed are shown on the figure. It is assumed that " δ " is less than the manufacturing tolerance. The drastic changes in feed rates have been specified for the purpose of emphasizing the demands which might be made on the system during actual operation.

The first obvious command to the system will be the initial table movement to A, which being non-cutting will be a 'rapid traverse.' For execution of this attention is drawn to Fig. 5 and the related discussion. The remaining blocks represent cutting operations. Block No. 1 calls for a movement of 2.9813" at the rate of 40 inch/min and the slope $\tan \theta_1 = 2.0$. This information is then acted upon by the logic of the m/c tool director to produce the following information:

$$\text{feed rate along X axis} = 4/6 \cos\theta_1 = .2981"/\text{sec}$$

$$\text{feed rate along Y axis} = 4/6 \sin\theta_1 = .5962"/\text{sec.}$$

Similarly for the remaining blocks we have

```

feed rate along X axis = .5962"/sec } Block 2
feed rate along Y axis = .2981"/sec

feed rate along X axis = .0298"/sec } Block 3
feed rate along Y axis = .0149"/sec

feed rate along X axis = .0304"/sec } Block 4
feed rate along Y axis = .0137"/sec

feed rate along X axis = .0313"/sec } Block 5
feed rate along Y axis = .0115"/sec

```

These, therefore, will be the successive inputs to the X and Y servos respectively. To be able to simulate the operation, the responses of the servos to these input ramps have to be expressed as functions of time. By generating the outputs against time and plotting the same using a Calcomp type offline plotting system a simulation of the system operation can be obtained. The major work lies in obtaining the response expressions. Since the initial conditions are not zero from block 2 onwards, the time domain expressions obtained from the closed loop transfer functions are not valid. We can either solve the system differential equation separately for each block, making use of the specific initial conditions, or we can set up a state space model representation for the system dynamics. The latter is preferable as it can be used for any combination of initial conditions and input commands. However, the state space representation for higher order

systems involves a considerable amount of computational labor and in order to maintain a reasonable degree of accuracy (up to 4 decimal places) one has to take recourse to machine computing. An alternative course of action would be a computer solution of the system differential equations. This approach has the added advantage that the system transient response can be optimized simultaneously by varying the compensator parameters.

The major steps involved in developing such a model for our system are outlined here. Because of time limitations the details could not be worked out. The closed loop transfer function of our system is

$$\frac{C(s)}{R(s)} = \frac{-.435s^5 + .41 \times 10^3 s^4 + .107 \times 10^7 s^3 + 2.76 \times 10^8 s^2 + 1.62 \times 10^{10} s}{s^6 + 2.49 \times 10^2 s^5 + 5.72 \times 10^4 s^4 + 7.14 \times 10^6 s^3 + 5.12 \times 10^8 s^2}$$

$$\frac{+1.01 \times 10^{11}}{+5.12 \times 10^9 s + 1.01 \times 10^{11}}$$

This is after discarding the two outlying poles. The state equations are obtained as*

*Ref. 22 pages 107-110

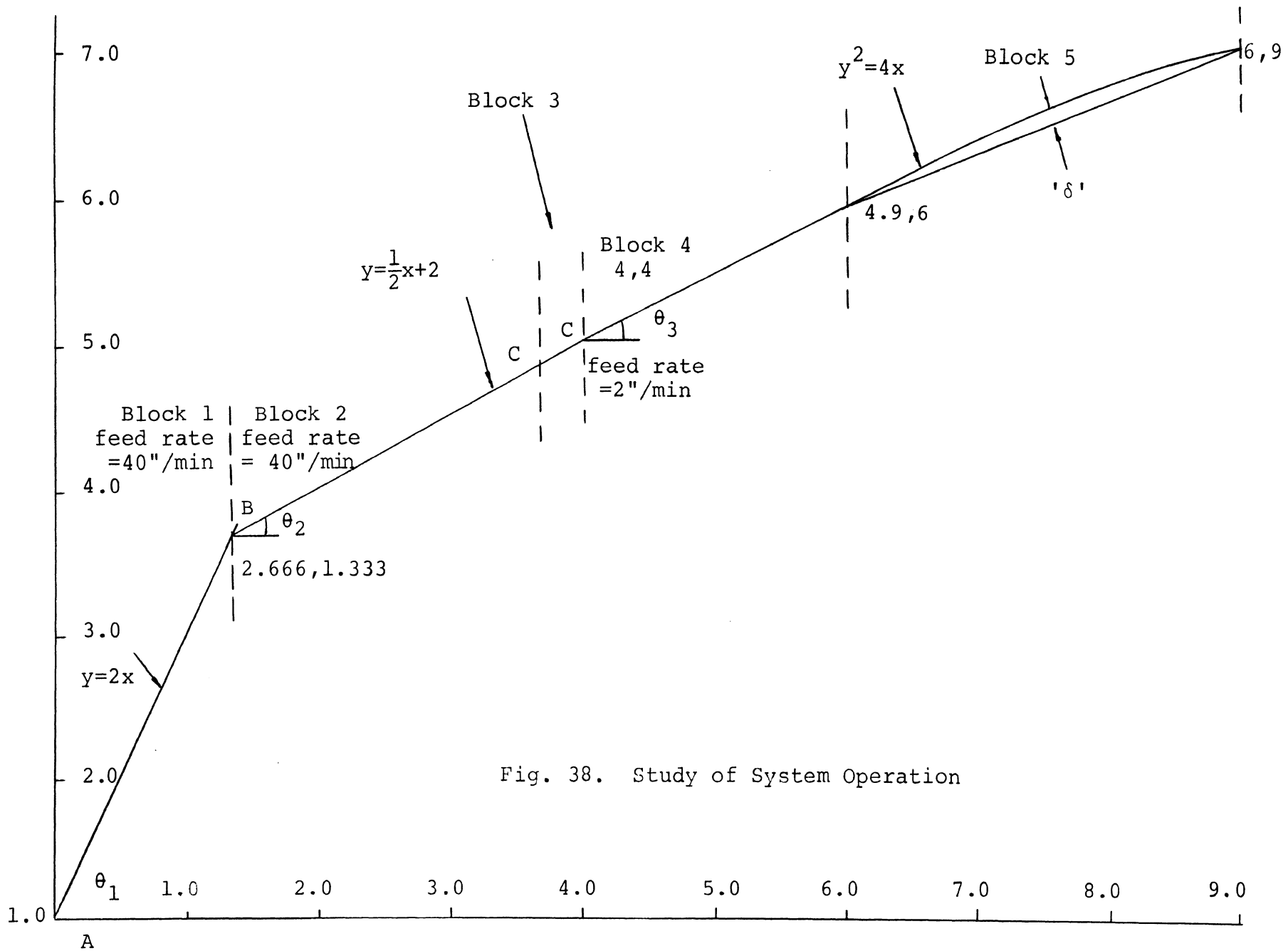


Fig. 38. Study of System Operation

$$\frac{dx_1(t)}{dt} = x_2(t) + (4.183 \times 10^2)r(t)$$

$$\frac{dx_2(t)}{dt} = x_3(t) + (.991 \times 10^6)r(t)$$

$$\frac{dx_3(t)}{dt} = x_4(t) + (8.4 \times 10^6)r(t)$$

$$\frac{dx_4(t)}{dt} = x_5(t) - (4.534 \times 10^{10})r(t)$$

$$\frac{dx_5(t)}{dt} = x_6(t) + (3.6225 \times 10^{12})r(t)$$

$$\begin{aligned} \frac{dx_6(t)}{dt} = & -(1.01 \times 10^{11})x_1(t) - (5.12 \times 10^9)x_2(t) - (5.12 \times 10^8) \\ & x_3(t) - (7.14 \times 10^6)x_4(t) - (5.72 \times 10^4)x_5(t) - \\ & (2.49 \times 10^2)x_6(t) + (1.122 \times 10^{15})r(t) \end{aligned}$$

Output equation is

$$c(t) = x_1(t) - (.435)r(t)$$

Using the matrix representation we have

$$\begin{bmatrix} \frac{dx_1(t)}{dt} \\ \frac{dx_2(t)}{dt} \\ \frac{dx_3(t)}{dt} \\ \frac{dx_4(t)}{dt} \\ \frac{dx_5(t)}{dt} \\ \frac{dx_6(t)}{dt} \end{bmatrix} = \begin{bmatrix} 0 & 1 & 0 & 0 & 0 & 0 \\ 0 & 0 & 1 & 0 & 0 & 0 \\ 0 & 0 & 0 & 1 & 0 & 0 \\ 0 & 0 & 0 & 0 & 1 & 0 \\ 0 & 0 & 0 & 0 & 0 & 1 \\ -1.01 \times 10^{12} & -5.12 \times 10^9 & -5.12 \times 10^8 & -7.14 \times 10^6 & -5.72 \times 10^4 & -2.49 \times 10^2 \end{bmatrix} \begin{bmatrix} x_1(t) \\ x_2(t) \\ x_3(t) \\ x_4(t) \\ x_5(t) \\ x_6(t) \end{bmatrix}$$

A

$$+ \begin{bmatrix} 4.183 \times 10^2 \\ .991 \times 10^6 \\ 8.4 \times 10^6 \\ -4.53 \times 10^{10} \\ 3.6225 \times 10^{12} \\ 1.122 \times 10^{15} \end{bmatrix} r(t)$$

B

The solution for the above dynamic model can be expressed as

$$\underline{x}(t) = \Phi(t-t_0)\underline{x}(t_0) + \int_{t_0}^t \Phi(t-\tau)\mathbf{B}r(\tau)d\tau$$

where the transition matrix Φ is given by the inverse Laplace transform of the matrix

$$[SI - \mathbf{A}]^{-1}$$

An obvious simplification would be to diagonalize the \mathbf{A} matrix. Defining the diagonalizing matrix as \mathbf{P} we have

$$\underline{\mathbf{X}} = \mathbf{P} \underline{\mathbf{y}}$$

where $\underline{\mathbf{y}}$ is a vector in the vector space whose coordinate axes are the eigenvectors of the \mathbf{A} matrix. Substituting for \mathbf{X} in terms of \mathbf{y} in the dynamic model we have

$$\frac{d\underline{\mathbf{y}}}{dt} = \mathbf{D} \underline{\mathbf{y}} + \mathbf{P}^{-1} \mathbf{B} r(t)$$

where \mathbf{D} is the diagonalized matrix having the eigenvalues of \mathbf{A} as its elements. For the special state variable selection as above \mathbf{P} is given by*

$$\mathbf{P} = \begin{bmatrix} 1 & 1 & 1 & 1 & 1 & 1 \\ \lambda_1 & \lambda_2 & \lambda_3 & \lambda_4 & \lambda_5 & \lambda_6 \\ \lambda_1^2 & \lambda_2^2 & \lambda_3^2 & \lambda_4^2 & \lambda_5^2 & \lambda_6^2 \\ \lambda_1^3 & \lambda_2^3 & \lambda_3^3 & \lambda_4^3 & \lambda_5^3 & \lambda_6^3 \\ \lambda_1^4 & \lambda_2^4 & \lambda_3^4 & \lambda_4^4 & \lambda_5^4 & \lambda_6^4 \\ \lambda_1^5 & \lambda_2^5 & \lambda_3^5 & \lambda_4^5 & \lambda_5^5 & \lambda_6^5 \end{bmatrix}$$

*Ref 23 pages 147-148

where the λ 's are the roots of the characteristic equation or the eigenvalues of the \mathbf{A} matrix, and in this case are

$$\lambda_1 = -7.1715, \lambda_2 = -75.4385, \lambda_3 = -58.2 + j51.31,$$

$$\lambda_4 = -58.2 - j51.31, \lambda_5 = -25.34 + j174.091 \text{ and } \lambda_6 = -25.34 - j174.091$$

\mathbf{P}^{-1} is best obtained by machine computation using a numerical technique such as the Gaus-Jordan method. The developing of a computer program to invert matrices having complex elements should be an interesting problem. Also the initial conditions are defined in the 'y' domain as

$$\underline{y}(0) = \mathbf{P}^{-1} \underline{x}(0)$$

In the general case there will be two such models, one for the x and y servos. Once the above model is completed it is a simple matter to generate the output for any input and initial conditions.

The plotter used in carrying out the above simulation should have a resolution comparable with that of the designed control system. Fine deviations from the commanded path can then be detected under magnified conditions. A satisfactory simulation automatically ensures that the transient behavior of the x and y servos are adequately matched. The following comments on the machining of the profile shown in Fig. 38 bring out some additional characteristics of contouring control.

At point B a change in feed rates along the two axes is necessitated on account of change in direction. Because of the inherent time delays this transition requires a finite time during which, say for example, the x servo starting from .2981"/sec attempts to reach a steady state velocity of .5962"/sec and the y servo has to change from .5962"/sec to .2981"/sec. During this finite time the m/c-tool table is traveling and gradually changing its direction from $\tan\theta_1=2$ to $\tan\theta_2=1$. The result of this finite time delay manifests itself in a smooth transition of direction which is characterized by an absence of a sharply defined corner at B. The amount of deviation from the actual profile depends (for a given servo) entirely on how drastic a change is entailed by the desired change in direction. For most contouring applications (e.g. blocks 5,6,etc) the feed rates are small and the change in directions are not so drastic. Therefore, deviations from commanded profile are negligible. However, for all part drawings which call for "sharp corners", the programmer has to insert a special code which the logic system recognizes and which leads to an automatic retardation as the corner is approached. This retardation is a consequence of changed inputs. The execution of the next block is started from rest. The slight overshoot indicated in the figure occurs while the table seeks a null position at B.

CC' is the 'deceleration block' introduced so that the commanded feed rate reduction can be achieved while the table traverses this block. It is assumed that the programmer has introduced this change in feed rate since the machine is required to go from a 'skimming' (fast material removal) to a 'contouring' operation. The length of CC' is shown exaggerated but is actually of the order on .010" . In practice the lengths of these 'compensatory' blocks will depend on the time constant associated with the least responsive slide. Ideally the x and y servos should have identical time domain responses to steps in ramp inputs, i.e. rise time, settling time, peak overshoot etc.

The information on 'acceleration deceleration' block lengths has to be furnished by the m/c tool manufacturer in form of charts. The problem of developing these charts can be greatly simplified by approximating the control system response to ramp inputs by a first order 'type 0' system response to 'step inputs'. First order 'type 0' system will typically exhibit a step response which can be expressed as

$$C(t) = Q(1 - e^{-t/\tau})$$

where Q is the step size and τ is the time constant. In establishing the correlation between our system response to changes in ramp inputs and the above we can make use of the correlation expressed in the last section and

establish value of τ . Note for this purpose we are assuming that

$$\frac{M_m}{k_1(1+k_o)} < 1 \text{ for } k_o = 80$$

so that relation 4 in the last section can be used. Thus the correlated system response is given by

$$V_t = V_i + \Delta V(1 - e^{-t/\tau})$$

Integrating the above expression for output velocity will give us the distance travelled in carrying out the transition to completion.

$$S = \int_0^{4\tau} \{V_i + \Delta V(1 - e^{-t/\tau})\} dt$$

Substituting for τ this gives a relation between S , ΔV and V_i which can be expressed in form of charts or monographs.

V. THE MODERN DESIGN APPROACH

As opposed to the essentially trial and error approach used in the preceding chapter, the philosophy of modern control theory is to first determine the overall transfer function $C(s)/R(s)$ which will satisfy the design criterion and the physical realisability of the controller (compensator). Knowing $C(s)/R(s)$ and also the characteristics of the plant it is then possible to work back to the controller transfer characteristics. An essential feature of this approach is the emphasis on 'optimality' of the resulting design. The designed control system can be claimed to be the 'best' according to some prescribed criterion. It should, however, be noted that the criterion selected may or may not lead to a design which is best for the particular application in mind. Quite often the performance criteria selected are often based on mathematical convenience. Among the many different types of optimal control design problems, the time-optimal control and the minimum-integral control are the most common. The first type deals with the system which is able to bring the states of the system from some initial point to equilibrium in the shortest possible time. The second type is the minimization or maximization of a certain function of the system variables e.g. the minimization of the mean square error design, quadratic performance index design.

The importance of this design approach is directly linked to the development of digital computers and their use as components in the feedback systems. Digital computers when inserted in the control loop have the ability to handle a wide variety of compensation procedures. Another great advantage is the possibility of time sharing of these sophisticated controllers among several control loops. In the present context since our m/c tool is already equipped with a logic unit to carry out data processing and interpolation functions it is logical that this facility be made more sophisticated and used to provide a certain degree of optimality in the functioning of our control system. Because of time limitations it is not possible to carry out an exhaustive design on the above lines. The main objective is to enunciate the design problem and to comment on the technique which may be used for carrying out a successful design.

Figure 39 shows the block diagram of our control system and comparing this with Fig. 4 we note the following changes. The digital to analog converter is now represented by an ideal sample and hold combination. The digital controller is a special computer introduced in the place of network compensators. The additional sampler T_1 represents a true physical phenomenon since the information in this part of the loop is in form of numbers or pulses. The two samplers T_1 and T_2 may or may not be synchronized.

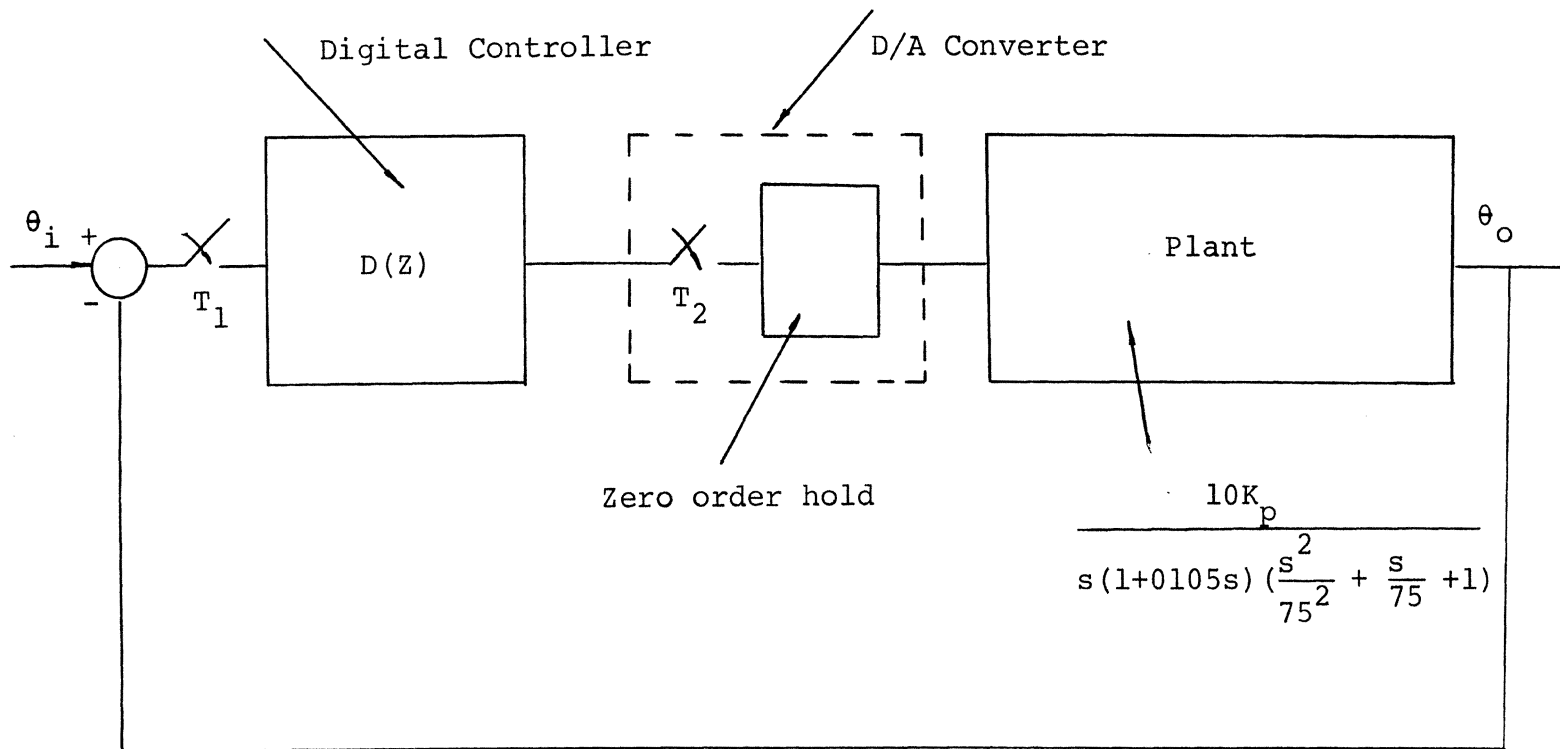


Fig. 39. Sample-Data Representation of Feed Control System

However, the analysis is made much simpler if both are assumed to be synchronized. Once the controller has been designed it is possible to observe the effects of varying T_1 and T_2 by digital simulation. The present representation does not show any velocity monitoring. This, however, is of no great consequence. As has been pointed earlier this part of the control system is not critical to the basic operation. It only serves to provide a fast damping of velocity transients. The analysis is considerably simplified by ignoring this during preliminary stages of design. During final simulation this additional feedback may be introduced and its effects studied.

The steps involved in carrying out a successful design will be:

- 1) Specify performance criterion which will form basis for design optimality
- 2) Specify the transfer function θ_o/θ_i which will meet this criterion successfully
- 3) Knowing the transfer function of the plant work back to a design for the digital controller $D(Z)$.
- 4) Digital simulation of the control system.

Without commenting in details it is sufficient to mention here that the 'optimal' control system for our application will be one which gives a 'time optimal' response for ramp

inputs. This is easily seen to be true for 'contouring control' where the cutting action is continuous. In addition to this time domain specification the control system must successfully meet our frequency domain specifications which have been expounded in detail in the previous chapters.

VI. CONCLUSION

The problems facing a potential N.C. feed drive designer have been adequately demonstrated in this work. A method of design, based on conventional techniques of analysis, has been presented. It is worthwhile, at this stage, to summarize the major steps involved in following this procedure and also to list the data required at the outset in order to be able to define the plant characteristics.

The first step is to establish the transfer characteristics of the plant under control which in this case consists of the power amplifiers, the actuator, the transmission and the machine table and slide characteristics. Referring to Fig. 16 we see that the values of the following parameters must be known viz. B_m , β_e , D_m , K_{ce} , K_q , J_T and V_T . All the above parameters excepting B_m and J_T will have to be obtained from the specification manuals of the hydraulic actuators. The latter two are decided by the machine tool table weight, slide friction and the transmission ratio.

Once the transfer characteristics of the plant have been established the next step is to decide on the minimum signal amplifications which are necessary. These amplification levels were established by studying the sensitivity and accuracy requirements for the control system. Once

these amplification levels are established we are in a position to complete the block diagram representation and then continue on to the system response study. Having successfully set up the problem our next step is to carry out an analysis in the frequency domain so as to ensure system stability and also to make the response conform to our frequency domain specifications of M_{peak} , bandwidth etc. Compensator parameters are established for optimum steady state response. Further an estimate is made on the range of values which should be incorporated while physically implementing these. As a check at this stage the system transient response is simulated to a step and ramp input.

Having completed the above the only step remaining is optimization of transient response. This, as has been pointed out earlier, is most easily accomplished using an analog computer.

For all control design problems one is faced with the choice of either following the conventional approach, wherein one is essentially relying on trial and error techniques and to a large extent on final simulation, or one has the choice to follow the modern techniques of optimization and go through a lot of preliminary maths to ensure least reliance on final simulation. For the case in hand the application of both methods would definitely bring out advantages of one over the other. A comparison can be made

if the design problem as enunciated in Chapter V, is carried to completion.

The effect of load transients on system response is an area which needs to be examined further. Output impedance for electronic amplifiers is defined as the parameter which relates the changes in output voltage and current with load impedance. The lower this impedance the less the effect of variations in load on the amplifier output voltage. An analogy can be drawn for a servomechanism whose controlled output is velocity and the disturbance is the external torque. Output impedance can be defined by simply relating the two variables from the block diagram. It is advisable, while designing compensators and deciding gain levels, to check the effect these have on the value of the impedance function. Disturbance effects can also be studied while simulating on an analog computer. The second aspect which needs to be stressed is the final simulation of an actual machining operation. This holds the advantage of insuring that servos controlling different axes are matched and further offers a definite proof of successful operation of the system. Lastly, a worthwhile extension would be to incorporate the effects of common non-linearities in the preliminary design. This could be accomplished by using analytic techniques such as 'describing functions' to represent such common non-linearities as backlash in gearing, saturation effects in amplifiers and Coulomb friction of machine slides.

BIBLIOGRAPHY

1. Mergler H.W., Numerical Machine Tool Control System Operating from Coded Punched Paper Tape.
Unpublished Ph.D. Dissertation: Case Institute of Technology - 1956.
2. Hadekel, R., "Hydraulic Control of Automatic Machinery Synthesis of Systems", Automation, Aug.-Oct.-Dec. 57 and Feb.-April-June-Aug 1957.
3. Rausch, R.C., "Analysis of Valve Controlled Hydraulic Servomechanisms", Bell Systems Tech. Journal, V. 38, N. 6, Nov. 59.
4. "Hydraulic Servo Performance in N.C. m/c Tools", Hydraulics and Pneumatics, V. 13, N. 6, June 1960.
5. Royle, J.K., Cowley, A., "Design of High Performance Position Control System for Machine Tool Profiling Operations", International Journal of Machine Tool Design and Research, V. 1, N. 1-2, Sept. 1961.
6. Seleno, A.P., "Hydraulic Servo Drives", Machine Design, October 1963.
7. Ogden, H., "Mechanical Design Aspects of Electronically Controlled Machine Tools", Advances in Machine Tool Design and Research, 1963.

8. Marklew, C.K. and McCall, R.H., "Design Considerations for a Low Cost N.C. Machine Tool", Advances in Machine Tool Design and Research, 1963.
9. Zeleny, J., "Feed Drives for N.C. Machine Tools", Advances in Machine Tool Design and Research, 1965.
10. Rhoades, J.M., "Matching Machine Tools and Hydraulic Servos", Control Engr., Vol. 12, No. 4, 1965.
11. Bakel, J.F., "Factors to Consider in Design of Machines Equipped with Automatic Controls", International Machine Tool Design and Research Conference, 6th Proc., Sept. 1965, Pages 89-94.
12. Cordes, E.V., "Incremental vs. Absolute Control System", Machine and Tool Blue Book, Vol. 61, No. 5, May 1966.
13. Fischer, K., "General Purpose Programmed Control System", Brown Boveri Review, U. 53, No. 4-5, April, May 1966, p 365-370.
14. Taft, C.K., Lutz, F.N., Mazol, M., "Dynamic Accuracy in N.C. Systems", Tool and Mfg. Engineer, Vol. 58, No. 5,6, May 1967.
15. "Position Measuring Systems for Numerically Controlled Machine Tools", Brown Boveri Review, Vol. 54, No. 8, Aug. 1967.

16. "Continuous Path Control System", Brown Boveri Review, Vol. 54, No. 8, Aug 1967.
17. "How to Match Machine Elements and Servo Systems for Best Total Performance", Machine Design, Vo. 39, No. 10, April 1967.

BOOKS

18. Herbert E. Meritt, "Hydraulic Control Systems", John Wiley and Sons, Inc., 1967.
19. Howard L. Harrison and John G. Bellinger, "Introduction to Automatic Controls", International Textbook Company, 1963.
20. Francis H. Raven, "Automatic Control Engineering", McGraw-Hill Book Company, 1968.
21. Cornelius T. Leondes, "Computer Control Systems Technology", McGraw-Hill Book Company, 1961.
22. Benjamin C. Kuo, "Automatic Control Systems", Prentice-Hall, Inc. 1967.
23. Katsuhiko Ogata, "State Space Analysis of Control Systems", Prentice-Hall Inc., 1967.

VITA

Subash Bhatia was born on December 30, 1944 in Pakistan. He received his primary and secondary education in New Delhi. In July 1966 he received his Bachelor's degree in Mechanical Engineering from Indian Institute of Technology, Bombay. Subsequent to that he was employed in Bombay for a period of four years.

He has been enrolled in the Graduate School of the University of Missouri-Rolla since September, 1970.

APPENDIX A
HYDRAULIC SERVO ANALYSIS

Section 1: Linear Electro-Hydraulic Servo-Analysis

For an ideal critical center valve with matched and symmetrical orifices the expression for flow is

$$Q_L = C_d \omega X_v \left(\frac{1}{\rho} (P_s - P_L) \right)^{1/2}$$

where P_s - designed supply pressure

P_L - designed load pressure

C_d - coefficient of discharge

ω - area gradient for rectangular ports

X_v - displacement from line-on-line position

Taking the variables as X_v and $(P_s - P_L)$ and linearizing the equation we get

$$Q_L = K_q X_v - 2K_c P_L \quad (1)$$

where K_q - flow gain constant defined as flow rate per unit displacement of spool in³/sec/in

and K_c - flow pressure coefficient defined as change in flow per unit increase in load pressure and has units in³/sec/p.s.i.

Figure 40a shows a schematic representation of the valve and linear receiving unit.

$P_L = (P_1 - P_2)$ is the load pressure difference. A change in P_L is twice that which occurs across a port. Therefore, expression (1) can be expressed as

$$Q_1 = K_q X_v - 2K_c P_1$$

$$Q_2 = K_q X_v + 2K_c P_2$$

Adding these two equations we get

$$Q_L = K_q X_v - K_L P_L \quad (2)$$

The flow pressure coefficient K_c for each port is twice that for the valve as a whole because K_c is defined w.r.t. P_L and a change in P_L is twice that which occurs across a port. Also,

$$Q_L = \frac{Q_1 + Q_2}{2} = \text{load flow in}^3/\text{sec}$$

$$P_L = P_1 - P_2 = \text{load pressure difference p.s.i.}$$

Equation (2) represents the linearized flow equation for the servo-valve. The load flow Q_L represents the average of the flows in the lines and is equal to the flow in each line only if the external leakage is zero.

Applying the continuity equations to each of the piston chambers gives

$$Q_1 - C_{ip}(P_1 - P_2) - C_{ep}P_1 = \frac{dV_1}{dt} + \frac{V_1}{\beta_e} \frac{dP_1}{dt} \quad (3)$$

and

$$C_{ip}(P_1 - P_2) - C_{ep}P_2 - Q_2 = \frac{dV_2}{dt} + \frac{V_2}{\beta_e} \frac{dP_2}{dt} \quad (4)$$

where

C_{ip} - internal or cross-port leakage coefficient
of piston in³/sec/p.s.i.

C_{ep} - external leakage coefficient of piston
in³/sec/p.s.i.

β_e - effective bulk modulus of the system (includes
oil, entrapped air, and mechanical compliance
of chambers) p.s.i.

$V_T = V_1 + V_2 = 2V_o$ where V_o = volume of chamber when
piston is centered

= total volume of fluid under
compression in both the
chambers.

Substituting, equations (3) and (4) reduce to

$$Q_L = A_p \frac{dx_o}{dt} + C_{tp} P_L + \frac{V_t}{4\beta_e} \frac{d}{dt} P_L \quad (5)$$

where

x_o - displacement of piston

A_p - area of piston in.²

$C_{tp} - C_{ip} + C_{ep}/2$ = total leakage coefficient of
piston in³/sec/p.s.i.

Writing the expression for force balance on the piston we
have

$$F_g = A_p P_L = M_t s^2 X_o + B_p s X_o + F_L \quad (6)$$

where

F_g - total force generated by piston

B_p - viscous damping coefficient of piston in.-lb.-sec

Transforming eq. (5) and solving equations (2), (5) and (6)

simultaneously we get the overall transfer function for this valve and cylinder receiving unit as

$$X_O = \frac{K_q/A_P X_V - \frac{K_{ce}}{A_P} (1 + \frac{V_t}{4\beta_e K_{ce}} s) F_L}{\frac{V_t M_t}{4\beta_e A_P^2} s^3 + (\frac{K_{ce}}{A_P} M_T + \frac{B_P V_t}{4\beta_e A_P^2}) s^2 + (1 + \frac{B_P K_{ce}}{A_P^2}) s}$$

where

$$K_{ce} = K_c + C_{ip} + C_{ep}/2 = \text{total flow pressure coefficient in}^3/\text{sec/p.s.i.}$$

The factor $\frac{B_P K_{ce}}{A_P^2}$ is usually much smaller than unity and therefore can be eliminated conveniently. Thus, with this simplification the transfer function reduces to the form shown in Fig. 40b.

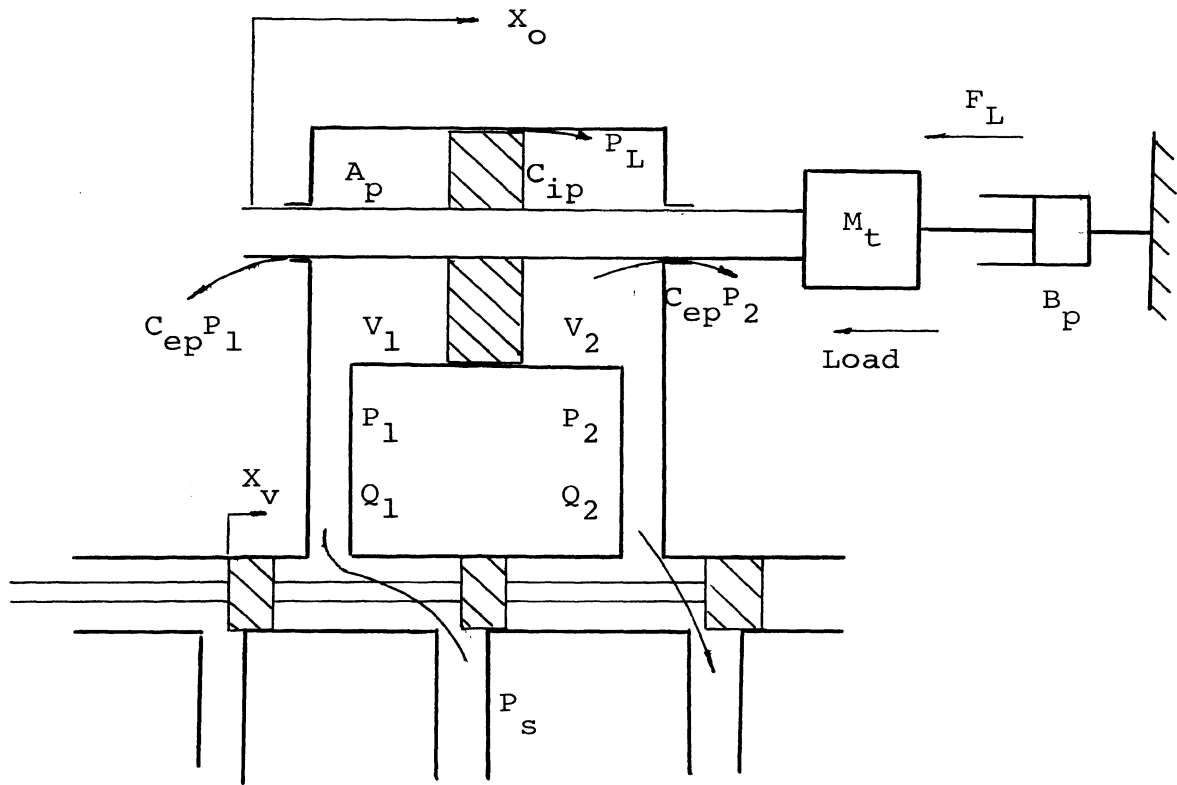
Section 2. Valve Controlled Motor

In this section we develop the transfer function for a valve controlled fixed displacement axial piston motor. The basic flow equation of the servo-valve as applicable here is same as Eq. (2) section I, i.e.

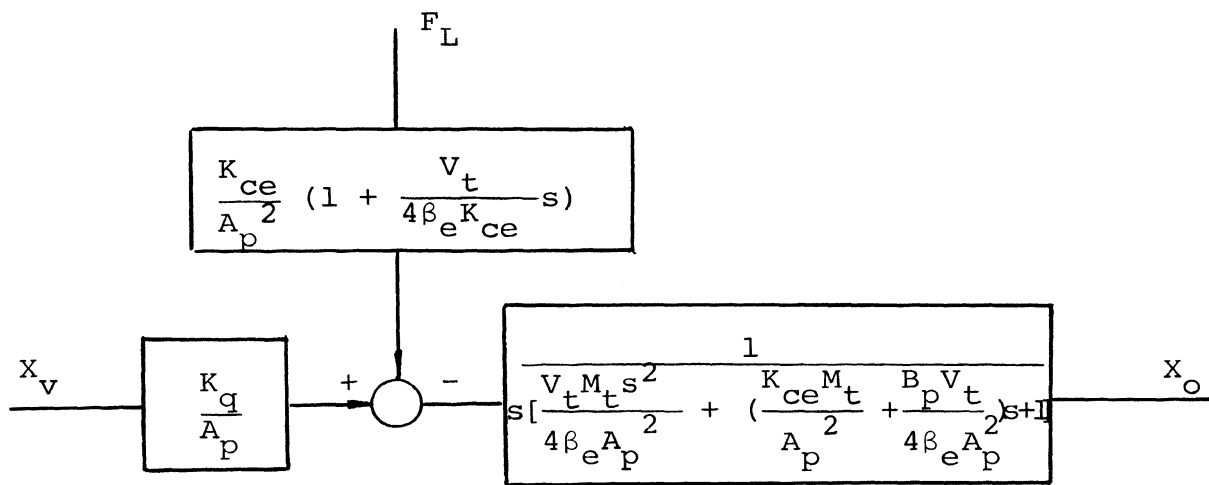
$$Q_L = K_q X_V - K_c P_L \quad (1)$$

Assuming the presence of following idealized conditions.

- a) Pressure in each motor chamber is uniform and does not saturate or cavitate.



40a



40b

Fig. 40. Valve Controlled Cylinder and Piston

- b) Fluid velocities in the chambers are small so that minor losses are negligible,
- c) Line phenomenon are absent,
- d) temperature and density are constant

we can write the following equations of continuity as before

$$Q_1 - C_{im}(P_1 - P_2) - C_{em}P_1 = \frac{dV_1}{dt} + \frac{V_1}{\beta_e} \frac{dP_1}{dt} \quad (8)$$

$$C_{im}(P_1 - P_2) - C_{em}P_2 - Q_2 = \frac{dV_2}{dt} + \frac{V_2}{\beta_e} \frac{dP_2}{dt} \quad (9)$$

where C_{im} is the internal or crossport leakage coefficient of motor in³/sec/p.s.i. and C_{em} is the external leakage coefficient of motor

β_e - effective bulk modulus of system p.s.i.

V_1 - volume of forward chamber in³

V_2 - volume of return chamber in³

$V_t = V_1 + V_2 =$ total contained volume of both high pressure and low pressure chambers

Also,

$$\frac{dV_1}{dt} = D_m \frac{d\theta_o}{dt} = - \frac{dV_2}{dt} \quad (10)$$

where $D_m =$ volumetric displacement of motor, in³/rad.

Simplifying equations (7), (8), (9), and (10) simultaneously we get

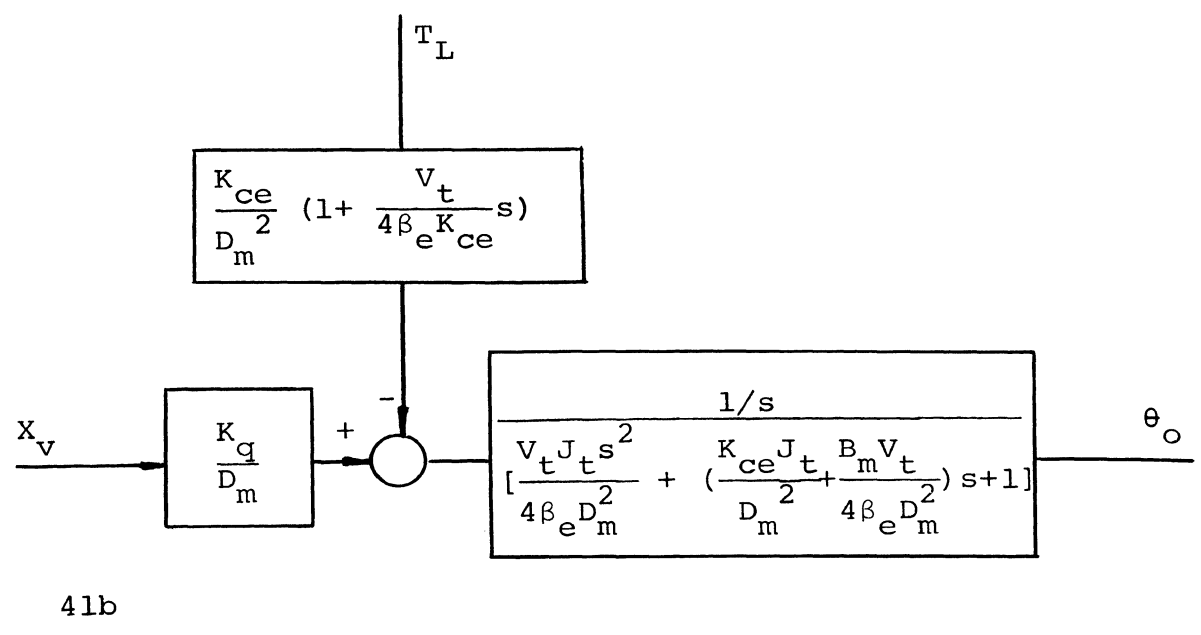
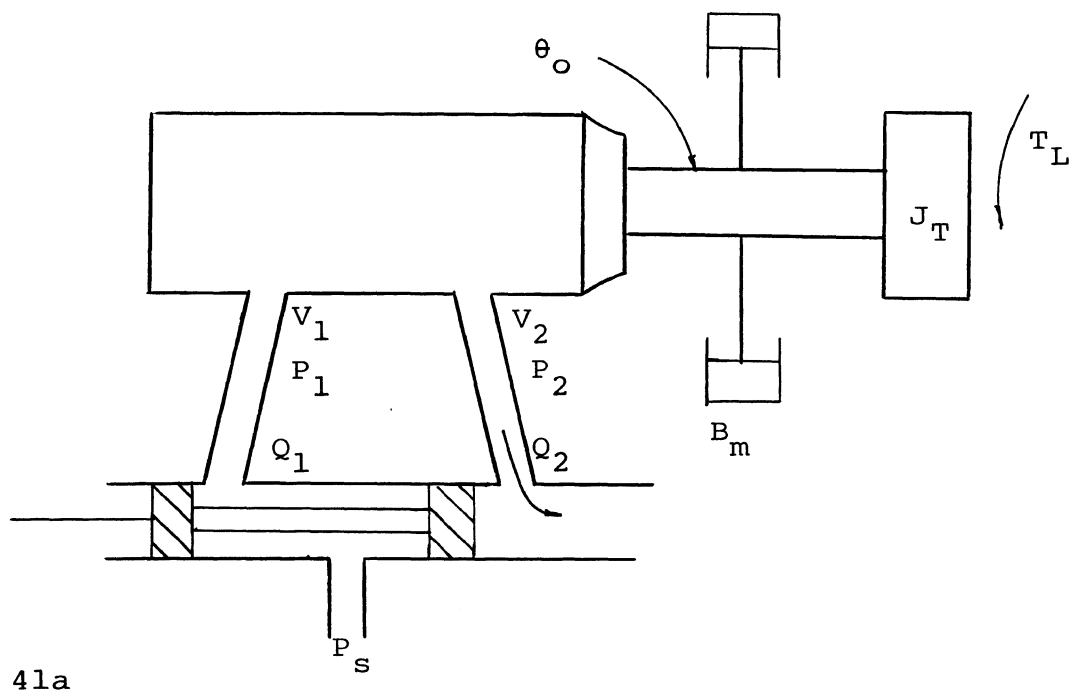


Fig. 41. Valve Controlled Hydraulic Motor

$$Q_L = D_m \frac{d\theta_o}{dt} + (C_{im} + \frac{C_{em}}{2}) (P_1 - P_2) + \frac{V_o}{2\beta_e} \frac{d}{dt} (P_1 - P_2)$$

Substituting $C_{tm} = C_{im} + \frac{C_{em}}{2}$ = total leakage coefficient of motor (in³/sec/p.s.i.) and taking the Laplace transform we get

$$Q_L = D_m s \theta_o + C_{tm} P_L + \frac{V_t}{4\beta_e} s P_L \quad (11)$$

Equation (11) is basic for all hydraulic actuators and may be simply interpreted in the following way. The total load flow Q_L is consumed by leakage, flow stored due to compressibility and flow to cause the displacement of the actuator.

Writing the torque balance for the motor we have

$$T_g = (P_1 - P_2) D_m = J_t s^2 \theta_o + B_m s \theta_o + T_L \quad (12)$$

where

T_g = torque generated or developed by motor in lbs.

J_t = total inertia of motor and load (referred to motor shaft) in-lb-sec²

T_L = reflected load torque on motor in-lbs

Combining equations (7), (11) and (12) and simplifying we get

$$\theta_o = \frac{\frac{K_q}{D_m} x_v - \frac{K_{ce}}{D_m} (1 + \frac{V_t}{4\beta_e K_{ce}} s) T_L}{s \left[\frac{V_t J_t s^2}{4\beta_e D_m^2} + \left(\frac{K_{ce} J_t}{D_m^2} + \frac{B_m V_t}{4\beta_e D_m^2} \right) s + \left(1 + \frac{B_m K_{ce}}{D_m^2} \right) \right]}$$

where

$$K_{ce} = K_c + C_{tm} = \text{total flow pressure coefficient} \\ \text{in}^3/\text{sec}/\text{p.s.i.}$$

The quantity $\frac{B_m K_{ce}}{D_m^2}$ is very small as compared to unity and can normally be neglected. Thus the overall transfer function for this valve-motor combination can be expressed as shown in Fig. 41b.

Section 3. Torque-Motor Analysis

Referring to Fig. 42 the two coils on a torque motor are generally supplied from a push-pull source. A voltage E_{bb} in the amplifier driving the torque motor establishes a quiescent current I_o in each coil but there is no net torque on the armature because the currents oppose each other. An increase in the input to the amplifier causes the current in one coil to increase as the current in the other coil decreases simultaneously by the same amount. Thus,

$$i_1 = I_o + i$$

$$i_2 = I_o - i$$

where i_1, i_2 = current in each coil respectively, and

I_o = quiescent current in each coil,

i = signal current in each coil

$$\Delta i = i_1 - i_2 = 2i$$

The flux in the armature, and consequently the developed torque, is proportional to Δi . Signal voltages for push-

pull operation are $e_1 = e_2 = \mu e_g$ where

e_1, e_2 = signal voltages from amplifiers

μ = amplifier gain

e_g = signal voltage input to amplifier.

The voltage equations for each coil circuit are

$$E_{bb} + e_1 = i_1(Z_b + R_c + r_p) + i_2 Z_b + \frac{N_c}{10^8} \frac{d\phi_a}{dt}$$

$$E_{bb} - e_2 = i_2(Z_b + R_c + r_p) + i_1 Z_b - \frac{N_c}{10^8} \frac{d\phi_a}{dt}$$

where

R_c = resistance of each coil in ohms

N_c = number of turns in each coil

ϕ_a = total magnetic flux through the armature

r_p = internal plate resistance of amplifier

E_{bb} = constant voltage for constant current

Z_b = impedance in common lines of coils

The above two equations can be combined to yield the fundamental voltage equation for the torque motor.

$$2\mu e_g = (R_c + r_p) \Delta i + \frac{2N_c}{10^8} \frac{d\phi_a}{dt} \quad (13)$$

The expression for the armature flux relation can be shown to be¹⁸

$$\phi_a = \frac{\frac{M_o}{R_G} (X/g) + \frac{N_c \Delta i}{R_g}}{1 - X^2/g^2}$$

where

M_o = total m.m.f. of all permanent magnets amp-turns

$R_g = g/\mu_o A_g$ = reluctance of each air gap at neutral
amp-turns/line

$N_c \Delta i$ = net m.m.f. due to control currents amp-turns

X = displacement of the armature tip from neutral
position in

A_g = pole face area at the air gaps in²

$\mu_o = 3.19$ = permeability of air

g = length of each air gap at neutral ins.

Torque motors are normally designed so that $\frac{X^2}{g^2} \lll 1$ and can be neglected. Therefore, the expression for armature flux is simplified to

$$\phi_a = \frac{M_o}{R_g} \frac{x}{g} + \frac{N_c \Delta i}{R_g} \quad (14)$$

Differentiating (14), substituting in (13) and taking the transform we get

$$2\mu e_g = (R_c + r_p) \Delta i + 2K_b s\theta + 2L_c s \Delta i \quad (15)$$

where

$$K_b = 2 \times 10^{-8} (a/g) N_c \frac{M_o}{2R_g}$$

= back e.m.f. constant for each coil volts/rad/sec.

$$L_c = (10^{-8}) \frac{N_c^2}{R_g} = \text{self inductance of each coil henrys.}$$

The torques developed in the two air gaps are in opposition. The net torque developed is given by the relation¹⁸

$$T_d = \frac{(1 + x^2/g^2)K_t \Delta i + (1 + \theta_c^2/\theta_g^2)K_m \theta}{(1 - x^2/g^2)^2}$$

where

$$\phi_c = \frac{N_c \Delta i}{2R_g}$$

$$\phi_g = \frac{M_o}{2R_g}$$

$$K_t = 4(4.42 \times 10^{-8}) (a/g) N_c \theta_g = \text{torque constant for the torque motor in-lbs/amp.}$$

$$K_m = 8(4.42 \times 10^{-8}) (a/g)^2 R_g \phi_g = \text{magnetic spring constant of torque motor in.lb/rad.}$$

For most torque motors $(\frac{x}{g})^2 \ll 1$ and $(\theta_c/\theta_g)^2 \ll 1$ and therefore can be neglected. Thus the expression for the torque developed reduces to

$$T_d = K_t \Delta i + K_m \theta$$

Equating the torque to the forces acting on the armature we get

$$K_t \Delta i = J_a s^2 \theta + B_a s \theta + (K_a - K_m) \theta + T_L \quad (16)$$

where

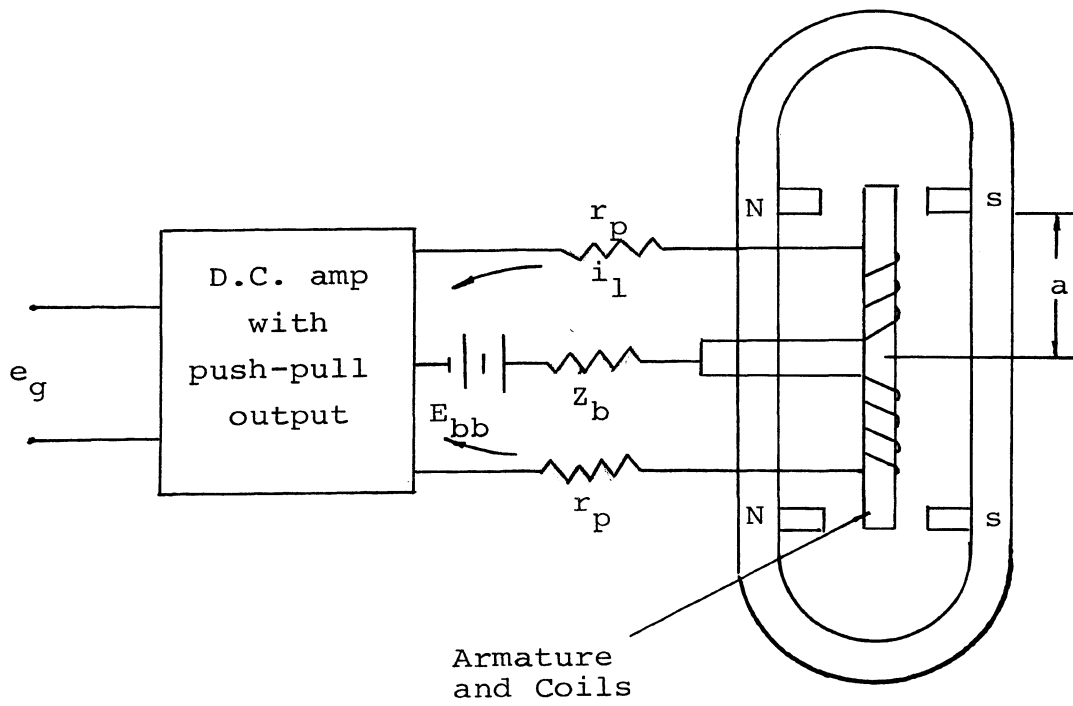


Fig. 42. Torque Motor

J_a = inertia of armature and any attached load in-lb-sec²

B_a = viscous damping coefficient of armature mounting

K_a = mechanical torsion spring constant of armature pivot in-lb/rads.

T_L = arbitrary load torque on the armature in-lbs.

Neglecting mechanical damping B_a equations (15) and (16) can be combined to give

$$\theta = \frac{K_o e_g - \left[\frac{1}{K_a (1 - K_m/K_a)} \right] (1 + s/\omega_a) T_L}{\frac{s^3}{\omega_a \omega_m^2 (1 - K_m/K_a)} + \frac{s^2}{\omega_m^2 (1 - \frac{K_m}{K_a})} + \frac{s}{\omega_a (1 - \frac{K_m}{K_a})} + 1}$$

where

$$K_o = \frac{2K_t \mu}{(R_c + r_p) K_a (1 - K_m/K_a)} = \text{static gain constant rads/volt}$$

$$\omega_a = \left(\frac{R_c + r_p}{2L_c} \right) = \text{armature circuit break frequency for each coil rad/sec.}$$

$$\omega_m = \sqrt{\frac{K_a}{J_a}} = \text{natural frequency of armature}$$

Neglecting T_L the above expression reduces to the form

$$\theta = \frac{K_o e_g}{(s/\omega_r + 1) \left(\frac{s^2}{\omega_o^2} + \frac{2\xi_o}{\omega_o} s + 1 \right)}$$

where

$$\omega_r \approx \omega_a$$

$$\omega_o \approx \omega_m$$

$$\xi_o \approx 1/2 (K_m/K_a)$$

Multiplying by 'r' we get

$$X_v = r\theta = \frac{K_s e_g}{(s/\omega_r + 1) \left(\frac{s}{\omega_o} + \frac{2\xi_o}{\omega_o} s + 1 \right)}$$

where

r = radius of armature coil, and
 $K_s = K_o r$ = overall gain constant in/volt.

This is the form of the transfer function which is used for most dynamic analysis of systems incorporating torque motors.

APPENDIX B

Transfer Functions of Electric-Servo

The power amplification is obtained by a Ward-Leonard drive and the actuator is an armature controlled d.c. motor. Figure 43a shows the circuit diagram for winding of the motor. E_a is the error signal from the generator of the power amplifier set. The circuit equation for the armature is

$$E_a - K_e I_f \dot{\theta} = R_a I_a + L_a D I_a = R_a [1 + \tau_a D] I_a$$

where the term $K_e I_f \dot{\theta}$ represents the back e.m.f. developed. Taking transform and regrouping we get

$$I_a = \frac{E_a}{R_a [1 + \tau_a s]} - \frac{K_e I_f \dot{\theta}}{R_a [1 + \tau_a s]} \quad (1)$$

Torque developed by the motor is given by the expression

$$T = K_m I_f I_a$$

where K_m is a constant having units in-lbs. Also torque balance for output shaft is

$$T = (B_m s + J_t s^2) \theta + T_L \quad (2)$$

The error signal of the servo is amplified by the static amplifier having gain K_v . This error signal is then applied across the field winding of the Ward-Leonard

drive generator. The circuit is shown in Fig. 43b. The following basic relationships follow from the figure.

$$E = (R_{fg} + L_{fg}s)I_{fg}$$

Also, $E_g = K'_c E$ where K'_c is the generator constant and

$E_g = E_a$. Therefore,

$$E_a = \frac{(K'_c/R_{fg})}{(1+\tau_{fg}s)} \quad (3)$$

The transfer function for this drive can be derived from equations (1), (2), and (3). Figure 43c shows the transfer function in block diagram form.

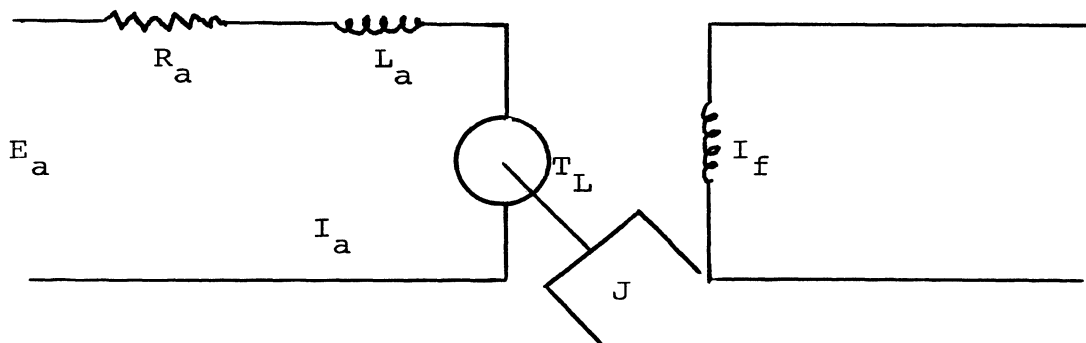


Fig. 43a

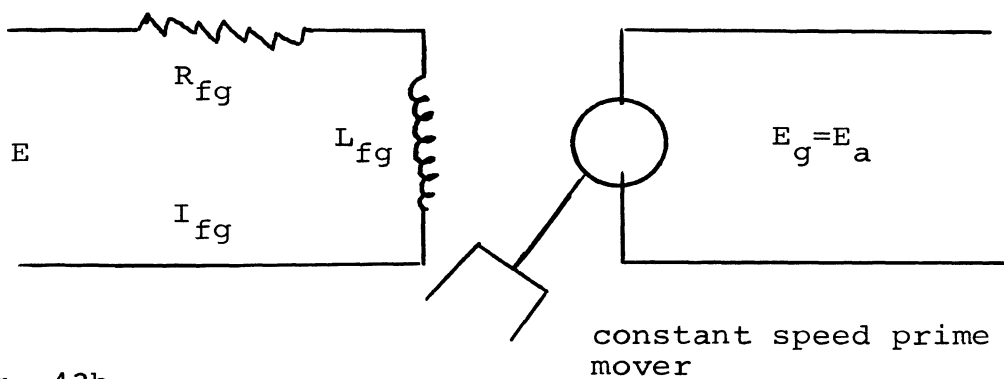


Fig. 43b

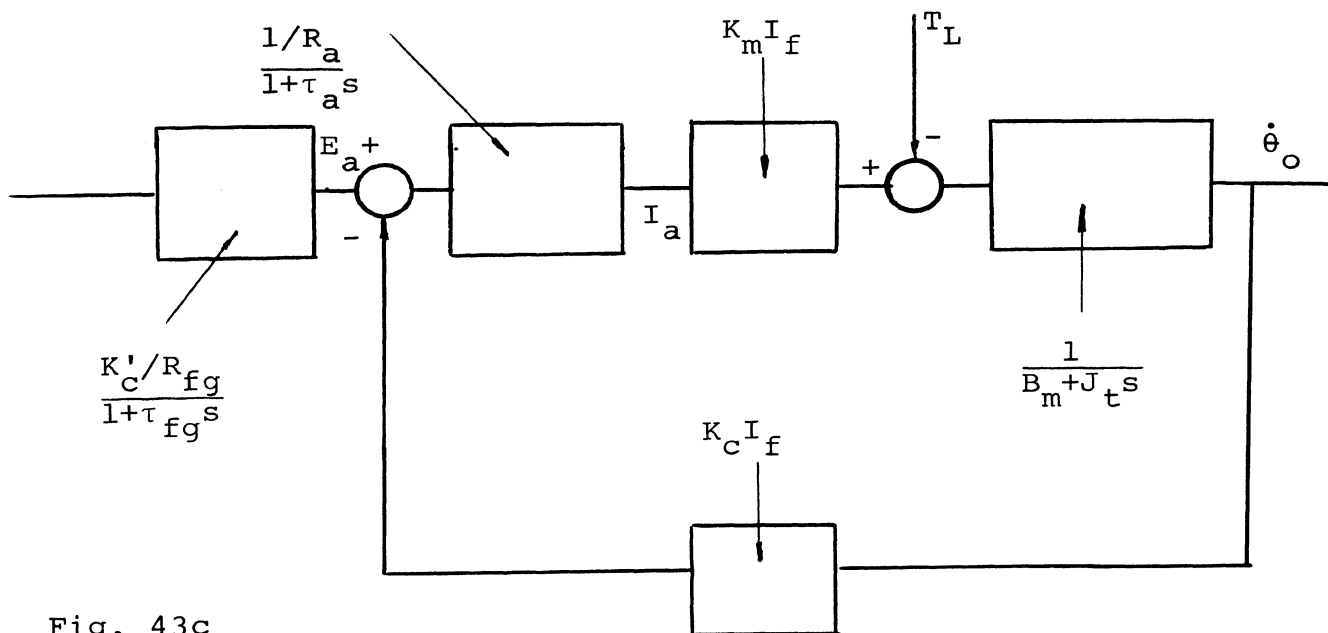


Fig. 43c

Fig. 43. Electric Servo-System

APPENDIX C

LAG-LEAD COMPENSATOR CHARACTERISTICS

A lag-lead compensator is a series combination of a lag and a lead network. The general transfer function is

$$\frac{E_o(s)}{E_{in}(s)} = \frac{(1+\tau_1s)(1+\tau_2s)}{(1+(\tau_1+\tau_2+\tau_{12})s + \tau_1\tau_2s^2)}$$

The log-magnitude diagram for a typical lag-lead compensator is shown in Fig. 44. The slope between the break points is -1 log units/decade. The time constant τ_{12} is decided by the placing of break point '3' or '4'. Consider an example where $\tau_1=1/50$, $\tau_2 = 1/250$ and also the break corresponding to point '3' is to be at 5 rads/sec. Then

$$\frac{E_o(s)}{E_{in}(s)} = \frac{(1+\tau_1s)(1+\tau_2s)}{1+(\tau_1+\tau_2+\tau_{12})s+\tau_1\tau_2s^2} = \frac{(1+s/50)(1+s/250)}{(1+\frac{1}{5}s)(1+\tau_4s)}$$

or, we have

$$\tau_1 + \tau_2 + \tau_{12} \approx \frac{1}{5} + \tau_4 \quad (1)$$

and

$$\tau_1\tau_2 \approx \frac{1}{5} \tau_4 \quad (2)$$

From (2) we get $\tau_4 = \frac{1}{2500}$. Also from (1) we get $\tau_{12} = \frac{441}{2500}$. It should further be noted from the figure that the maximum phase lead or lag obtainable depends entirely on

the constant τ_{12} which in turn will be decided by the relative position of break points '1' and '3'. Further

$$\left(\frac{E_0}{E_i \text{ min.}}\right) = \frac{\tau_1 + \tau_2}{\tau_1 + \tau_2 + \tau_{12}}$$

and corresponds to frequency

$$\omega = \frac{1}{\sqrt{\tau_1 \tau_2}}$$

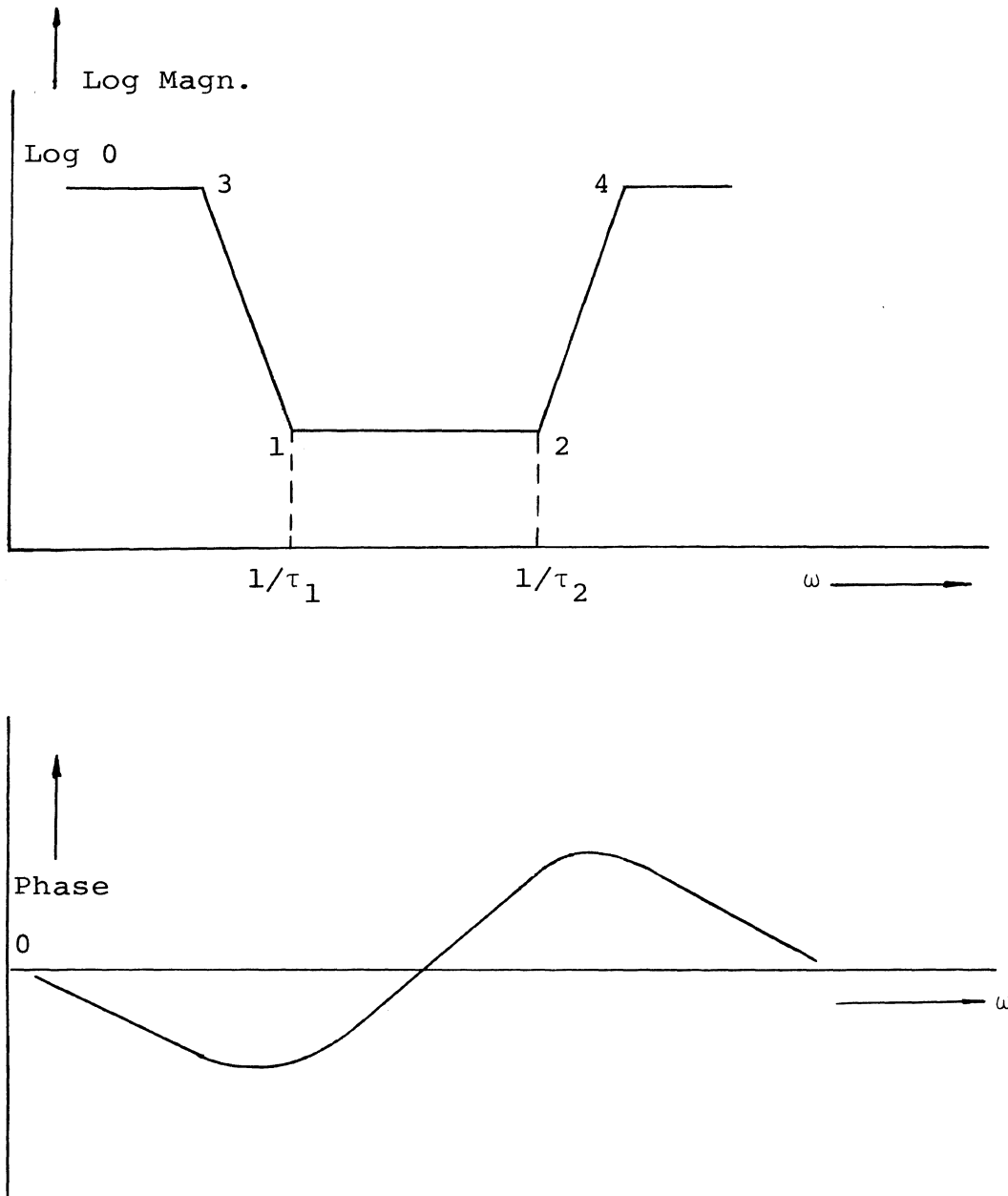


Fig. 44. Lag-Lead Compensator Characteristics

202940